COMPLEX OXIDES AS MOLECULAR MATERIALS: STRUCTURE AND BONDING IN HIGH-VALENT EARLY TRANSITION METAL COMPOUNDS

J.C. GOLOBOY, W.G. KLEMPERER *, T.A. MARQUART, G. WESTWOOD and O.M. YAGHI
Frederick Seitz Materials Research Laboratory
Department of Chemistry
University of Illinois
Urbana, Illinois 61801, U.S.A.

Key words: molybdenum compounds, complex oxides, metal oxides, molecular materials, structure, bonding.

1. Introduction

Complex oxides of the early transition metals in their highest oxidation states display a remarkable variety of properties, including catalytic [1], electrooptic [2], high-κ dielectric [3], electromechanical [4], ferroelectric [5], and charge density wave [6] behavior. The structural basis for this behavior, although understood in general terms, is not well understood on the atomic-molecular size scale, and as a result, these properties are difficult or impossible to control chemically. A first step toward addressing this problem is clear definition of structure and bonding in these materials, the subject of this Chapter.

Structural diversity is a hallmark of early transition metal oxide chemistry [7]. In high-valent oxides, coordination numbers range from four to seven, coordination geometry is often severely distorted from idealized polyhedral geometry, and coordination polyhedra are linked by vertex-, edge-, and face-sharing [8]. From this point of view, coordination compounds, polyoxometalates, and lattice compounds have little in common, especially when blues [9], bronzes [10], and so-called nonstoichiometric phases [11] are taken into account. A far different sit-

* e-mail: wklemper@uiuc.edu

J.J. Borrás-Almenar et al. (eds.), Polyoxometalate Molecular Science, 79–174.

uation is obtained, however, if the structures of these compounds are represented in terms of metal-oxygen bonding interactions [12–16] as opposed to linkages between coordination polyhedra. By first distinguishing between relatively weak bonds and relatively strong bonds and then defining structural building units to be those groups of atoms interconnected by strong bonds, a large number of different structures can be reduced to a relatively small number of different structural building units. Complex oxides are in this fashion reduced to molecular materials, molecular materials in the same sense as polyoxometalates in the solid state [17, 18].

Alfred Werner discussed oxide polymers in terms of principal valency and auxiliary valency but considered the distinction of only secondary importance in this context [19]. The important distinction between strong (principal) and weak (auxiliary) metal-oxygen bonding in polymeric oxides was first recognized by Kihlborg in his analysis of the α-MoO_3 structure [20]. When all metal-oxygen bonds are taken into account, α-MoO_3 has the layer structure shown in **1**.

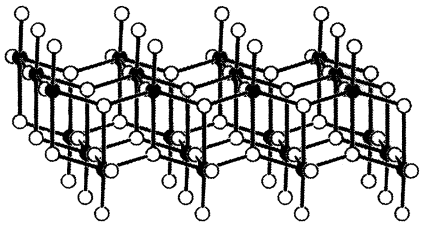

1

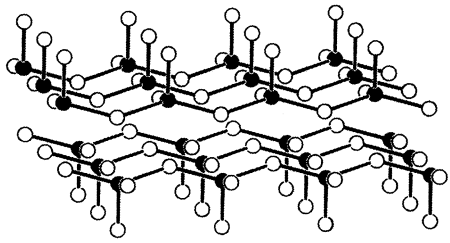

2

Kihlborg noted that molybdenum(VI) coordination geometry in α-MoO_3 is quite irregular and deviates substantially from idealized octahedral geometry, with Mo–O distances ranging from 1.67 to 2.33Å and O–Mo–O angles deviating by up to 37° from their octahedral values. By disregarding the two weak Mo–O bonds [d(Mo–O) = 2.25 and 2.33Å] and focusing on the four strong bonds [d(Mo–O) = 1.67, 1.73, and 2×1.95Å], he produced an alternative representation of the α-MoO_3 structure shown in **2**. Here, four-coordinate molybdenum(VI) centers have distorted tetrahedral geometry, and the structure is a chain structure, not a sheet structure as in **1**. This type of chain is conveniently represented by the valence structure **3**, where the short 1.67- and 1.73-Å bonds are drawn as double bonds and the longer 1.95-Å bonds are drawn as single bonds.

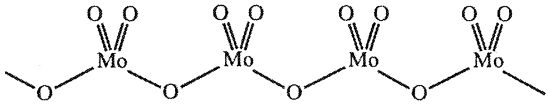

3

Since molybdenum(VI) coordination geometry in α-MoO_3 is intermediate between octahedral and tetrahedral, both of the structural representations **1** and **2** are valid, and each of them provides a useful description in its own fashion. The octahedral sheet description **1** is required, for example, to demonstrate the geometric relationship between α-MoO_3 and the V_2O_5 or TiO_2 (anatase) structures [21, 22], and the tetrahedral chain description **2** is required to appreciate the close relationship between the α-MoO_3 and the CrO_3 structures [21].

In this Chapter, Kihlborg's analysis of α-MoO_3 is extended to oxometalate coordination compounds, polyoxoanions, and lattice compounds of the early transition elements in their highest oxidation states. By disregarding relatively weak metal-oxygen interactions and focusing exclusively on strong metal-oxygen bonds, a set of structural building units is generated that reveals common features among a surprisingly wide range of different materials. The following Section provides background material and guidelines for reducing compounds to their structural building units. In the third Section, one specific family of compounds, oxomolybdenum(VI) compounds, is treated in detail, and several families of structural building units based on metal-oxygen chains, rings, and cages are described. This approach is generalized in the fourth and final Section, where structural analysis of other classes of early transition metal oxide compounds and mechanistic analysis of structural phase transitions are considered. The closing paragraphs address the central issue of structure-property relationships when structure is defined in terms of structural building units.

2. Identification of Structural Building Units

The identification of structural building units in early transition metal oxides derives from irregular metal-oxygen coordination geometry that allows for more than one plausible assignment of coordination number. This Section deals with three aspects of this irregularity: first, its physical origin; second, its manifestation in different metal-oxygen coordination polyhedra; and third, its role in defining structural building units.

2.1. STRUCTURE AND BONDING

The forces responsible for the irregular coordination geometry frequently observed in high-valent early transition metal oxo compounds are perhaps most clearly identified in Henry Taube's analysis of "yl" ions [23]. Vanadium(IV) exists in acid solution as $VO(H_2O)_5^{2+}$, that is, as a hydrated vanadyl ion. Taube addressed the specific question of why V(IV) adopts an unsymmetrical structure with one O^{2-} ligand and five H_2O ligands as opposed to a more symmetrical structure involving two OH^- ligands and four H_2O ligands. More generally, he

considered the relative stability of the isomeric $HOM^{z+}OH$ (**4**) and $H_2OM^{z+}O$ (**5**) ions:

4

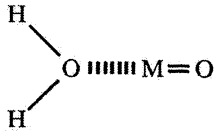

5

Taube rationalized the driving force behind formation of the "yl" ion in **5** in terms of the relative polarizabilities of O^{2-}, OH^-, and H_2O ligands and the polarizing power of various M^{z+} ions, noting that the polarizability of O^{2-} decreases enormously with addition of the first proton but much less with addition of the second. As a result, an electrophilic metal center is able to acquire more electron density in **5** than in **4**. When invoking these concepts, Taube emphasized that polarizability and polarizing power involve not only classical charge/radius concepts, but also the $p\pi$ donor capabilities of oxo ligands and the $d\pi$ acceptor capabilities of certain high-valent early transition metal cations, concepts invoked by Ballhausen and Gray in their early computational study of the vanadyl ion [24]. Polarizability and orbital energy arguments provide classical and quantum mechanical descriptions of the same physical phenomenon: strong with metal-oxygen d-p π bonding interactions arise in high valent early transition metal oxo compounds when the metal cation is strongly polarizing (relatively low-lying empty d orbitals) and the oxygen ligand is easily polarized (relatively high-lying occupied p orbitals). Reducing the argument to its simplest terms, multiple bonding to an oxo ligand plus weak bonding to an aquo ligand as in **5** is energetically favorable relative to formally single bond formation to a pair of hydroxyl ligands as in **4** when conditions for metal-oxygen d-p π bonding interactions are favorable.

The factors responsible for irregular coordination geometry in solid oxides of the high-valent early transition metals have been discussed extensively in terms of off-center displacement [25, 26]. Typically, a six-coordinate metal center is surrounded by a fairly regular octahedral array of close-packed oxygen atoms. Instead of occupying the center of this octahedron, however, the metal is displaced away from the center, usually toward an octahedral edge, vertex, or face, and hence away from the opposite edge, vertex, or face, such that relatively short metal-oxygen bonds are *trans* to relatively long metal-oxygen bonds. Qualitatively, Megaw explained that off-center displacement occurs when metal-oxygen bonds are stressed, that is, metal-oxygen distances obtained when the metal occupies the center of the octahedron are greater than the distance associated with the minimum of the metal-oxygen potential energy curve and oxygen-oxygen repulsions inhibit relief of this stress through contraction of the coordination polyhedron. Since d-p π bonding is short-range relative to d-p σ bonding, the factors favoring "yl" ion formation also favor off-center displacement. In this case, close

packing of oxygen atoms is not a precondition, and when the metal center is not coordinatively saturated, relatively short metal-oxygen bonds are not necessarily *trans* to relatively long metal-oxygen bonds. These qualitative arguments are reproduced by semi-quantitative molecular orbital and band structure calculations [27].

The structural analogy between off-center displacement in lattice compounds and irregular coordination polyhedra in oxo complexes was recognized by Orgel [28], who also recognized their common origin, metal-oxygen π bonding. Donohue [29] independently noted the geometric regularity of the close-packed oxygen octahedron surrounding Mo(VI) in coordination compounds where the bond distances and angles at molybdenum are quite irregular, implicitly forming another connection between off-center displacement and "yl" ion formation. Off-center displacement in solid oxides differs from "yl" ion formation in mononuclear complexes, however, in that the latter is a localized phenomenon and the former is usually delocalized in the form of bond length alternation. Consider, for example, the classic example of tetragonal $BaTiO_3$ [30], where octahedrally-coordinated titanium(IV) centers are linked by bridging oxygen atoms such that idealized octahedral coordination would generate symmetric, approximately linear chains of the type shown in **6**. Chains of this type are observed in cubic $BaTiO_3$, but off-center displacement toward an octahedral vertex is observed in tetragonal $BaTiO_3$, yielding unsymmetric chains of the type shown in **7**.

6

7

8

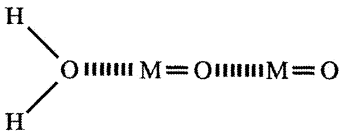

This displacement must be cooperative if the same type of metal-oxygen bonding is to be maintained throughout the chain, and as a result, these chains are polar. The close relationship between "yl" ion formation (**5**) and cooperative off-center displacement (**7**) is depicted in **8**, the hypothetical case of water coordination at the end of a polytitanyl chain. Note also that collective effects are not restricted to linear systems, but can in principal occur in cyclic systems as well:

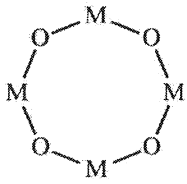

9

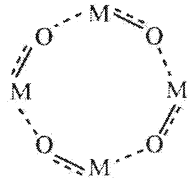

10

2.2. COORDINATION GEOMETRY

Molybdenum(VI) is a representative early transition metal π acceptor, and the coordination geometries usually adopted by six-coordinate Mo(VI) centers bonded only to oxygen atoms are shown in Scheme I by valence structures labeled Type I [31, 32], Type II [31, 32], and Type III, where double lines represent Mo–O bonds shorter than 1.80Å (double bonds), dashed lines represent Mo–O bonds longer than 2.10Å (weak bonds), and single lines represent Mo–O bonds where 2.10Å $\geq$ d(Mo–O) $\geq$ 1.80Å (single bonds).

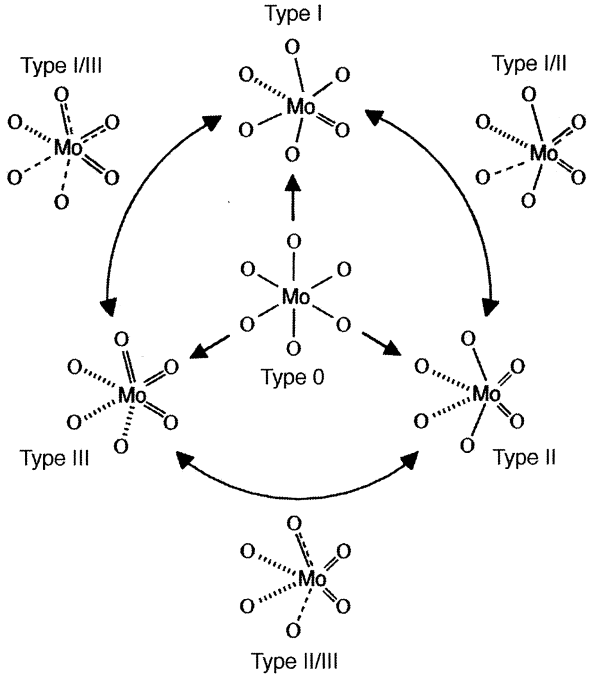

Scheme I

Type 0 coordination geometry, also shown in Scheme I, is extremely rare in oxomolybdenum(VI) compounds [33–36], where off-center displacement is al-

most invariably observed. In Scheme I, single-headed arrows represent off-center displacement toward an octahedral vertex (Type I geometry), edge (Type II geometry), or face (Type III geometry), such that one, two, or three "yl" groups are formed. The double-headed arrows drawn in Scheme I represent intermediate types of off-center displacement, namely, displacement toward the vertex of an octahedral face (Type I/III geometry), the edge of an octahedral face (Type II/III geometry), or the vertex at an octahedral edge (Type I/II geometry). In Type 0, Type I, Type II, and Type III coordination geometry, single bonds are always *trans* to single bonds, double bonds are always *trans* to weak bonds, and weak bonds are always *trans* to double bonds. When this is not the case, the longer of the two *trans* bonds is represented by a broken line and the shorter of the two is represented by a broken plus a single line, and coordination geometry is classified as Type I/II, Type II/III, or Type I/III geometry as indicated in Scheme I.

The valence structures used to represent metal-oxygen bonding in Scheme I are an extension of those employed by Schröder and Hartman [37] to describe metal-oxygen bonding in tungsten(VI) oxides. The bond length criteria are designed to be consistent with empirical bond length/bond strength correlations that associate double bonds with *ca.* 1.7 Å bond lengths and single bonds with *ca.* 1.9 Å bond lengths [38–40]. As employed here, bond strength should not be confused with bond order in the quantum mechanical sense, since Mo–O bond orders of up to three are possible [41–43]. Multiple molybdenum-oxygen bonds are collectively classified as double bonds purely for the sake of convenience, following standard usage [44].

Coordination numbers five and seven are also observed in oxomolybdenum(VI) compounds, and appropriate valence structures can be derived from the structures shown in Scheme I. Type I and Type II coordination geometry at five-coordinate centers is represented by valence structures **11** and **12**, respectively, where double lines are drawn when d(Mo–O) < 1.80Å (double bonds), dashed lines when d(Mo–O) > 2.05Å (weak bonds), and single lines when 2.05 Å ≥ d(Mo–O) ≥ 1.80Å (single bonds).

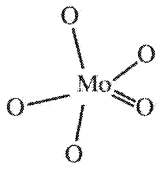

11

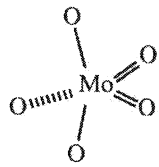

12

Valence structure **13** is often appropriate for representing bonding at seven-coordinate centers, where single, double, and weak bonds are assigned using the same bond length criteria described above for six-coordinate species.

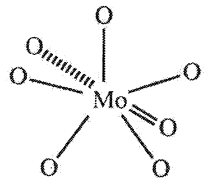

13

2.3. REDUCTION TO STRUCTURAL BUILDING UNITS

Wells has pointed out that there is no dividing line between complex oxides, oxo molecules and ions, and polyoxometalates [30], and these compounds are treated here as a single class of compounds. For example, all compounds containing at least one molybdenum(VI) center bonded exclusively to oxygen atoms are collectively called oxomolybdenum(VI) compounds. Structural building units are groups of metal and oxygen atoms interconnected by strong metal-oxygen bonds, and in oxomolybdenum(VI) compounds, strong bonds are single and double bonds as defined in Section 2.1. In this Section, the process of reducing compounds to their structural building units is illustrated by analyzing three oxomolybdenum(VI) compounds in detail.

The sodium phosphomolybdate hydrates, $Na_6Mo_5P_2O_{23}(H_2O)_n$, $n = 13$ [45] and $n = 14$ [46], both contain the $P_2Mo_5O_{23}^{6-}$ anion shown in **14**. All five molybdenum centers have Type II coordination geometry, where double bonds [d(Mo–O) = 1.69 to 1.73 Å] are *trans* to weak bonds [d(Mo–O) = 2.17 to 2.40 Å] and single bonds [d(Mo–O) = 1.89 to 1.95 Å], are *trans* to single bonds as indicated in Scheme I.

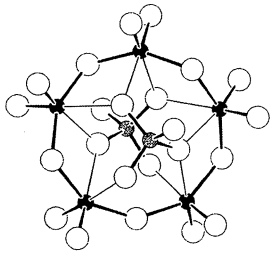

14

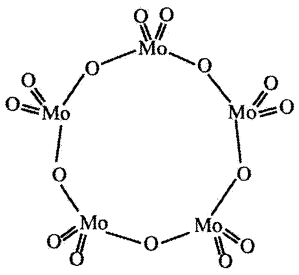

15

In **14**, weak Mo–O bonds are drawn as thin lines and strong Mo–O bonds, that is, single and double bonds, are drawn as thick bonds. Five molybdenum atoms and a total of fifteen oxygen atoms are interconnected by strong bonds, and these twenty atoms constitute an Mo_5O_{15} structural building unit. This cyclic species has the valence structure **15** and the $P_2Mo_5O_{23}^{6-}$ anion can be assigned the structural formula $[(PO_4^{3-})_2(Mo_5O_{15})]$, where the overall charge has been partitioned according to formal oxidation states.

The calcium uranium molybdate $CaUMo_4O_{16}$ [47] contains Ca^{2+} and UO_2^{2+} cations that serve as counterions for $Mo_4O_{14}^{4-}$ sheets. All of the Mo(VI) centers have Type II octahedral coordination geometry (see Scheme I), and the sheet is formed from $Mo_2O_7^{2-}$ building units as shown in **16**, where thin lines represent weak bonds and thick lines represent strong bonds.

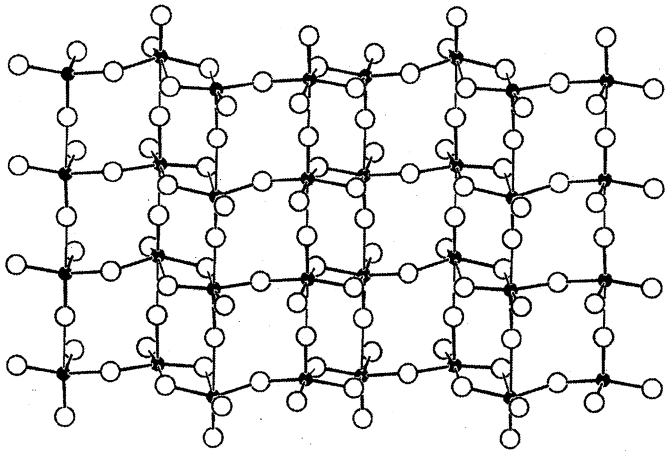

16

The metal-oxygen framework shown in **16** is derived from the α-MoO_3 structure **1** by systematic removal of MoO_2^{+} groups such that $Mo_3O_9 = Mo_2O_7^{2-} + MoO_2^{+}$. In terms of structural building units, the $Mo_4O_{14}^{4-}$ sheets in $CaUMo_4O_{16}$ are $(Mo_2O_7^{2-})_\infty$ polymers.

When reducing an oxomolybdenum(VI) compound to its structural building units, molybdenum(VI) and oxygen centers are treated as closed shell Mo^{6+} and O^{2-} ions, and charge balance is maintained by treating the remaining atoms or groups of atoms as cations for purposes of electron bookkeeping. In main group chemistry, this process is well-precedented: silicate esters such as tetraethylorthosilicate $Si(OC_2H_5)_4$ and silicate salts such as tetrasodiumorthosilicate Na_4SiO_4 are both identified as derivatives of the orthosilicate ion SiO_4^{4-}. In general, this formalism removes the distinction between oxides, alkoxides, esters, oxoanions, coordination complexes, and polyoxoanions. Consider, for example, $\{[Mg_2Mo_8O_{22}(MeO)_6(MeOH)_4]^{2-}[Mg(MeOH)_6]^{2+}\}\cdot 6MeOH$, Me = CH_3 [48]. This compound is a solvated magnesium salt of the

$[Mg_2Mo_8O_{22}(MeO)_6(MeOH)_4]^{2-}$ aggregate shown in **17**. Of the eight molybdenum atoms, four are Mo(V) centers forming the two $Mo_2O_4^{2+}$ groups shown at the top and bottom of **17**, and the remaining four are Mo(VI) centers.

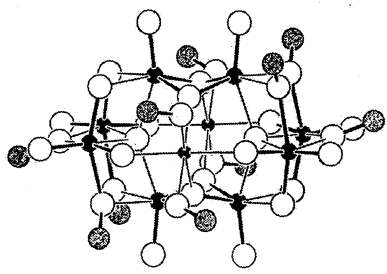

17

In **17**, strong and weak bonds at the four Mo(VI) centers are drawn with thick and thin lines, respectively, and examination of bond lengths indicates Type II coordination geometry at all of the Mo(VI) centers. Reduction of this structure to its oxomolybdenum(VI) building units therefore yields four MoO_4^{2-} units. Since none of the atoms in one unit are bonded to atoms in any other unit, the MoO_4^{2-} units are monomers. Note carbon and magnesium centers are treated in an equivalent fashion when reducing the $[Mg_2Mo_8O_{22}(MeO)_6(MeOH)_4]^{2-}$ aggregate to its structural building units. For purposes of electron bookkeeping, the formal charges assigned to CH_3^+ and $Mg(MeOH)_2^{2+}$ groups bonded to MoO_4^{2-} building units serve to emphasize their common role as counterions required to maintain charge balance; they play the same role as ethyl "cations" in tetraethyl orthosilicate and sodium "cations" in tetrasodium orthosilicate. By ignoring the distinction between covalent and ionic interactions, structural building units may be defined without relying on any preconceived notions regarding the nature of the counterion-oxygen bond.

3. Structural Building Units in Oxomolybdenum(VI) Compounds

When a large number of different oxomolybdenum(VI) compounds are reduced to their structural building units, several different families of building units emerge. In some building units, each of the molybdenum atoms is connected to two oxygen atoms by double bonds, forming an MoO_2 dioxomolybdenum group. In others, molybdenum atoms are doubly-bonded to one or three oxygen atoms, forming MoO monoxomolybdenum or MoO_3 trioxomolybdenum groups, respectively. Families of structural building units containing dioxomolybdenum groups are discussed first, followed by treatment of structural building units containing monoxomolybenum and/or trioxomolybdenum groups.

Bonding at four-coordinate molybdenum(VI) centers was not discussed in Section 2 because four-coordinate molybdenum(VI) centers generally have regular, undistorted, tetrahedral coordination geometry. Since tetrahedral molybdenum(VI) centers are often found in compounds containing Type II octahedral

molybdenum(VI) centers, they are treated in this Section for purposes of convenience. Molybdenum-oxygen bonds at tetrahedral molybdenum(VI) centers are treated as strong bonds when they are shorter than 2.10 Å.

Unless specified otherwise, structural drawings in this Section follow the same conventions adopted in **14**, **16**, and **17**: molybdenum atoms are represented by small, filled spheres and oxygen atoms are represented by large, open spheres; weak molybdenum(VI)-oxygen bonds are represented by thin lines and strong molybdenum(VI)-oxygen bonds are represented by thick lines. In order to avoid excessive length, the number of examples treated in this Section is very limited. Several excellent reviews are available that provide far more comprehensive coverage [49–51].

3.1. DIOXOMOLYBDENUM CHAIN BUILDING UNITS

The α-MoO_3 structure [20, 52–54] occupies a central position in oxomolybdenum(VI) chemistry since its $Mo_\infty O_{3\infty}$ structural building units **3** are end members of a large family of $Mo_nO_{3n+1}^{2-}$ chain building units. The manner in which $Mo_\infty O_{3\infty}$ chains are linked together in α-MoO_3 is of prime importance, since several other $Mo_nO_{3n+1}^{2-}$ chain building units are linked in a similar fashion. Two types of weak Mo–O bonds link $Mo_\infty O_{3\infty}$ chains in α-MoO_3. One type involves coordination of singly-bonded, bridging oxygen atoms from one chain to molybdenum centers in an adjacent chain such that $(Mo_\infty O_{3\infty})_2$ double chains **18** are formed. The other type involves coordination of doubly-bonded terminal oxygen atoms in one chain to molybdenum atoms in an adjacent chain as in **19** such that $(Mo_\infty O_{3\infty})_\infty$ sheet polymers **19** are formed. The α-MoO_3 structure **20** is generated either by polymerizing $(Mo_\infty O_{3\infty})_2$ double chains **21** or by dimerizing $(Mo_\infty O_{3\infty})_\infty$ sheets **22**.

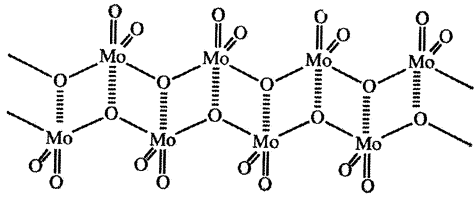

18

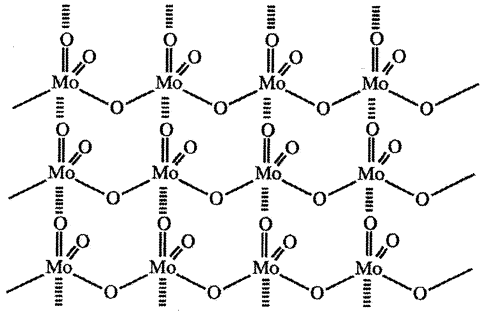

19

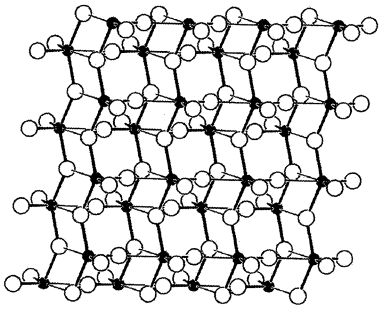

20

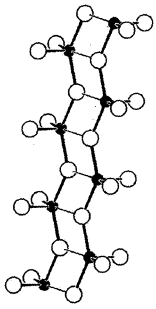

21

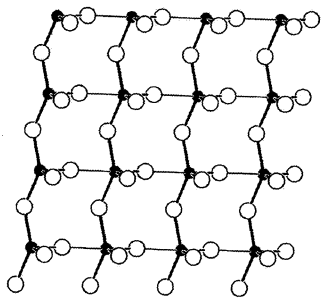

22

The remainder of this Section deals with structures containing $Mo_nO_{3n+1}^{2-}$ chain building units, and discussion will proceed in order of increasing chain length, beginning with the $n = 1$ case, MoO_4^{2-}. Unless specified otherwise, all five- and six-coordinate molybdenum(VI) centers treated in this Section have Type II coordination geometry as defined in Section 2.2.

3.1.1. *Orthomolybdate Building Units*

A vast number of oxomolybdenum(VI) compounds contain monomeric orthomolybdate structural building units. These MoO_4^{2-} groups frequently aggregate by formation of weak Mo–O bonds between oxygen atoms in one MoO_4^{2-} unit and molybdenum atoms in another MoO_4^{2-} unit. Structures containing MoO_4^{2-} structural building units can therefore be treated systematically according to their degree of aggregation.

Monomeric MoO_4^{2-} Units. Many oxomolybdenum(VI) structures contain isolated MoO_4^{2-} units where four-coordinate, approximately tetrahedral molybdenum(VI) centers do not form weak bonds to any additional oxygen atoms. In some cases, all four MoO_4^{2-} oxygen atoms are essentially equivalent, as in the hydrated potassium 18-crown-6 salt, $(C_{12}H_{24}O_6)_2K_2MoO_4 \cdot 5H_2O$ [55], where Mo–O distances range between 1.75 and 1.77 Å. In other cases, one or more MoO_4^{2-} oxygen may interact with counterions. In $[(C_6H_5)_3Si]MoO_4[(n\text{-}C_4H_9)_4N]$ [56], one long bond, d(Mo–O) = 1.88 Å, and three short bonds, d(Mo–O) = 1.70, 1.69, and 1.71 Å, bonds are observed. The $\{(\kappa^2 O\text{-}MoO_4)_3(\kappa^3 O\text{-}MoO_4)_2[Mo(NNC_6H_5)_2]_3\}^{4-}$ anion [57, 58] shown

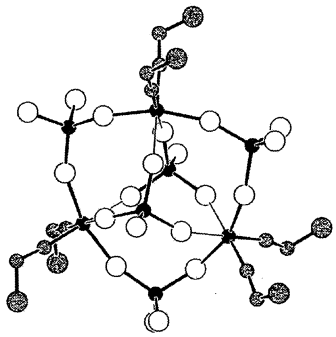

23

in **23** illustrates cases where isolated MoO_4^{2-} ions interact with two or three $[Mo(NNC_6H_5)_2]^{2+}$ counterions.

Type II octahedral coordination geometry is observed in the 1,3-diphenylpropanedianoto complex $MoO_2(PhCOCHCOPH)_2$ **24** [60] and its ethylene glycolate analogue, $MoO_2(OCH_2CH_2OH)_2$ [59]. Type II octahedral coordination is observed in these compounds, but in other cases such as **25**, the trimetaphosphate complex $[(P_3O_9)MoO_2(OCH_2CH_3)]^{2-}$ [61], the coordination geometry is less symmetric. Here, double bonds to the two terminal oxygen atoms [d(Mo–O) = 1.68 and 1.69 Å] are both *trans* to weak Mo–O bonds [d(Mo–O) = 2.20 and 2.25 Å], but the single bond to the alkoxide oxygen [d(Mo–O) = 1.88 Å] is *trans* to a weak Mo–O bond [d(Mo–O) = 2.11 Å]. The coordination geometry is therefore Type II/III as defined in Section 2.2. For purposes of comparison with **24**, the Type II/III coordination may be idealized to Type II geometry by treating the 2.11-Å bond as a long single bond, and from this point of view, the structural building unit in **25** is a distorted MoO_4^{2-} dioxomolybdenum building unit. If the 1.88-Å bond to the alkoxide ligand is treated as a long double bond, the structural building unit is a distorted MoO_3 trioxomolybdenum building unit. This alternative description is useful for comparing **25** with related compounds containing trioxomolybdenum building unit (see Section 3.7).

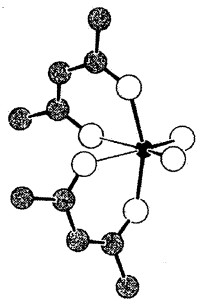

24

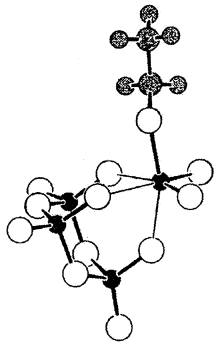

25

MoO_4^{2-} Dimers. Orthomolybdate units sometimes dimerize as in **26**, where both molybdenum centers are five-coordinate. This $(MoO_4^{2-})_2$ group is a segment of the $(Mo_\infty O_{3\infty})_2$ double chain **18**. The orthomolybdate dimers **27** and **28** are observed in $Bi_2(MoO_4)_3$ [62, 63] and $[(\mu^5\text{-}C_5H_4CH_3)_2Mo]_2(MoO_4)_2$ [64, 65], respectively. The same dimer is observed in the 2,2-dimethylpropanediolate complex $\{[CH_2C(CH_3)_2CH_2](MoO_4)(H_2O)\}_2$ **29** [66], where molybdenum centers are six-coordinate.

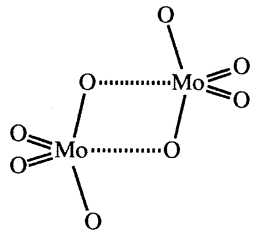

26

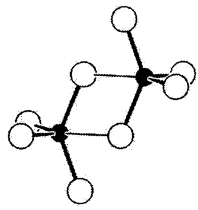

27

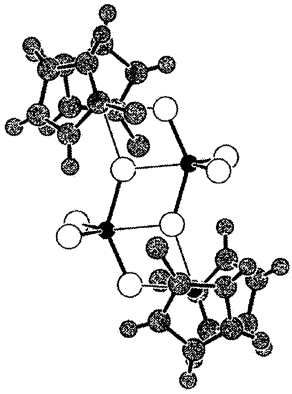

28

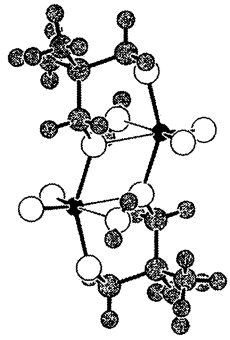

29

MoO_4^{2-} Tetramers. Two dimers **26** are combined to form a tetramer in the $[(\mu^5\text{-}C_5Me_5)Rh]_4(MoO_4)_4$ molecule **30** [67].

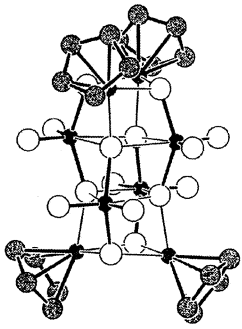

30

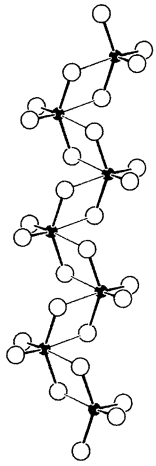

31

MoO_4^{2-} Polymers. Dimers **26** may also polymerize, forming the polymers **31** observed in $HgMoO_4$ [68] and $AgIn(MoO_4)_2$ [69]. This $(MoO_4^{2-})_\infty$ chain polymer utilizes singly-bonded oxygen atoms to form weak bonds between MoO_4^{2-} structural building units **26**. Doubly-bonded oxygen atoms may also be utilized to link MoO_4^{2-} building units as in the sheet polymer **32**. In Bi_2MoO_6, these $(MoO_4^{2-})_\infty$ sheets are separated by $(BiO^+)_\infty$ sheets that serve as countercations [70, 71]; similar orthomolybdate sheets are observed in the Sb_2MoO_6 structure [72], where the $(MoO_4^{2-})_\infty$ sheets are far more puckered than in Bi_2MoO_6.

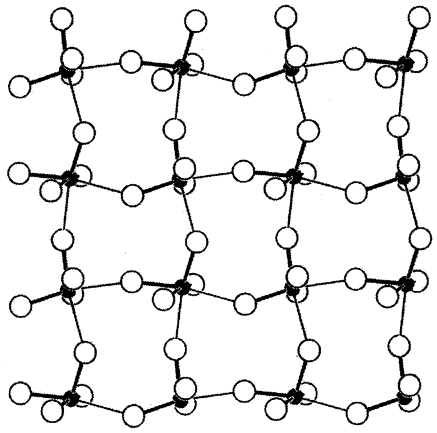

32

3.1.2. *Dimolybdate Chain Building Units*

Dimolybdate chain building units offer more possibilities for oligomerization than orthomolybdate units, and some of these possibilities are shown in **33-37**. In valence structure **34**, dimolybdate units are joined in the same fashion observed for MoO_4^{2-} units in **26**, and linkages **36** and **37** resemble those formed between $Mo_\infty O_{3\infty}$ chains in **18** and **19**, respectively.

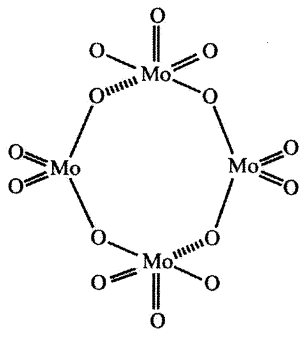

33

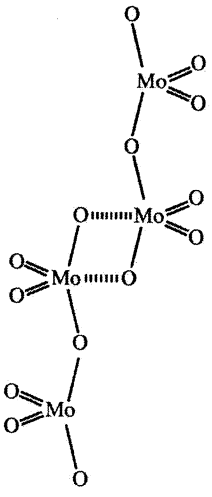

34

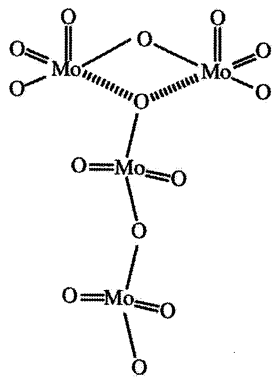

35

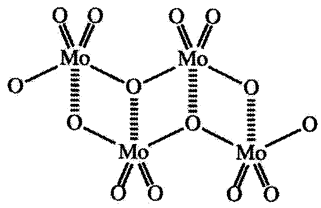

36

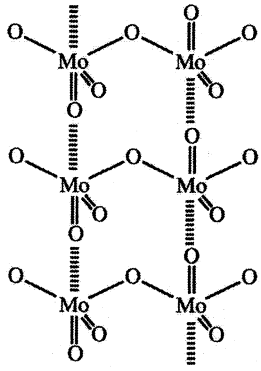

37

Monomeric $Mo_2O_7^{2-}$ units. Several compounds contain $Mo_2O_7^{2-}$ groups where both molybdenum centers are four-coordinate, including $[(n\text{-}C_4H_9)_4N]_2Mo_2O_7$ [73, 74], $MgMo_2O_7$ [75], $Ce_6(MoO_4)_8(Mo_2O_7)$ [76, 77], $K_2Mo_2O_7 \cdot KBr$ [78], and $(C_{58}H_{51}O_2MoP_4Pt)_2(Mo_2O_7) \cdot CH_2Cl_2$ [79]. The conformation shown in **38** is adopted by the tetra-*n*-butylammonium salt in the solid state [73]. In other cases, additional oxygen atoms are weakly bonded to the molybdenum centers in $Mo_2O_7^{2-}$ building units such that Type II coordination geometry is obtained as in the 3,5-*tert*-butylcatecholate complex $Mo_2O_5(3,5\text{-}DBCat)_2^{2-}$ **39** [80] as well as analogous catecholate [81–86], manitolate [87, 88], erythritolate [89], lyxose [90], and tetrahydroxytetramethylfuranose [91] complexes; the oxalate complex $\{[MoO_2(C_2O_4)(H_2O)]_2O\}^{2-}$ **40** [92, 93]; and the $As_4Mo_4O_{26}^{8-}$ arsenomolybdate **41** [94]. The $(RhCp^*)_4Mo_6O_{22}$ molecule [95] contains two monomeric dimolybdate building units and two monomeric MoO_4^{2-} building units that are interconnected by weak Mo–O bonds as shown in **42**.

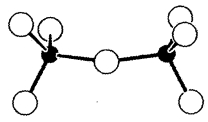

38

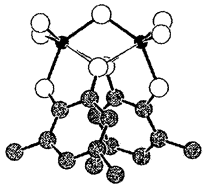

39

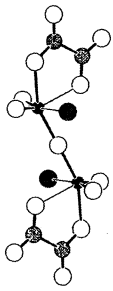

40

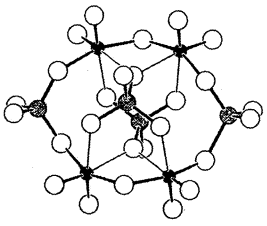

41

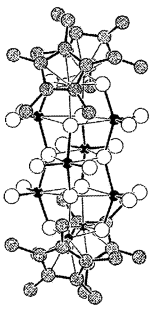

42

$Mo_2O_7^{2-}$ Dimers. Linkage of two $Mo_2O_7^{2-}$ units by weak bonds according to **33** is observed in the $Mo_4O_{10}(OCH_3)_6^{2-}$ anion **43** [96, 97], where two oxygen atoms in each $Mo_2O_7^{2-}$ unit are methylated, and the cyclic dimer is capped above and below by CH_3O^- ligands such that Type II octahedral coordination geometry is achieved at all four molybdenum centers.

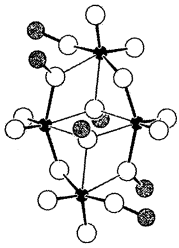

43

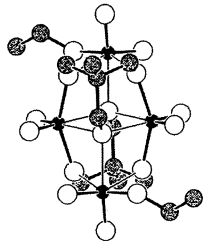

44

Two additional oxygen atoms are alkylated in the $Mo_4O_8(CH_3CH_2O)_2[CH_3C(CH_2O)_3]_2$ molecule **44** [98]. This molecule contains two MoO_4^{2-} units and two MoO_3 units, not two dimolybdate building units. The C_2H_5O–Mo bonds are 1.85 Å long, however, and as a result, two of the molybdenum centers in **44** have Type II/III geometry. Type II/III coordination geometry in **44** may be idealized to Type II geometry, and in this case, the structural building units are distorted $Mo_2O_7^{2-}$ units. Alternatively, the Type II/III molybdenum centers may be idealized to Type III geometry such that two orthomolybdate and two distorted trioxomolybdenum building units are obtained.

$Mo_2O_7^{2-}$ Tetramers. In cyclic tetramer **45**, each of four $Mo_2O_7^{2-}$ building units is linked to two nearest neighbors by weak bonds as in **34**.

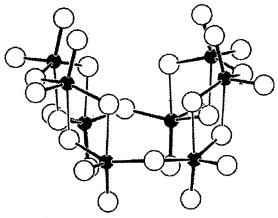

45

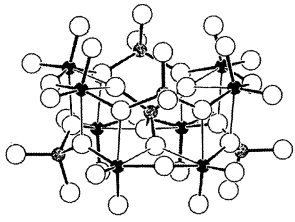

46

The $V_5Mo_8O_{40}^{7-}$ anion structure **46** is generated from **45** by connecting second-nearest neighbor $Mo_2O_7^{2-}$ units with VO_2^+ groups and placing a tetrahedral VO_4^{3-} anion at the center of the structure as shown in **46** [99]. Taking a somewhat broader perspective, the Mo(VI) and V(V) centers in **46** can be treated in an equivalent fashion since they both have low-lying, empty d orbitals well-suited for d-p π bonding with oxygen. From this point of view the vanadium atoms

are heteroatoms, and **46** contains two cyclic $V_2Mo_4O_{18}^{2-}$ building units and one orthovanadate building unit. The $V_2Mo_4O_{18}^{2-}$ rings in **46** are formed from $Mo_2O_7^{2-}$ units in **45** and VO_2^+ groups in the same fashion that $Mo_\infty O_{3\infty}$ chains are formed from $Mo_2O_7^{2-}$ units in **16** and MoO_2^{2+} groups (see Section 2.3).

$Mo_2O_7^{2-}$ Hexamers. When six $Mo_2O_7^{2-}$ building units adopt the conformation shown in **38**, they may be placed at the vertices of an octahedron and linked together by weak bonds as in **35** to form the oxomolybdenum(VI) framework of the T_h $[M(IV)Mo_{12}O_{42}]^{8-}$ structure shown in **47** where M(IV) = Ce(IV) or U(IV). Here, the tetravalent metal center is located at the center of the anion [100–106].

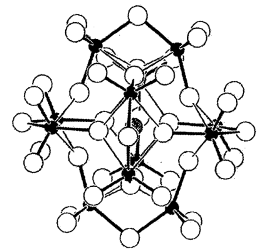

47

$Mo_2O_7^{2-}$ Chain Polymers. The $(Mo_2O_7^{2-})_\infty$ chains in *o*-$(NH_4)_2Mo_2O_7$ [107, 108], $K_2Mo_2O_7$ [109], $Ce_2(MoO_4)_2(Mo_2O_7)$ [110], and $Pr_2(MoO_4)_2(Mo_2O_7)$ [111] all have structure **48**, where both four-and six-coordinate molybdenum(VI) centers are observed. Each $Mo_2O_7^{2-}$ unit is bonded to neighboring units by weak Mo–O bonds as shown in **49** (see **33**) and **50** (see **34**). In the $K_2Mo_2O_7{\cdot}H_2O$ structure **51** [76, 112], each $Mo_2O_7^{2-}$ unit is bonded to one neighbor as in **52** (see **34**) and a second neighbor as in **53** (see **36**) such that five- and six-coordination is achieved. Linkages **34** and **53** are also utilized to join dimolybdate units in the $Ag_2Mo_2O_7$ structure [113] (see **54**). Here, each $Mo_2O_7^{2-}$ unit is linked as in **34** to *two* neighboring units to form the $(Mo_2O_7^{2-})_\infty$ single chains **55**. Double chains are formed from these single chains by linking $Mo_2O_7^{2-}$ units pairwise as shown in **56**.

48

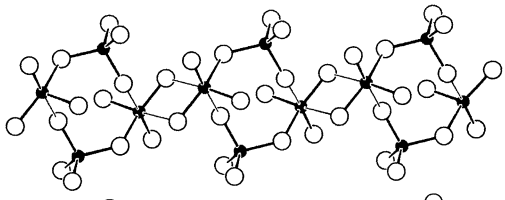

49

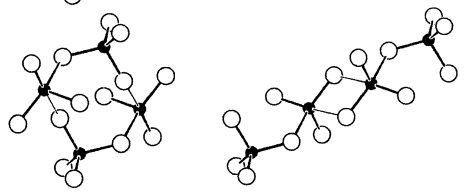

50

51

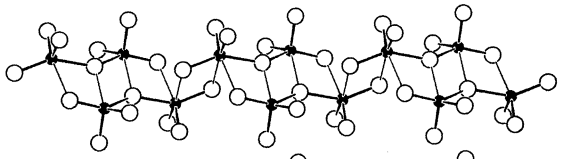

52

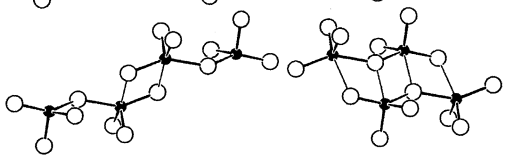

53

54

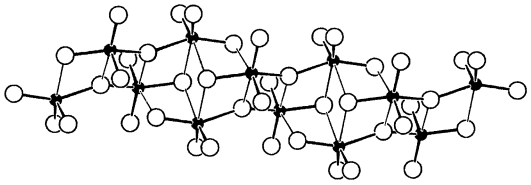

55

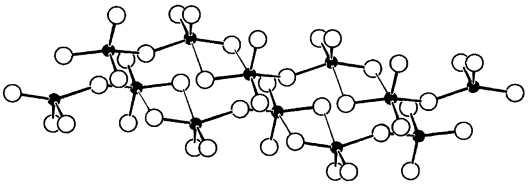

56

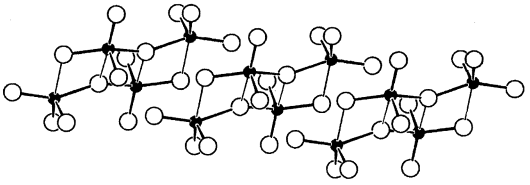

$Mo_2O_7^{2-}$ Sheet Polymers. When dimolybdate units form single chains **57** using linkage **34**, each $Mo_2O_7^{2-}$ unit can form weak bonds to dimolybdate units in two neighboring chains using its doubly-bonded oxygen atoms as in **37** to form the $Mo_2O_7^{2-}$ sheet polymer **16** discussed in Section 2.3.

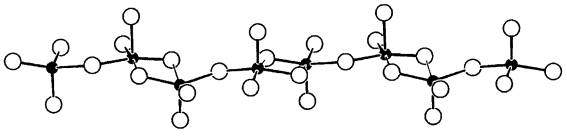

57

3.1.3. *Trimolybdate Chain Building Units*

Valence structures **58-61** illustrate several of the possibilities available for linking trimolybdate building units. Valence structures **58** and **59** involve the same linkages as **33** and **34**, respectively, but **60** and **61** involve linkages not discussed thus far. Although orthomolybdate and dimolybdate anions are known where molybdenum(VI) centers are four-coordinate, the corresponding trimolybdate is unknown.

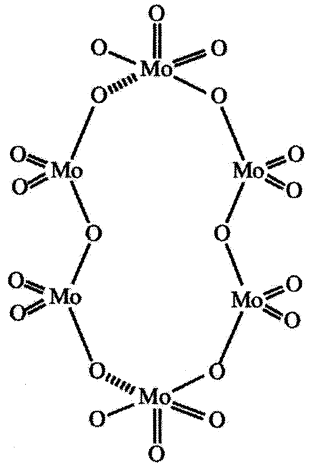

58

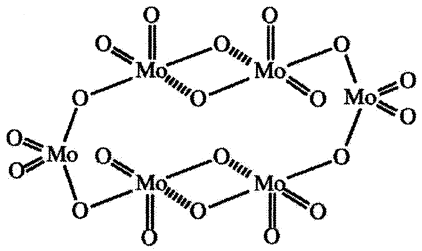

59

60

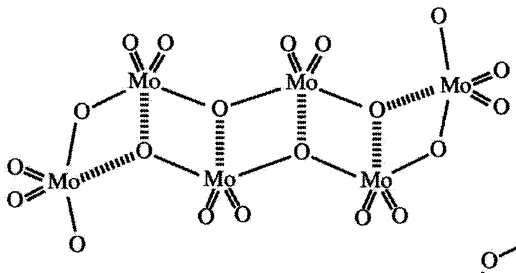

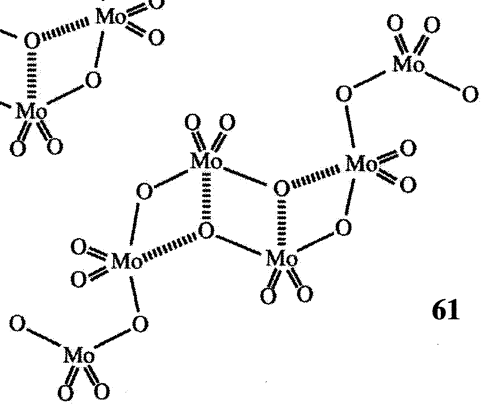

61

Monomeric $Mo_3O_{10}^{2-}$ Units. Three examples of complexes containing monomeric $Mo_3O_{10}^{2-}$ units are shown in **62-64**. In the $\{(Mo_3O_{10}^{2-})(CH_3O^-)_2[Mo(NNC_6H_5)_2^{2+}]\}^{2-}$ anion **62** [114, 58] and the pinacolate complex $\{Mo_3O_8[OC(CH_3)_2C(CH_3)_2O]_2\}^{2-}$ **63** [115], the two peripheral molybdenum centers are both five-coordinate, but in the $Sb_5Mo_5O_{36}H_{10}^{7-}$ anion **64** [116], all three molybdenum centers are six-coordinate. Note that **64** also contains two symmetry-equivalent MoO_4^{2-} building units in addition to a trimolybdate building unit.

62

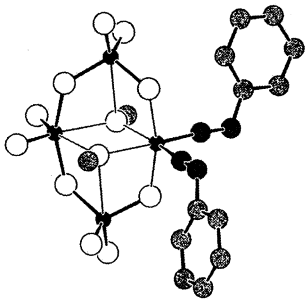

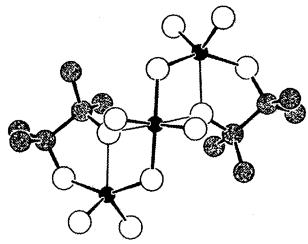

63

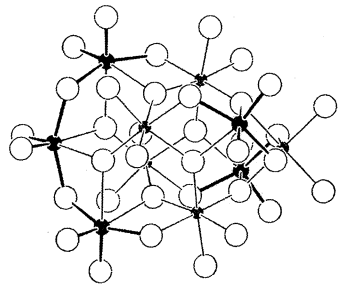

64

$Mo_3O_{10}^{2-}$ Dimers. The β-$V_2Mo_6O_{26}^{6-}$ anion **65** [117] contains two trimolybdate chain building units linked by weak Mo–O bonds as shown in valence structure **59**. If the vanadium(V) centers in the β-$V_2Mo_6O_{26}^{6-}$ anion are treated as heteroatoms, the structural formula $[(VMo_3O_{12}^-)_2(O^{2-})_2]$ is obtained.

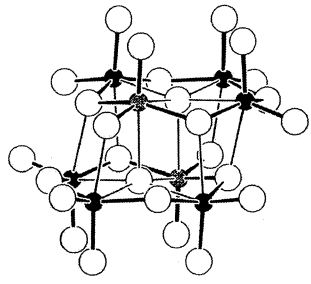

65

Two closely-related structures contain $Mo_3O_{10}^{2-}$ building units linked together by weak Mo–O bonds as in **58**. In the $Mo_8O_{28}(CH_3)_4^{4-}$ anion [118], the $Mo_3O_{10}^{2-}$ chains have the conformation shown in **66**, and the complete structure **67** is obtained by placing an MoO_4^{2-} dimer **26** in the center of **66** and dimethylating both $Mo_3O_{10}^{2-}$ units. In the $Mo_8O_{28}H_2^{6-}$ anion [119], $Mo_3O_{10}^{2-}$ chains have the conformation shown in **68**, and addition of an MoO_4^{2-} dimer **26** plus two protons yields the observed structure, **69**. The $[(Mo_3O_{10}^{2-})_2(MoO_4^{2-})_2]$ structures shown in **67** and **69** are valence isomers, that is, they have the same connectivity but different valence structures, and are designated α-$Mo_8O_{28}^{8-}$ and β-$Mo_8O_{28}^{8-}$, respectively. Further β-$Mo_8O_{28}^{8-}$ derivatives are known where the two hydroxyl groups in β-$Mo_8O_{28}H_2^{6-}$ are replaced with formate [120], methionite [121], and *N*-propylsalicylideneiminate [121] groups. In these derivatives, the oxygen atoms bonded to carbon atoms form weak, 2.11- to 2.12-Å Mo–O bond lengths, implying Type II/III coordination geometry at the two molybdenum centers in question.

66

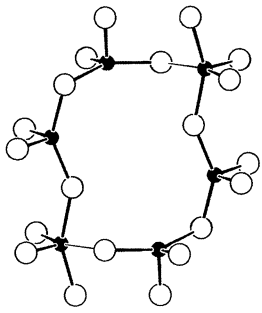

67

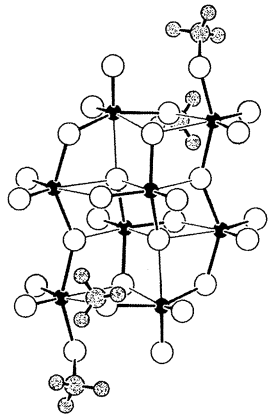

68

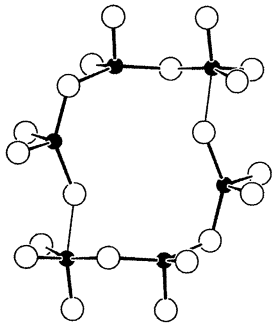

69

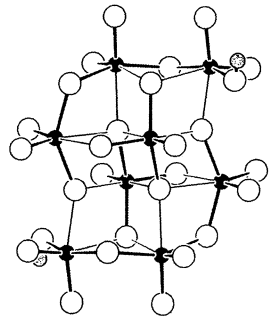

The $Cu_4Mo_6O_{20}$ structure [122] contains trimolybdate building units linked together as in **60** but it also contains Mo_6O_{18} ring building units and is therefore described in Section 3.2.3.

$Mo_3O_{10}^{2-}$ Polymers. The rubidium trimolybdate $Rb_2Mo_3O_{10}$ [123, 124] and its potassium [123, 125] and cesium [123] analogues have a common structure where $Mo_3O_{10}^{2-}$ units form chain polymers **70**. Each $Mo_3O_{10}^{2-}$ unit has the conformation adopted by the $Mo_3O_{10}^{2-}$ unit in the pinacolate complex **63** and is linked by weak Mo–O bonds to two neighboring trimolybdate units as in **61**.

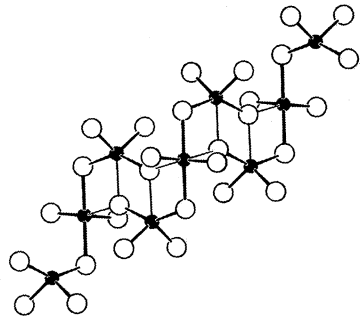

70

3.1.4. *Tetramolybdate Chain Building Units*

In the family of structures based on $Mo_4O_{13}^{2-}$ building units, a large number of different $Mo_4O_{13}^{2-}$ linkage are observed, and a summary listing such as those provided above for di- and trimolybdates is not offered in this Section. Instead, only selected linkage modes are represented as valence structures, and these are incorporated in the text when relevant.

Monomeric $Mo_4O_{13}^{2-}$ Units. The so-called dimolybdomalate complex $[Mo_4O_{11}(C_4H_3O_5)_2]^{4-}$ **71** [126–128] contains two triply-deprotonated malic acid ligands ($^-O_2CCH_2CH(O^-)CO_2^-$).The two alkoxide oxygen atoms form single bonds to the two terminal molybdenum atoms in the $Mo_4O_{13}^{2-}$ chain, and six of the total of eight carboxylate oxygen atoms form weak Mo–O bonds *trans* to the eight double-bonded, terminal oxygen atoms in the chain. This structure is also observed for the analogous citrate complex where both malate methine hydrogens are replaced by uncoordinated CH_2COOH groups [129]. In the closely-related structure **72** adopted by $[Mo_4O_{11}(C_2H_2O_4)(HCO_2)]^{3-}$ [130]. One pair of geminal alkoxide oxygen atoms in a quadruply deprotonated glyoxal dihydrate ligand ($^=O_2CHCHO_2^=$) forms single bonds to the two terminal molybdenum atoms in the $Mo_4O_{13}^{2-}$ chain, and the remaining two glyoxalic oxygen atoms plus the two formate oxygen atoms form weak molybdenum-bonds to the two

central molybdenum atoms in the $Mo_4O_{13}^{2-}$ chain. In a related compound, the bridging diacetal unit is derived from 9,10-phenanthroquinone instead of glyoxal, and a hydroxyl group bridges the central molybdenum atoms instead of a formate group [131].

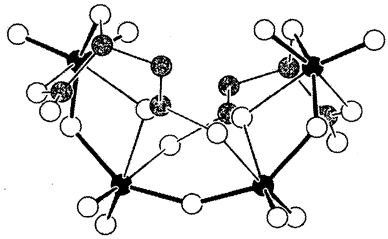

71

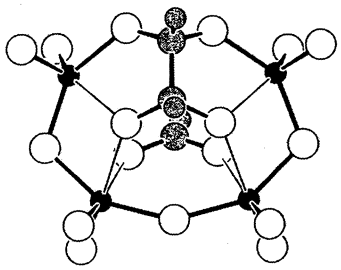

72

The isomeric $Mo_{10}O_{34}^{8-}$ ions **73** and **74** both contain two $Mo_4O_{13}^{2-}$ chains linked by weak Mo–O bonds to form a ring enclosing an MoO_4^{2-} dimer. The α-$Mo_{10}O_{34}^{8-}$ isomer **73** is known as NH_4^+ [132–134] and Tl^+ [135] salts, and the β-$Mo_{10}O_{34}^{8-}$ isomer **74** has been observed in $(CH_3NH_3^+)_8(Mo_{10}O_{34})\cdot 2H_2O$ [136]. The α- and β-$Mo_{10}O_{34}^{8-}$ structures are derived from the α- and β-$Mo_8O_{28}^{8-}$ structures **67** and **69**, respectively, by addition of MoO_3 groups.

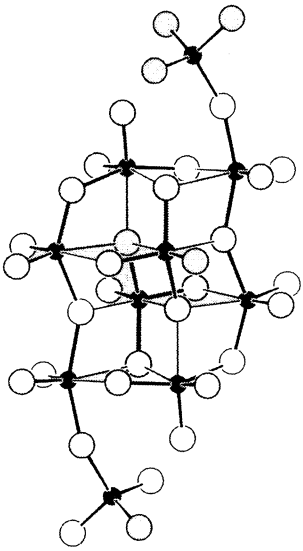

73

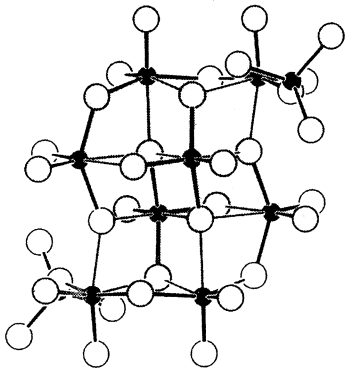

74

$Mo_4O_{13}^{2-}$ Chain Polymers. Insertion of an MoO_3 unit into each of the $Mo_3O_{13}^{2-}$ chains in **59** yields the tetramolybdate dimer **75**. Valence structure **75** illustrates one of the linkages between $Mo_4O_{13}^{2-}$ units in the $Cu_4Mo_5O_{17}$ structure [137, 138], where each dimer **75** encloses an orthomolybdate dimer. These $(Mo_4O_{13}^{2-})_2(MoO_4^{2-})_2$ assemblies are linked by weak Mo–O bonds to form the chain polymer **76**.

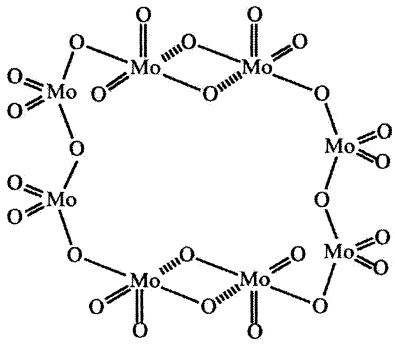

75

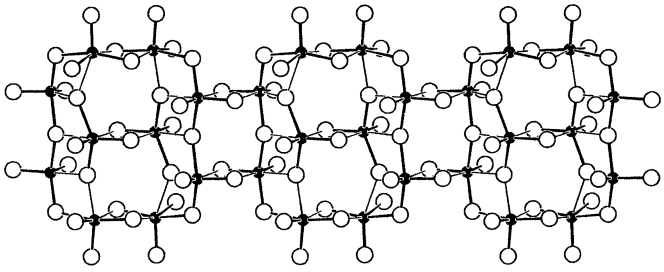

76

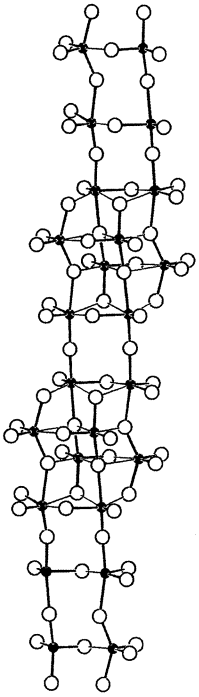

77

Terminal molybdenum atoms in each tetramolybdate chain have Type II/III coordination geometry that has been idealized to Type II geometry in **76**. Note that **73**, **74**, and **76**, all have the same composition in terms of their structural building units, namely, equal numbers of MoO_4^{2-} and $Mo_4O_{13}^{2-}$ units.

The hydrated sodium molybdate $Na_2Mo_4O_{13}{\cdot}6H_2O$ [139] is a poorly characterized compound that appears to contain the $(Mo_4O_{13}^{2-})_\infty$ double chains **77**. Structure **77** contains the same group of eight edge-sharing MoO_6 octahedra found in **67** and **69**. However, its valence structure is different, and the $Mo_8O_{28}^{8-}$ substructure in **77** is identified as δ-$Mo_8O_{28}^{8-}$ in order to distinguish it from the α- and β-$Mo_8O_{28}^{8-}$ ions.

Tetramolybdate polymers **78** observed in $K_2Mo_4O_{13}$, $Rb_2Mo_4O_{13}$, and t-$(NH_4)_2Mo_4O_{13}$ [140–142], are double chain polymers, and the constituent single chain are more readily identified in **79**, where weak bonds linking the two single chain polymers have been deleted and the two chains have been separated.

Within each single chain, $Mo_4O_{13}^{2-}$ units are linked by the weak Mo–O bonds shown in valence structure **80**. Structure **78** contains the same grouping of eight edge-sharing MoO_6 octahedra observed in **73** and several other structures discussed above, but since the octamolydate subunit in **78** has a different valence structure, it is designated ε-$Mo_8O_{28}^{6-}$.

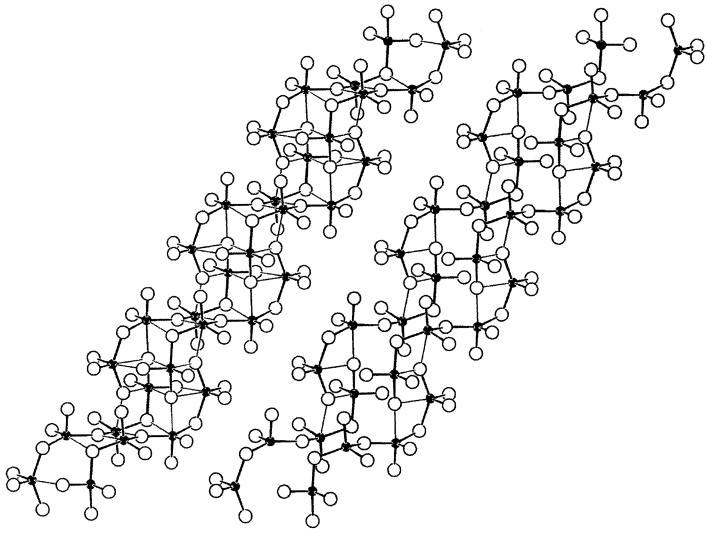

78 **79**

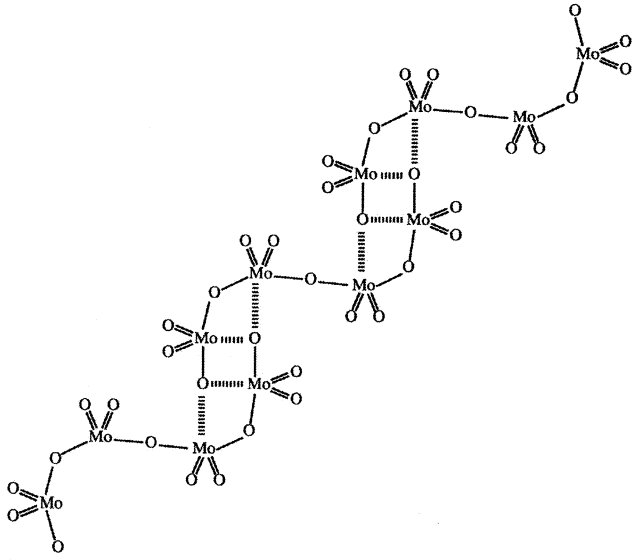

80

For purposes of comparison with tetramolybdate sheet polymers to be discussed next, it is instructive to take a second look at the $K_2Mo_4O_{13}$ structure from a different viewpoint. In **81**, the double chain structure is viewed almost parallel to the planes defined by molybdenum atoms in its constituent $(Mo_4O_{13}^{2-})_\infty$ single chains (see **79**), and these single chains are drawn separately in **82** and **83** from the same viewpoint.

81

82

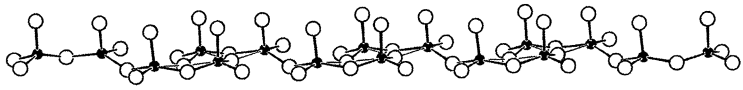

83

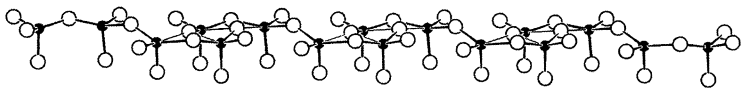

$Mo_4O_{13}^{2-}$ Sheet Polymers. The high temperature form of lithium tetramolybdate, H–$Li_2Mo_4O_{13}$ [143]; the low temperature form of lithium tetramolybdate, L–$Li_2Mo_4O_{13}$ [144]; thallium tetramolybdate, $Tl_2Mo_4O_{13}$ [145]; and *o*-$(NH_4)_2Mo_4O_{13}$ [142], all have sheet structures formed from $Mo_4O_{13}^{2-}$ structural building units. In each case, these sheets contain $(Mo_4O_{13}^{2-})_\infty$ single chain polymers where tetramolybdate units are linked together by weak Mo–O bonds as in **80**, but three different structures are observed corresponding to three different ways of linking these chains together into sheets.

The H–$Li_2Mo_4O_{13}$ sheet structure **84** is drawn from about the same viewpoint adopted in **81** for the $K_2Mo_4O_{13}$ double chain structure. Structure **84** contains the same double chains **81** found in $K_2Mo_4O_{13}$, but in H–$Li_2Mo_4O_{13}$, these double chains are linked together by tetramolybdate single chain polymers **85**. These single chain polymers have a significantly different conformation from the conformation adopted in $K_2Mo_4O_{13}$ (see **82** and **83**).

The L–$Li_2Mo_4O_{13}$ **86** resembles the H–$Li_2Mo_4O_{13}$ structure **84** in that both sheet structures contain tetramolybdate double chain polymers **81** linked by tetramolybdate single chain polymers. These single chain polymers are shown from the same viewpoint in **85** and **87**, where they are seen to have virtually identical conformations. In both structures, weak bonds are formed between molybdenum atoms in the single chains and doubly-bonded, terminal oxygen atoms in the double chains.

84

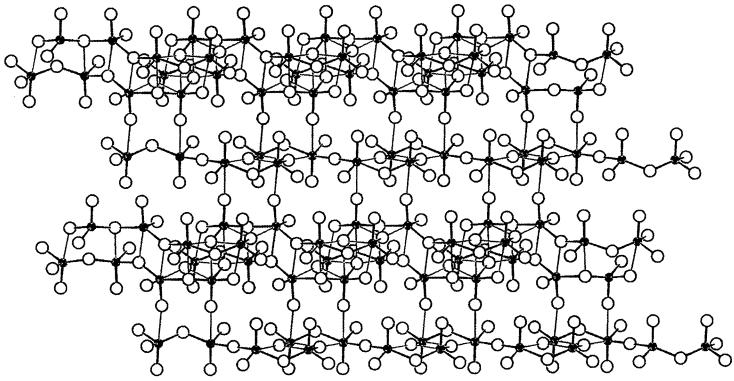

85

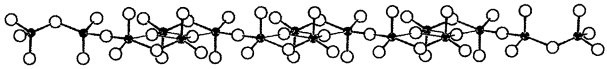

86

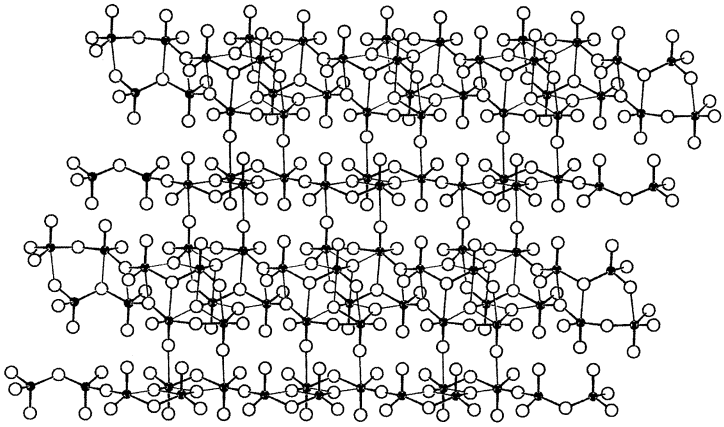

87

The differences between the H–$Li_2Mo_4O_{13}$ and L–$Li_2Mo_4O_{13}$ structures are most apparent in drawings of the two structures shown in **88** and **89**, respectively, where the double chains are drawn from the same viewpoint adopted in **78** for the $K_2Mo_4O_{13}$ structure. In these two drawings, the weak Mo–O bonds joining the single and double chains have been artificially lengthened for purposes of clarifying this difference. Structures **88** and **89** utilize different sets of doubly-bonded terminal oxygen atoms in the tetramolybdate double chains to form weak bonds with molybdenum atoms in the tetramolybdate single chains.

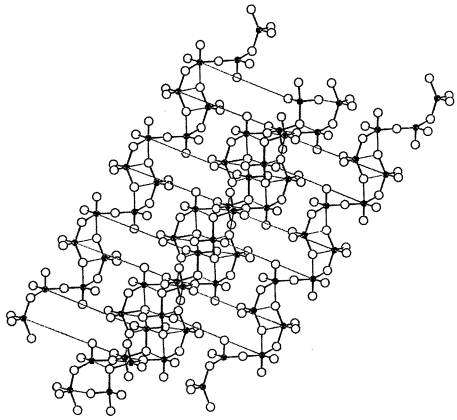

88

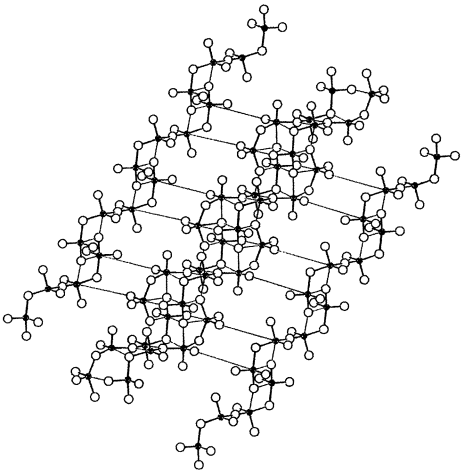

89

Referring back to structures **84** and **86**, the H–$Li_2Mo_4O_{13}$ and L–$Li_2Mo_4O_{13}$ structures may be interconverted by a shear motion within the tetramolybdate double chains where the single chains remain intact, but their relative positions are shifted. The metal-oxygen bond shifts involved may be traced by noting that the double chains in **84** are generated from the double chains in **86** when the upper single chain within each double chain is shifted to the right relative to the lower single chain in the same double chain. This mechanism will be reexamined in Section 4.3.

90

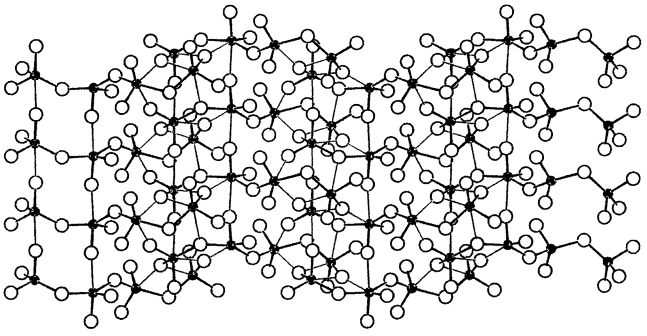

91

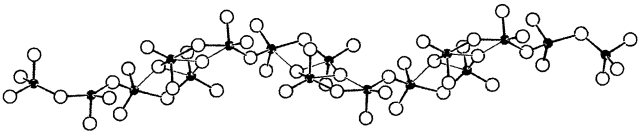

In the $Tl_2Mo_4O_{13}$ [145] and *o*-$(NH_4)_2Mo_4O_{13}$ [142] oxomolybdenum(VI) sheet structure **90**, tetramolybdate building units are once again linked as shown in valence structure **80** to form single chain polymers that have the conformation shown in **91**. This conformation is quite different from the conformations **82** and **85**, and tetramolybdate chain polymers **91** having this conformation may be stacked in an ABAB fashion to form the sheet polymer shown in **90.** Each chain polymer **91** in the sheet polymer **90** uses both its doubly-bonded, terminal oxygen atoms and its singly-bonded, bridging oxygen atoms to form weak Mo–O bonds with molybdenum atoms in neighboring chains.

3.1.5. *Penta-, Hexa-, and Heptamolybdate Chain Building Units*

Before approaching structures containing well-defined penta-, hexa-, and heptamolybdate dioxomolybdenum(VI) chain building units, the possibility of polydispersity warrants brief discussion in the context of the "pentamolybdate" $KMo_5O_{15}OH{\cdot}2H_2O$ [147] or $KMo_{5.33}[H_{4.5}]_{0.67}O_{18}$ structure [148], the $(Na{\cdot}2H_2O)Mo_{5.33}[H_{4.5}]_{0.67}O_{18}$ structure [148], and related defect structures [147–150] obtained by cation exchange. As defect structures based on hypothetical hexagonal MoO_3 structure, where countercations compensate for dioxomolybdenum vacancies, these structures appear to contain $Mo_nO_{3n+1}{}^{2-}$ chains since the hypothetical hexagonal MoO_3 structure contains infinite $Mo_\infty O_{3\infty}$ dioxomolybdenum(VI) chains as structural building units. Only statistical data is available, however, concerning chain lengths.

The $Sb_4Mo_{10}O_{50}{}^{20-}$ anion observed in crystalline $K_8(Sb_4Mo_{10}O_{40}H_{12}){\cdot}10H_2O$ [116] has the anion structure shown in **92**. The pentamolybdate chains in **92** are not interconnected by weak bonds, that is, they are monomeric. The $H_4Co_2Mo_{10}O_{38}{}^{6-}$ anion **93** in $(NH_4)_6[H_4Co_2Mo_{10}O_{38}]{\cdot}7H_2O$ [151, 101] also contains two $Mo_5O_{16}{}^{2-}$ chains, but here the two chains are interconnected by two sets of four weak bonds to form a cyclic dimer. Each set of four weak bonds forms a linkage identical to the linkage between two $Mo_4O_{13}{}^{2-}$ units in **80**.

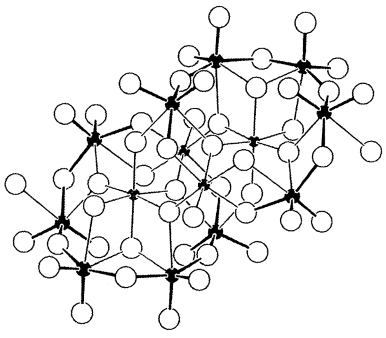

92

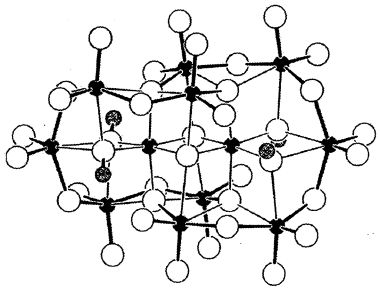

93

In $[(NH_4)_6[Mo_6O_{17}(HL)_2]\cdot 10H_2O$, L = $CH_3C(O)(PO_3)_2$ [152], the bis-diphosphonate complex $\{Mo_6O_{17}[CH_3C(O)(PO_3)_2]_2\}^{8-}$ has the structure shown in **94**. This anion contains a single $Mo_6O_{19}^{2-}$ chain building unit.

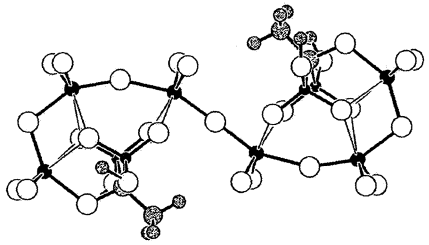

94

Both hexamolybdate chain polymers and orthomolybdate dimers are found in $(NH_4)_6Mo_8O_{27}\cdot 4H_2O$ [153, 154]. The $[(Mo_6O_{19}^{2-})_\infty(MoO_4^{2-})_{2\infty}]$ chain polymer **95** is a condensation polymer of $H_2Mo_8O_{28}^{6-}$ anions **69** obtained by condensing pairs of $Mo_3O_{10}^{2-}$ building units in the $[(Mo_3O_{10}^{2-})_2(MoO_4^{2-})_2]^{8-}$ "monomers" to form $Mo_6O_{19}^{2-}$ building units but otherwise retaining the linkages formed between structural building units in **69**.

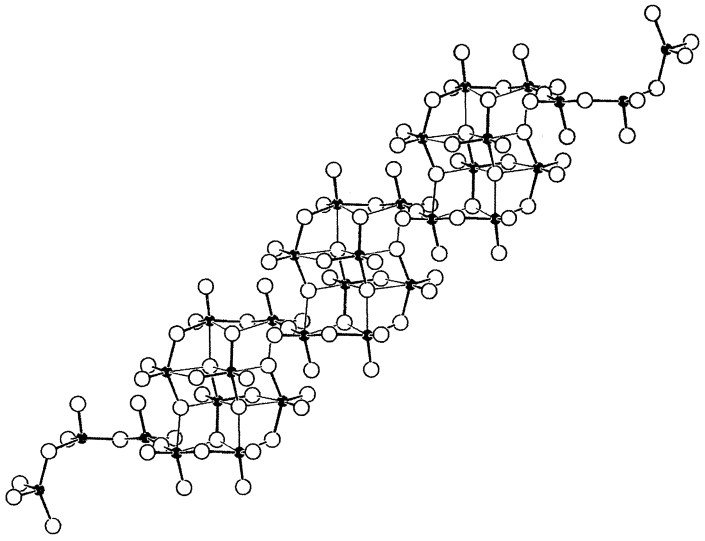

95

Pentamolybdate sheet polymers in $Cs_2Mo_5O_{16}$ [155] and heptamolybdate sheet polymers in $Cs_2Mo_7O_{22}$ [155], $Rb_2Mo_7O_{22}$ [155], and $Tl_2Mo_7O_{22}$ [156] are formed from chain polymers analogous to the $Mo_3O_{10}^{2-}$ chain polymer **70** found in $Cs_2Mo_3O_{10}$, $Rb_2Mo_3O_{10}$, and $K_2Mo_3O_{10}$. In these compounds, the $Mo_3O_{10}^{2-}$, $Mo_5O_{16}^{2-}$, and $Mo_7O_{22}^{2-}$ building units form the homologous series shown in **96**, **97** and **98**.

96

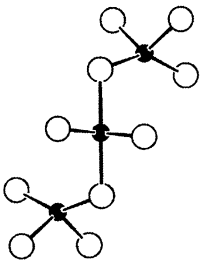

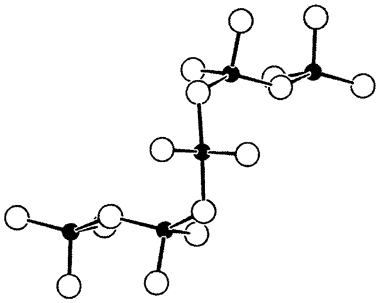

97

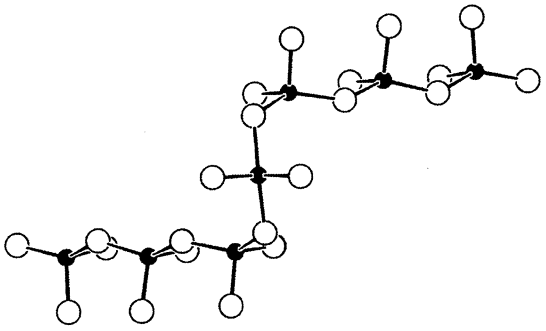

98

Pentamolybdate units **97** are linked as shown in **99** to form chain polymers **101** and heptamolybdate units **98** are linked as shown in **100** to form chain polymers **102** in precisely the same fashion that trimolybdate units **96** are linked as shown in **61** to form chain polymers **70** as described in Section 3.1.3. Note that segments of the α-MoO_3 double chain valence structure **18** are apparent in valence structures **99** and **100** and that the conformation of α-MoO_3 double chains shown in **21** is reproduced in the conformations of the corresponding double chain segments in **101** and **102**. Weak Mo–O bonds are formed between $Mo_5O_{16}^{2-}$ chain polymers **101** in $Cs_2Mo_5O_{16}$ to obtain the pentamolybdate sheet polymers **103**, and weak Mo–O bonds are formed between $Mo_7O_{22}^{2-}$ chain polymers **102** in $Cs_2Mo_7O_{22}$ to obtain heptamolybdate sheet polymers **104**.

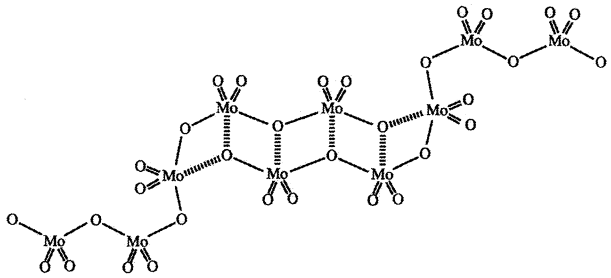

99

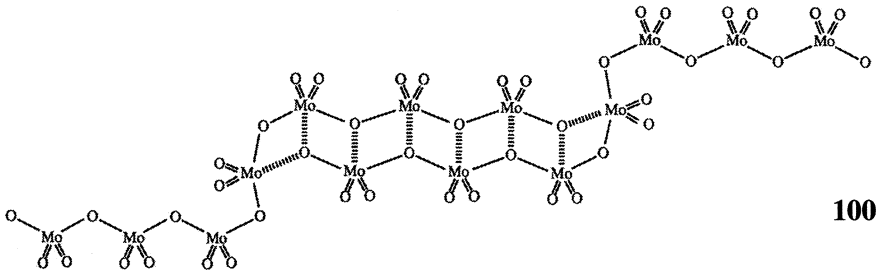

100

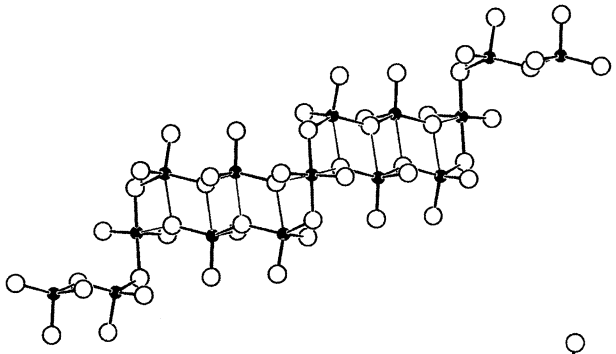

101

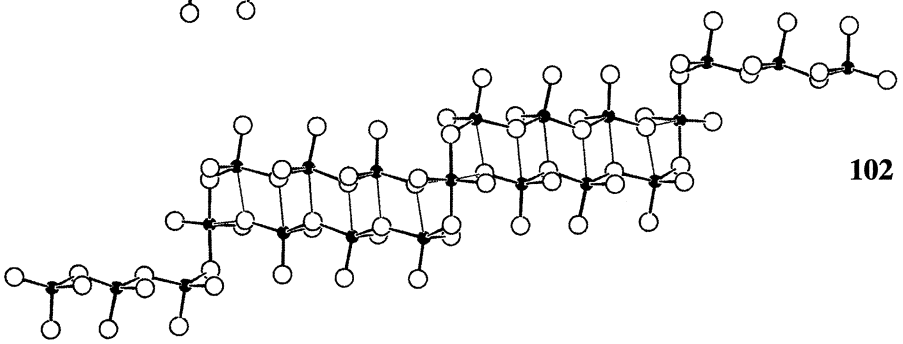

102

103

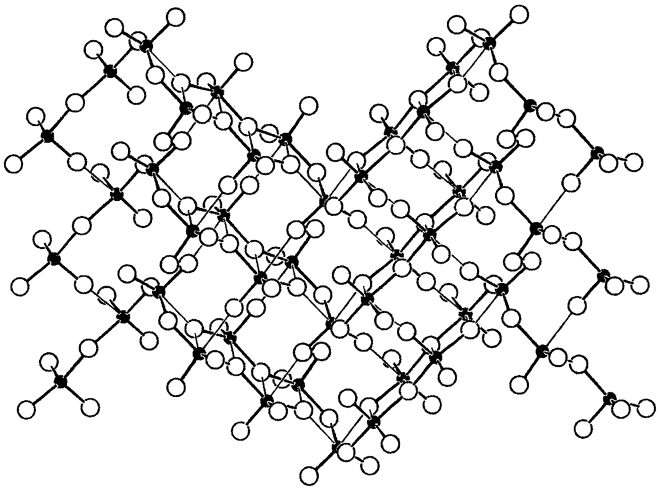

104

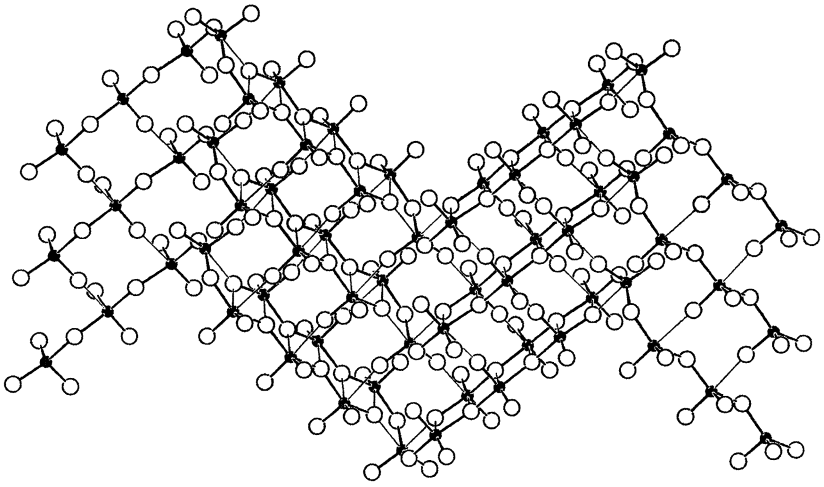

In both cases, staircase-like sheet polymers are obtained from the chain polymers by forming weak bonds between doubly-bonded oxygen atoms and molybdenum atoms in adjacent chains much in the same way that α-MoO_3 sheets **20** are obtained from double chain polymers **21**. As a result, the $Cs_2Mo_5O_{16}$ and $Cs_2Mo_7O_{22}$ structures both contain α-MoO_3 substructures evident in **103** and **104** by comparison with **21**. The α-MoO_3 structure is formally the $n = \infty$ end member of the homologous series $Cs_2Mo_{(2n+3)}O_{(6n+10)}$ generated from the $n = 1$ and 2 homologues **103** and **104**, respectively.

3.1.6. *$Mo_{\infty}O_{3\infty}$ Chain Building Units*

Structures based on $Mo_{\infty}O_{3\infty}$ chain building units **3** are discussed here in the same sequence followed above for structures based on other dioxomolybdenum chain building units. First, structures containing "monomeric" $Mo_{\infty}O_{3\infty}$ building units are treated, that is, structures where $Mo_{\infty}O_{3\infty}$ building units are not interconnected by weak Mo–O bonds. Next, structures containing $Mo_{\infty}O_{3\infty}$ "dimers" are treated, that is, structures containing $(Mo_{\infty}O_{3\infty})_2$ double chains. Finally, structures are treated that contain $Mo_{\infty}O_{3\infty}$ chains interconnected by weak bonds to form $(Mo_{\infty}O_{3\infty})_{\infty}$ infinite sheet structures.

Monomeric $Mo_{\infty}O_{3\infty}$ Units. Two different crystalline polymorphs of the dimethylsulfoxide adduct $Mo_3O_9{\cdot}4(CH_3)_2SO$ are known, α-$Mo_3O_9{\cdot}4(CH_3)_2SO$ [157] and β-$Mo_3O_9{\cdot}4(CH_3)_2SO$ [158]; the chain polymers formed in these compounds are shown in **105** and **106**, respectively.

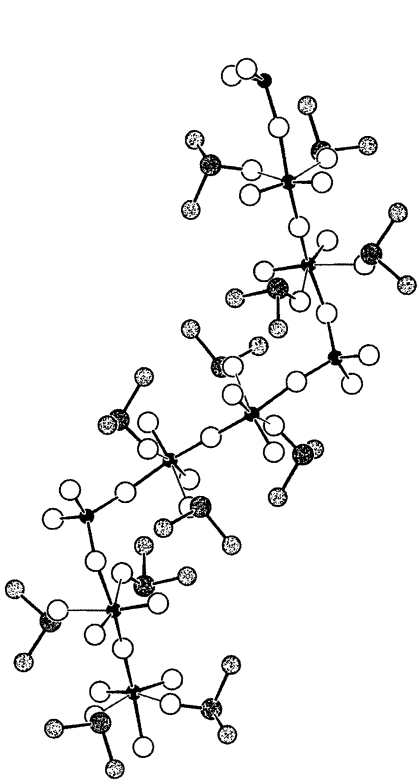

105

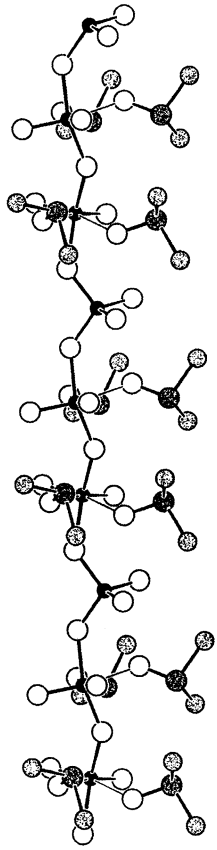

106

In both structures, every third molybdenum atom is four coordinate, but the remaining molybdenum atoms achieve six-coordination by forming weak bonds to oxygen atoms in dimethylsulfoxide ligands. The $Mo_{\infty}O_{3\infty}$ building units are not connected by weak bonds and therefore formally monomeric.

Crystalline $Na_2Mo_2O_7$ [159, 160] has the structural formula $[(Mo_{\infty}O_{3\infty})(MoO_4^{2-})_{\infty}]$. Here, each molybdenum atom in the $Mo_{\infty}O_{3\infty}$ chains forms two weak bonds to MoO_4^{2-} oxygen atoms in different orthomolybdate units as shown in **107**. In the trimolybdates $(NH_4)_2Mo_3O_{10}$ [161], $NaRbMo_3O_{10}$ [124], and $Rb_2Mo_3O_{10}{\cdot}H_2O$ [162], pairs of $Mo_{\infty}O_{3\infty}$ chains are bridged by MoO_4^{2-} units as shown in **108**. This $[(Mo_{\infty}O_{3\infty})_2(MoO_4^{2-})_{\infty}]$ structure is a substructure of the $[(Mo_{\infty}O_{3\infty})_4(MoO_4^{2-})_{2\infty}(Mo_4O_{13}^{2-})_{\infty}]$ structure adopted in $Na_6Mo_{10}O_{33}$ [163], where $Mo_{\infty}O_{3\infty}$, MoO_4^{2-}, and $Mo_4O_{13}^{2-}$ dioxomolybdenum structural building units are interconnected as shown in **109**.

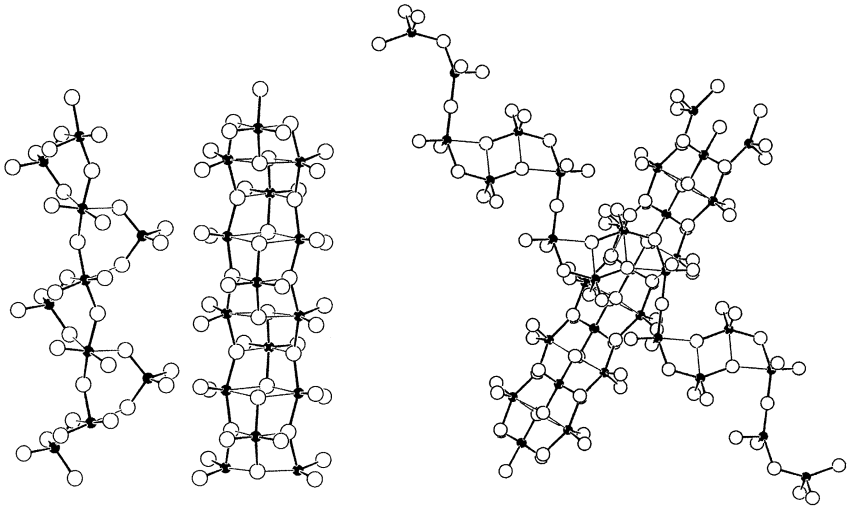

107 **108** **109**

The $Mo_4O_{13}^{2-}$ building units are linked into chains according to **80**, and these tetramolybdate chains have almost the same conformation adopted by tetramolybdate single chains in H– and L–$Li_2Mo_4O_{13}$ (see Section 3.1.5). These conformations may be compared by rotating **109** clockwise by 90° and comparing the tetramolybdate chains with the tetramolybdate single chains shown in **88**.

Each $Mo_4O_{13}^{2-}$ building unit is also linked to two MoO_4^{2-} units as shown in **110**. Note that MoO_4^{2-} building units are linked to $Mo_2O_7^{2-}$ chains in the $(RhCp^*)_4Mo_6O_{22}$ molecule **42** and MoO_4^{2-} are linked to $Mo_{\infty}O_{3\infty}$ chains in **108-110** in a very similar but not identical fashion.

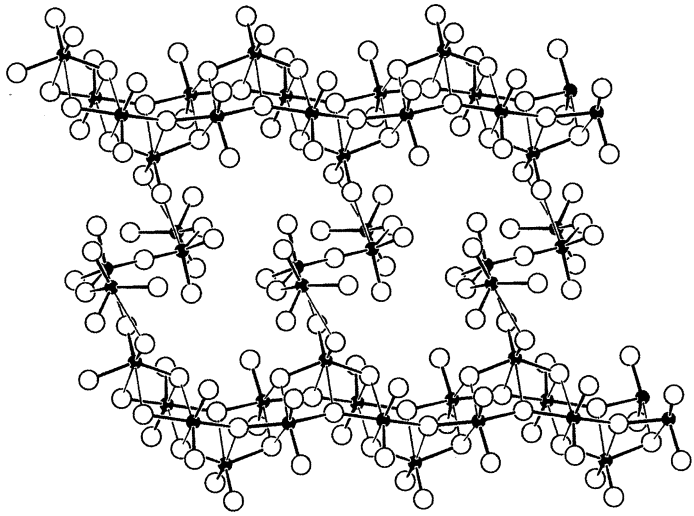

110

$Mo_{\infty}O_{3\infty}$ Dimers. Double chains **18** of the type observed in α-MoO_3 are also observed in the α-$MoO_3 \cdot H_2O$ structure [164, 165]. Here, each molybdenum atom also forms a weak bond to a water oxygen as shown in **111**, where the $Mo_{\infty}O_{3\infty}$ double chains have the same conformation adopted in α-MoO_3 (see **21**).

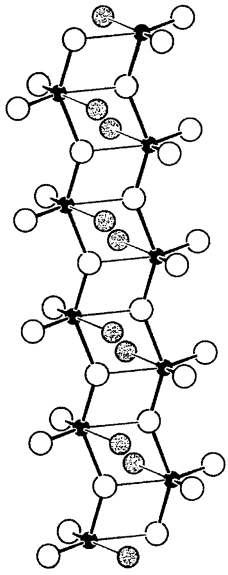

111

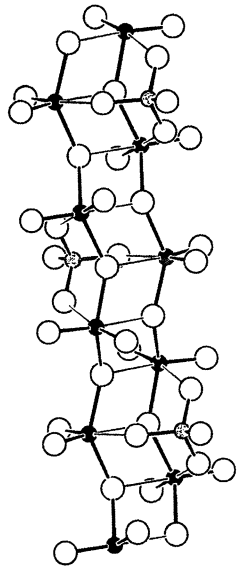

112

These double chains are also formed in $Rb_2SMo_3O_{13}$ [166] where they adopt a different conformation in order to accommodate weakly-bonded, tridentate sulfate groups (see **112**).

$Mo_\infty O_{3\infty}$ Polymers. Yellow molybdic acid, $MoO_3 \cdot 2H_2O$, contains the $MoO_3 \cdot H_2O$ sheets shown in **113** plus additional water molecules intercalated between these sheets [167–169]. The **113** $Mo_\infty O_{3\infty}$ chain building units that form $(Mo_\infty O_{3\infty})_\infty$ sheets in $MoO_3 \cdot 2H_2O$ differ in two respects from the $Mo_\infty O_{3\infty}$ building units that form sheet polymers **22** in α-MoO_3. First, the chains have different conformations such that terminal oxygen atoms in α-MoO_3 sheets **22** all lie on the same side of the sheet, but terminal oxygen atoms in $MoO_3 \cdot 2H_2O$ sheets **113** lie on both sides of the sheet. Second, only half of the molybdenum(VI) coordination polyhedra in $MoO_3 \cdot 2H_2O$ have Type II coordination geometry; the remainder have Type II/III geometry. When the distinction between strong and weak Mo–O bonds is disregarded, the metal-oxygen framework shown in **113** is seen to be identical to the corresponding metal-oxygen framework **32** of $(MoO_4^{2-})_\infty$ sheets in Bi_2MoO_6. The $(MoO_4^{2-})_\infty$ sheet **32** is literally the conjugate base of the $(H_2MoO_4)_\infty$ sheet **113**, and it is interesting to note that diprotonation of the $(MoO_4^{2-})_\infty$ sheet yields not a dihydroxy compound as in **4**, but instead an oxo-aquo compound as in **5**.

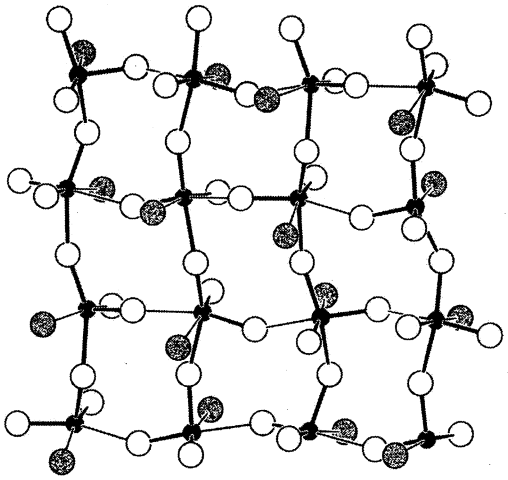

113

A high pressure polymorph of MoO_3 known as MoO_3-II contains $Mo_\infty O_{3\infty}$ double sheets **20**, but their stacking sequence is different from sequence adopted in the α-MoO_3 structure [170].

3.2. DIOXOMOLYBDENUM RING BUILDING UNITS

Three dioxomolybdenum rings of corner sharing MoO_4 tetrahedra are believed to exist in the gas phase [171–178]: Mo_3O_9, Mo_4O_{12}, and Mo_5O_{15}. This type of isolated ring has not been observed in fluid solution or in the solid state, but five dioxomolybdenum rings are known as structural building units in molecular and extended oxide structures: Mo_4O_{12}, Mo_5O_{15}, Mo_6O_{18}, Mo_8O_{24}, $Mo_{12}O_{36}$.

3.2.1. *Mo_4O_{12} Ring Building Units*

Mo_4O_{12} Ring Monomers. The Mo_4O_{12} ring building unit adopts a highly symmetric conformation in the peroxide complex $[(Mo_4O_{12})(O_2^{2-})_2]^{4-}$ **114** [179, 180]. When the two peroxide ligands are replaced by a μ_4-OH^- ligand and a bidentate $CH_2O_2^{2-}$ or $(CH_3)_2AsO_2^-$ ligand, a slightly less symmetric structure is observed. The $CH_2Mo_4O_{15}H^{3-}$ or $[(CH_2O_2^{2-})(Mo_4O_{12})(OH^-)]$ structure [181] is shown in **115**, and the $(CH_3)_2AsMo_4O_{15}H^{2-}$ or $\{[(CH_3)_2AsO_2^-](Mo_4O_{12})(OH^-)\}$ anion adopts the same structure [182–184]. A different ring conformation is evident in the $Mo_5(NO)O_{13}(OCH_3)_4^{3-}$ structure **116** [185].

114

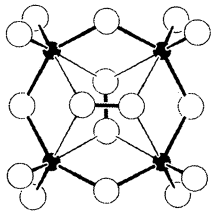

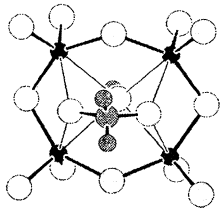

115

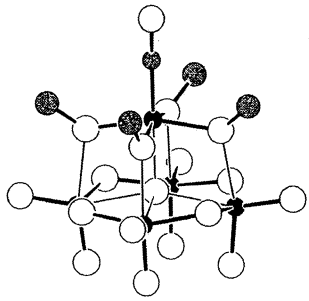

116

Monomeric Mo_4O_{12} building units are also observed in $Ag_6Mo_{10}O_{33}$, [186, 187] which has the structural formula $[(Mo_\infty O_{3\infty})_4(MoO_4^{2-})_2(Mo_4O_{12})_\infty(O^{2-})_\infty]$. Here, $Mo_\infty O_{3\infty}$ chains are linked by MoO_4^{2-} groups to form double chains of the type shown in **108**. These chains are linked together by Mo_4O_{12} rings to form infinite sheets **117**. The center of each Mo_4O_{12} ring is occupied by a μ_4-O^{2-}

ligand. In the $Ag_6Mo_{10}O_{33}$ structure, $[(Mo_4O_{12})(O^{2-})]$ groups play a role similar to the role assumed by $Mo_4O_{13}^{2-}$ building units in the $Na_6Mo_{10}O_{33}$ structure (see **110**).

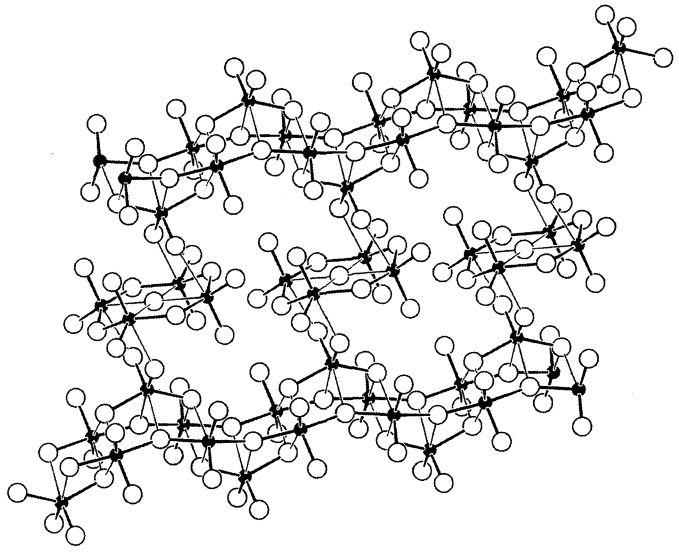

117

Mo_4O_{12} Ring Dimers. The structure of the β-$Mo_8O_{26}^{4-}$ has been determined in several different crystalline salts, including the ammonium salts $(NH_4)_4Mo_8O_{26}\cdot 5H_2O$ [188, 189] and $(NH_4)_4Mo_8O_{26}\cdot 4H_2O$ [76, 190, 191]; the pyridinium salt $(C_5NH_6)_4Mo_8O_{26}$ [192]; the 3-ethylpyridinium and 4-ethylpyridinium salts $(C_7NH_{10})_4Mo_8O_{26}$ [193, 194]; the 2-methylpyridinium and 3-methylpyridinium salts, $(C_6H_8N)_4(Mo_8O_{26})$ [195, 196]; $[NH_2(CH_3)_2]_4Mo_8O_{26}\cdot 2C_3H_7NO$ [197]; $Na_2[N(CH_3)_4]_2Mo_8O_{26}\cdot 2H_2O$ [198]; the melaminium salt $(C_3H_7N_6)_4Mo_8O_{26}$ [199]; $[HN(C_2H_5)_3]_3(H_3O)Mo_8O_{26}\cdot 2H_2O$ [200]; $[Na_4(CH_3OH)_8(H_2O)_2]Mo_8O_{26}$ [201]; $[(C_6H_5)_3PCH_2CO_2CH_2CH_3]_2[H_2N(C_2H_5)_2]_2Mo_8O_{26}$ [202]; the anilinium salt $(C_6H_5NH_3)_4Mo_8O_{26}\cdot 2H_2O$ [203]; and the dimethylanilinium salt $[C_6H_5NH(CH_3)_2]_4Mo_8O_{26}\cdot 2H_2O$ [204].

The β-$Mo_8O_{26}^{4-}$ or $[(Mo_4O_{12})_2(O^{2-})_2]$ anion structure **118** contains two Mo_4O_{12} rings that are linked by six weak oxygen-metal bonds, four involving Mo_4O_{12} bridging oxygen atoms and two involving Mo_4O_{12} terminal oxygen atoms. The $(Mo_4O_{12})(O^{2-})$ subunit in **118** is also present in **115**, **116**, and **117**.

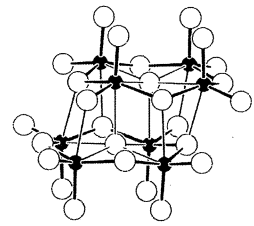

118

3.2.2. *Mo_5O_{15} Ring Building Units*

Pentanuclear dioxomolybdenum ring building units **15** have been observed in heteropolyanion structures containing two tridentate oxoanion ligands coordinated to opposite sides of the ring as shown in **14** for the $P_2Mo_5O_{23}^{6-}$ or $[(Mo_5O_{15})(PO_4^{3-})_2]$ anion [45, 46]. Species known to have the same structure include $[(Mo_5O_{15})(PO_4^{3-})(HPO_4^{2-})]$ [205, 206], $[(Mo_5O_{15})(HPO_4^{2-})_2]$ [207], $[(Mo_5O_{15})(CH_3PO_3^{2-})_2]$ [208], $[(Mo_5O_{15})(H_3NCH_2CH_2PO_3^{-})_2]$ [208], $[(Mo_5O_{15})(C_6H_5PO_3^{2-})_2]$ [209], $[(Mo_5O_{15})(HPO_3^{2-})_2]$ [210], $[(Mo_5O_{15})(C_3H_7AsO_3^{2-})_2]$ [211, 212], and $[(Mo_5O_{15})(SO_3^{2-})_2]$ [213].

3.2.3. *Mo_6O_{18} Ring Building Units*

Mo_6O_{18} Ring Monomers. When an Mo_6O_{18} ring building unit encloses an octahedral XO_6 group, two isomeric structures may be obtained. All six molybdenum atoms in the Mo_6O_{18} ring are coplanar in **119**, the D_{3d} α-$PtMo_6O_{24}^{8-}$ structure.

119

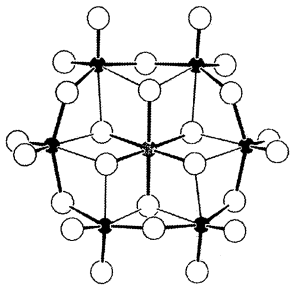

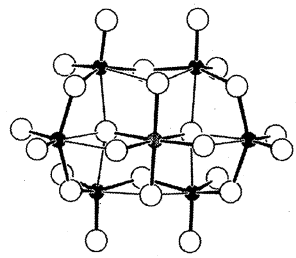

120

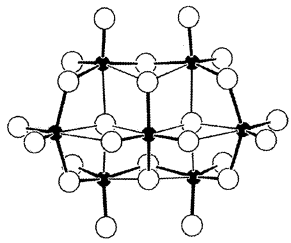

121

This structure is observed in the $PtMo_6O_{24}H_6^{2-}$ or $\{[Pt(OH)_6^{2-}](Mo_6O_{18})\}$ anion [214] as well as the hydrogen-bonded dimers $[(PtMo_6O_{24})_2H_7]^{9-}$ and $[(PtMo_6O_{24})_2H_9]^{7-}$ [214, 215]. Other species in this class include the $TeMo_6O_{24}^{6-}$ or $[(TeO_6^{6-})(Mo_6O_{18})]$ [216, 217], $CrMo_6O_{24}H_6^{3-}$ or $\{[Cr(OH)_6^{3-}](Mo_6O_{18})\}$ [218], $CuMo_6O_{24}H_6^{4-}$ or $\{[Cu(OH)_6^{4-}](Mo_6O_{18})\}$ [219], and $IMo_6O_{24}^{5-}$ or $[(IO_6^{5-})(Mo_6O_{18})]$ anions [220]. The isomeric C_{2v}

β-$PtMo_6O_{24}^{8-}$ structure **120** [214, 215] is adopted by the $PtMo_6O_{24}H_4^{4-}$ or $\{[PtO_2(OH)_4^{4-}](Mo_6O_{18})\}$ anion and represents the second family of structures where the Mo_6O_{18} building unit adopts a less symmetric, bent conformation. This family includes the $H_2SbMo_6O_{24}^{5-}$ or $\{[SbO_4(OH)_2^{5-}](Mo_6O_{18})\}$ structure [221] and the $Mo_7O_{24}^{6-}$ or $[(MoO_4^{2-})(O^{2-})_2(Mo_6O_{18})]$ structure **121** where the central molybdenum atom has Type II octahedral coordination geometry [216, 222–229]. This $Mo_7O_{24}^{6-}$ structure is a subunit of the $Pr_8Mo_{58}O_{200}(H_2O)_{26}^{28-}$ or $\{(MoO_4^{2-})[Pr^{3+}(H_2O)_4]_3[Pr^{3+}(H_2O)][(MoO_4^{2-})(O^{2-})_2(Mo_6O_{18})]_4\}_2$ aggregate in $(NH_4)_{28}Pr_8Mo_{58}O_{200}\cdot 40H_2O$ [230].

The Mo_6O_{18} ring in the α-$Mo_8O_{26}^{4-}$ or $[(Mo_6O_{18})(MoO_4^{2-})_2]$ structure **122** has the same conformation adopted in **119**. The α-$Mo_8O_{26}^{4-}$ anion is an isomer of the β-$Mo_8O_{26}^{4-}$ anion **118** and has been characterized in $[N(C_4H_9)_4]_4Mo_8O_{26}$ [231, 58] and $[(C_6H_5)_3P(CH_2CH_2CH_3)]_4Mo_8O_{26}\cdot CH_3CN\cdot H_2O$ [232, 74].

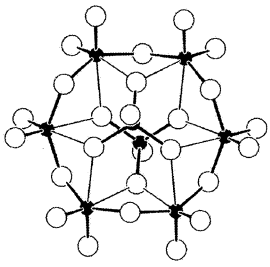

122

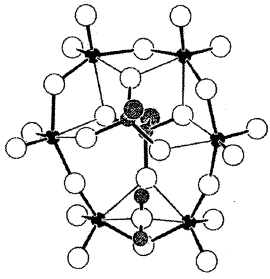

123

Several derivatives of the α-$Mo_8O_{26}^{4-}$ anion are known where the capping MoO_4^{2-} groups are replaced by other oxoanions as in $[(CH_3AsO_3^{2-})_2(Mo_6O_{18})]$ [233], $[(CH_3CH_2CH_2AsO_3^{2-})_2(Mo_6O_{18})]^{4-}$ [234, 211], and $[(VO_4^{3-})_2(Mo_6O_{18})]$ [235]. The last of these species, the α-$V_2Mo_6O_{26}^{6-}$ ion, and the β-$V_2Mo_6O_{26}^{6-}$ ion **65** are isomeric. Derivatives of the α-$Mo_8O_{26}^{4-}$ anion obtained by substitution of ring MoO_2 dioxomolybdenum units with other ML_2 units may result in significant structural rearrangement. For example, **23** is derived from **122** by replacing three MoO_2 groups in the Mo_6O_{18} ring with $Mo(NNC_6H_5)_2$ groups, and **41** is derived from **122** replacing two MoO_2 units with AsO_2 units and replacing both MoO_4^{2-} capping groups with AsO_4^{3-} groups. Monomeric Mo_6O_{18} ring building units may adopt several conformations different from those observed in **119–122**. Two of these conformations are shown in **123**, the $[(C_6H_5AsO_3^{2-})_2(Mo_6O_{18})(H_2O)]$ anion [236, 237], and **124**, the $[(CH_3AsO_3^{2-})(Mo_6O_{18})(H_2O)_6]$ anion [183].

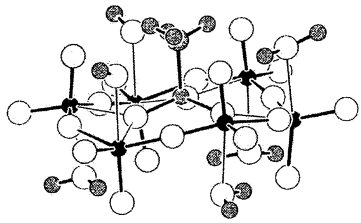

124

An even less symmetric conformation is adopted in the γ-$Mo_8O_{26}^{4-}$ structure [238]. Like the α-$Mo_8O_{26}^{4-}$ anion, the γ isomer has the structural formula $[(Mo_6O_{18})(MoO_4^{2-})_2]$. Its three-dimensional structure is very different, however, and may be derived from the β-$Mo_8O_{26}(OH)_2^{6-}$ structure **69** by removing both hydroxyl groups and converting the geometry of the square pyramidal molybdenum centers thus formed to trigonal bipyramidal geometry.

Monomeric Mo_6O_{18} building units are also found in the copper molybdate $Cu_4Mo_6O_{20}$ [122]. This compound has the structural formula $[(Mo_3O_{10}^{2-})_{2\infty}(Mo_6O_{18})_\infty(O^{2-})_{2\infty}]$ and contains polymeric chains **125** where two structurally distinct $Mo_6O_{19}^{2-}$ groups are linked by weak Mo–O bonds in an ABAB$\cdots$ fashion.

125

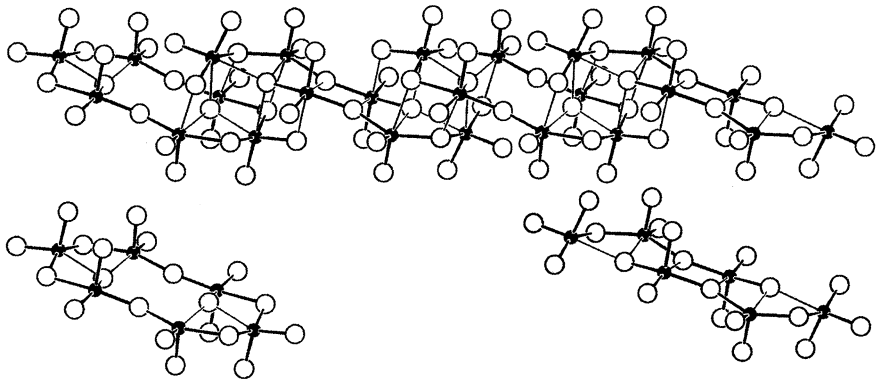

126 **127**

One $Mo_6O_{19}^{2-}$ group contains two μ_3-O^{2-} ligands connected by weak Mo–O bonds to an elongated Mo_6O_{18} dioxomolybdenum ring building unit as shown in **126**. This Mo_6O_{18} ring has been idealized in **125** and **126**: the two symmetry-equivalent molybdenum centers at opposite ends of the ring have Type II/III geometry, and these are drawn as Type II centers. The other $Mo_6O_{19}^{2-}$ group **127** contains two $Mo_3O_{10}^{2-}$ dioxomolybdenum chain building units connected by weak Mo–O bonds as shown in **60**.

Mo_6O_{18} Ring Dimers. The $As_2Mo_{12}O_{42}^{6-}$ anion, observed in $[(CH_3)_4N]_4Na_2(As_2Mo_{12}O_{42})\cdot 6H_2O$ [239], contains Mo_6O_{18} dioxomolybdenum ring dimers **128.**

128

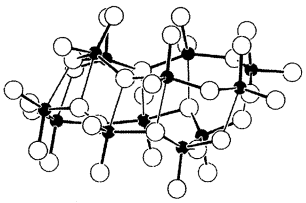

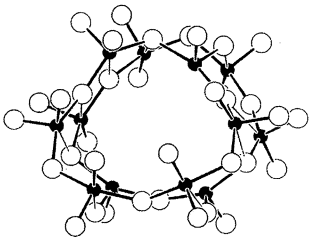

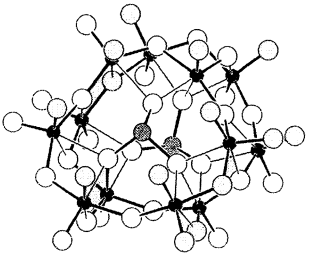

129 **130**

This side view of the dimer shows how nine weak bonds interconnect the two ring units, and the top view **129** of the same dimer reveals a central cavity that is occupied by two AsO_3^{3-} anions as shown in **130**. Three molybdenum centers in the $As_2Mo_{12}O_{42}^{6-}$ anion have Type I/II coordination geometry, and they have been idealized to Type II geometry in **130**. These molybdenum centers are the ones doubly-bonded to oxygen atoms that also form weak molybdenum-oxygen bonds interconnecting the two Mo_6O_{18} building units.

3.2.4. *Mo_8O_{24} Ring Building Units*

As shown in **131**, the eight peripheral molybdenum atoms in the $V_3Mo_9O_{38}^{7-}$ anion [240] all have Type II octahedral coordination geometry and therefore define an Mo_8O_{24} ring structural building unit. If all metal-oxygen bonds longer than 2.10Å are treated as weak bonds, the structure may be reduced to three structural building units: an Mo_8O_{24} dioxomolybdenum ring, a $V_2O_7^{4-}$ anion, and a $VMoO_7^{3-}$ anion.

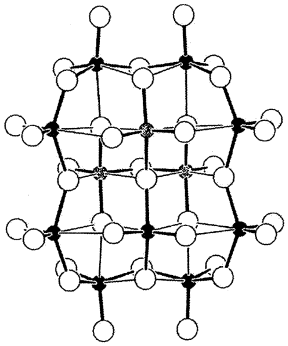

131

3.2.5. *$Mo_{12}O_{36}$ Ring Building Units*

The squarate complex $[(C_4H_9)_4N]_4[Mo_{12}O_{36}(C_4O_4H)_4]\cdot 10(C_2H_5)_2O$ [241] contains an ideally S_4 $Mo_{12}O_{36}$ dioxomolybdenum ring building unit linked to four monoprotonated squarate ions $C_4O_4H^-$ by weak Mo–O bonds as shown in **132**.

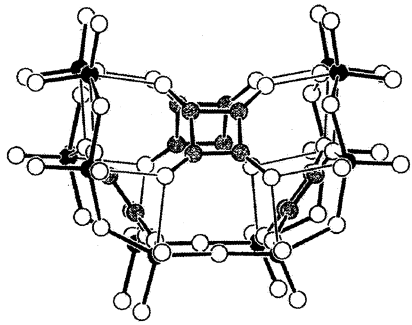

132

3.3. POLYCYCLIC DIOXOMOLYBDENUM BUILDING UNITS

The structural building units discussed in Section 3.2 are cyclic species formed from doubly-bridging oxygen atoms and dioxomolybdenum. Polycyclic cages may be formed from these rings by introducing triply-bridging oxygen atoms that serve as ring junctions.

3.3.1. *The Polycyclic $Mo_8O_{23}^{2+}$ Cage*

The $H_2TeMo_8O_{30}^{4-}$ anion **133** [242] contains the polycyclic $Mo_8O_{23}^{2+}$ building unit **134** connected to a TeO_6^{6-} ion and an H_2O molecule by weak Mo–O bonds.

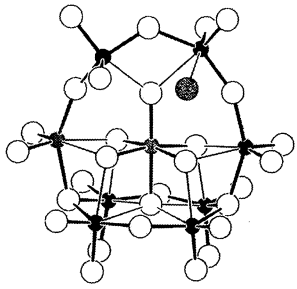

133

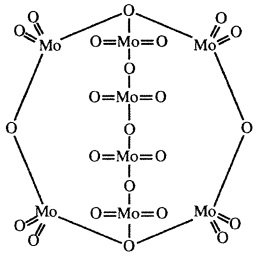

134

All of the molybdenum centers in this structure have Type II coordination geometry except for one of the six molybdenum atoms bonded to a trivalent oxygen atom. This center has Type II/III geometry by virtue of a long, 2.12-Å bond to a trivalent oxygen atom, and bonding at this molybdenum center has been idealized to Type II geometry in **133**.

The polycyclic $Mo_8O_{23}^{2+}$ cage building unit in **133** is drawn in **134** as an Mo_4O_{12} ring derivative obtained by transannular addition of an $[(MoO_2)_4O_3]^{2+}$ chain. The conformation of this Mo_4O_{12} ring (see **133**) is very similar to the conformation of the Mo_4O_{12} building unit in **116** and **118**. The polycyclic building unit **134** also contains two Mo_6O_{18} rings. Addition of an $[(MoO_2)_2O]^{2+}$ chain to the Mo_6O_{18} ring unit in either the known α-$TeMo_6O_{24}^{6-}$ anion **119** or the hypothetical β-$TeMo_8O_{24}^{4-}$ anion **120** yields the hypothetical $TeMo_8O_{29}^{4-}$ structure **135**. The $H_2TeMo_8O_{30}^{4-}$ structure **133** may be derived from **135** by cleaving two weak Mo–O bonds and adding a water molecule to one of the two resulting five-coordinate molybdenum centers. This hypothetical hydration process closely resembles hydration of the $[(C_6H_5AsO_3^{2-})_2(Mo_6O_{18})]$ anion **122**, known to yield **123**. In **123**, the water oxygen is bonded to two Mo_6O_{18} molybdenum atoms, not to only one as in **133**.

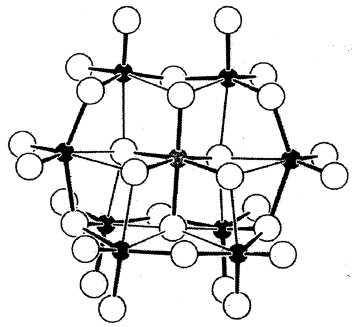

135

3.3.2. *The Polycyclic $Mo_9O_{26}^{2+}$ Cage*

The symmetric, tricyclic dioxomolybdenum structural building unit **136** is derived from an Mo_6O_{18} dioxomolybdenum ring unit by transannular addition of an $[(MoO_2)_3O_2]^{2+}$ chain.

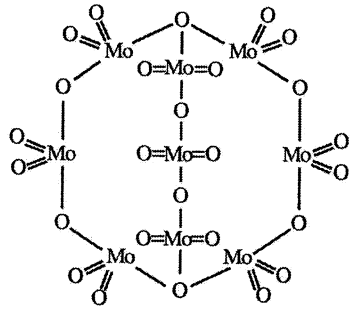

136

This polycyclic $Mo_9O_{26}^{2+}$ building unit is found in the $MnMo_9O_{32}^{6-}$ or $[(MnO_6^{8-})(Mo_9O_{26}^{2+})]$ anion [243–245] and its nickel analogue [246], where it adopts the D_{3d} conformation **137**. In $MnMo_9O_{32}^{6-}$, an MnO_6^{8-} group occupies the center of the cage as shown **138**, and each of the three constituent Mo_6O_{18} rings has the conformation observed in the β-$PtMo_6O_{18}^{8-}$ structure **120**. The relationship between the $MnMo_9O_{32}^{6-}$ and β-$PtMo_6O_{24}^{8-}$ structures be-

comes evident when an $[(MoO_2)_3O_2]^{2+}$ chain is removed from the $MnMo_9O_{32}{}^{6-}$ structure **138** to form the hypothetical β-$MnMo_6O_{24}{}^{8-}$ anion **139**.

137

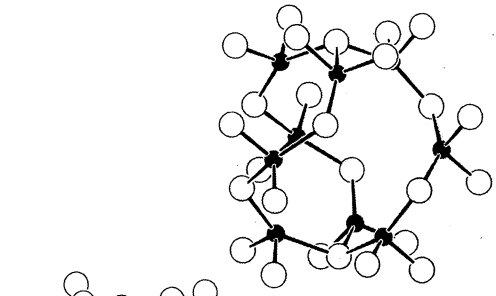

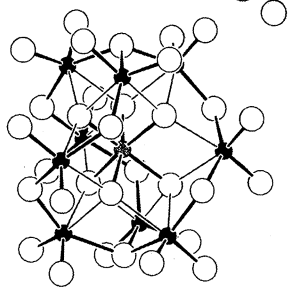

138

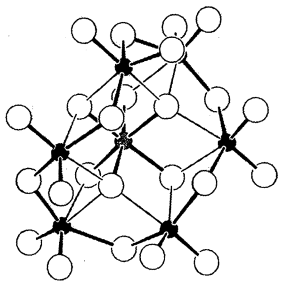

139

3.3.3. *The Polycyclic $Mo_{12}O_{34}{}^{4+}$ Cage*

The $H_4As_4Mo_{12}O_{50}{}^{4-}$ anion [247] contains a tetrahedral $Mo_{12}O_{34}{}^{4+}$ cage building unit **140** connected to four tridentate $HAsO_4{}^{2-}$ anions by weak Mo–O bonds as shown in **141**.

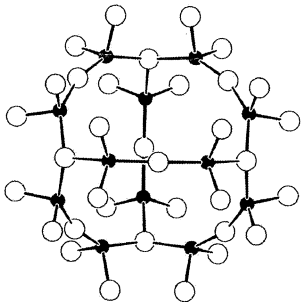

140

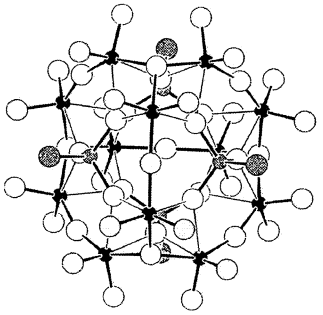

141

The $(p\text{-}H_3NC_6H_4As)_4Mo_{12}O_{46}$ molecule [248] contains the same cage building unit linked to four $^{+}H_3NC_6H_4AsO_3{}^{-}$ ligands. As shown in valence structure **142**, this polycyclic building unit contains both Mo_6O_{18} and Mo_8O_{24} rings.

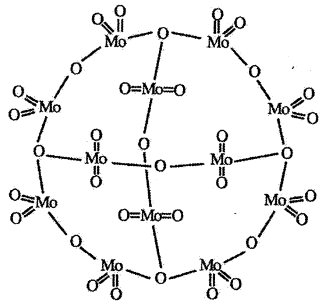

142

3.4. MONOXOMOLYBDENUM SHEET BUILDING UNITS

Although many topologies are possible for monoxomolybdenum sheet building units, the building units discussed in this Section are fragments of the $Mo_{\infty}O_{3\infty}$ monoxomolybdenum sheet **143**. These sheet building units are monoxomolybdenum analogues of dioxomolybdenum chain building units derived from the $Mo_{\infty}O_{3\infty}$ dioxomolybdenum chain **3**.

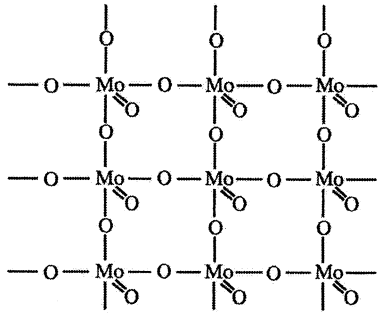

143

3.4.1. *MoO_5^{4-} Building Units*

The simplest monooxomolybdenum(VI) structural building unit often forms $(MoO_5^{4-})_2$ dimers **144**, analogues of the $(MoO_4^{2-})_2$ dimers **26** treated in Section 3.1.1. These dimers are observed in $[MoO(OCH_3)_4]_2$ [249], the bis(3,5-di-*tert*-butylcatecholato) complex $\{MoO[O_2C_6H_2(t\text{-}Bu)_2]_2\}_2$ [250], both isomers of the triolate ethoxide complex $\{MoO[(CH_3(CH_2O)_3](CH_3CH_2O)\}_2$ [251], and Li_4MoO_5 [252]. In the organic complexes, Type I coordination geometry is observed at both metal centers, but in Li_4MoO_5, the Mo–O bond *trans* to the 2.12-Å weak Mo–O bond is 1.81 Å long, formally implying Type 0/I coordination geometry.

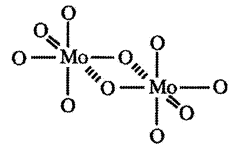

144

The MoO_5^{4-} building unit may also be linked to dioxomolybdenum(VI) building units by weak Mo–O bonds as in the arsenic(III) compound $Na_3[As_3Mo_3O_{15}]\cdot 10H_2O$ [253]. Here, the $Mo_3O_{13}^{8-}$ oxomolybdenum(VI) core structure has the structural formula $[(MoO_5^{4-})(Mo_2O_7^{2-})(O^{2-})]$.

3.4.2. $Mo_2O_9^{6-}$ *Building Units*

The μ-oxo-bis{[2,3-dimethyl-2,3-butanediolato(1-)][2,3-dimethyl-2,3-butanediolato(2-)]-oxomolybdenum(VI)} complex $\{[(OCMe_2CMe_2O)(HOCMe_2CMe_2O)MoO]_2O\}$ [254] has the structure shown in **145**. Since both molybdenum centers have Type I octahedral coordination geometry, this complex provides an example of the $Mo_2O_9^{6-}$ structural building unit **146**.

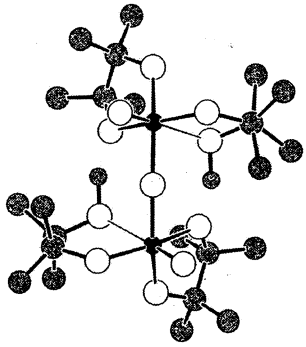

145

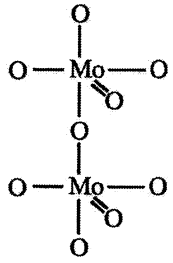

146

3.4.3. $Mo_{2\infty}O_{7\infty}^{2\infty-}$ *Building Units*

Infinite $Mo_{2\infty}O_{7\infty}^{2\infty-}$ double chains **147** are obtained upon reduction of the UMo_2O_8 structure [255] to its structural building units. These double chains are interconnected by weak bonds as shown in **148** to form sheet polymers. All of the molybdenum centers in this structure have Type I coordination geometry.

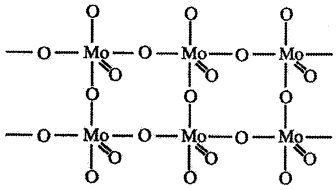

147

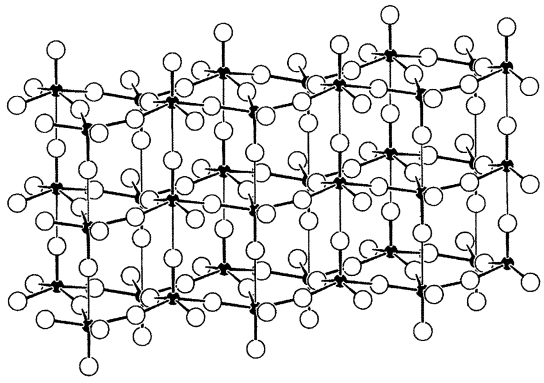

148

3.4.4. $Mo_\infty O_{3\infty}$ *Sheet Building Units*

The β'-MoO_3 structure [256, 257] reduces to $Mo_\infty O_{3\infty}$ sheets **149**, and each sheet is linked to two other sheets by weak molybdenum-oxygen bonds as shown

in **150** for two adjacent sheets. This $(Mo_{\infty}O_{3\infty})_{\infty}$ polymer has the ReO_3 structure. Molybdenum coordination geometry in the $Mo_{\infty}O_{3\infty}$ sheet building units **149** is extremely distorted from Type I coordination geometry, and since some of the molybdenum centers have Type II/III geometry, the building unit is technically a hybrid building unit of the type treated below in Section 3.6. The β'-MoO_3 structure is included here because its $Mo_{\infty}O_{3\infty}$ structural building unit approaches structure **143** more closely than any other $Mo_{\infty}O_{3\infty}$ sheet building unit characterized to date.

149

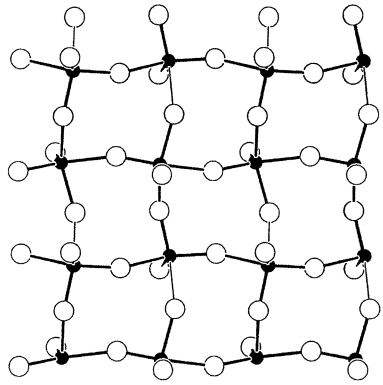

150

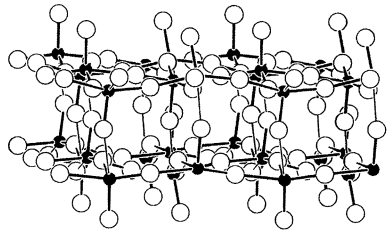

3.5. MONOXOMOLYBDENUM CAGE BUILDING UNITS

When monoxomolybdenum groups are linked by oxygen atoms as in **143** but on a closed surface instead of a plane, Mo_nO_{3n} cage building units are obtained. These cage units are monoxomolybdenum analogues of the Mo_nO_{3n} dioxomolybdenum ring building units derived from **3**. The topologies of *closo* cage building units treated in this Section are represented in Scheme II by regular-faced polyhedra, where edges represent bridging oxygen atoms and vertices represent monoxomolybdenum groups. In Scheme II, octahedron **a** represents the Mo_6O_{18} cage building unit, cuboctahedron **b** represents the α-$Mo_{12}O_{36}$ cage building unit, triangular orthobicupola ("anticuboctahedron") **c** represents the β-$Mo_{12}O_{36}$ cage building unit, and elongated triangular orthobicupola **d** represents the $Mo_{18}O_{54}$ cage building unit. The polyhedral fragments inscribed in the polyhedra shown in

Scheme II using thick lines represent *nido* cage building units derived from the *closo* cage building units.

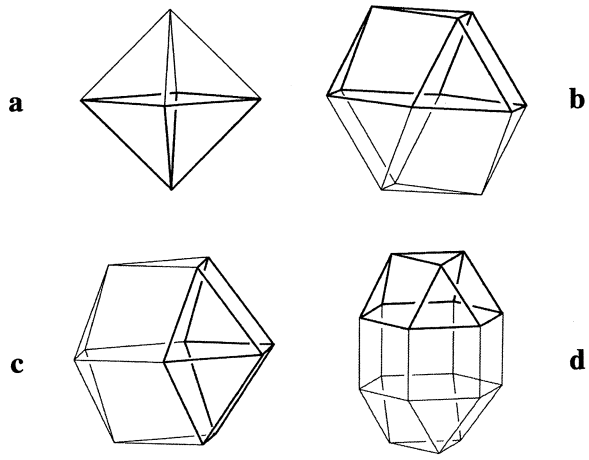

Scheme II

3.5.1. *Closo Cage Building Units*

Mo_6O_{18} Cages. The $Mo_6O_{19}^{2-}$ or $[(Mo_6O_{18})(O^{2-})]$ ion has the structure shown in **151** [258–261, 202]. Here, molybdenum centers all have Type I octahedral coordination geometry. Within the Mo_6O_{18} cage, Mo_4O_4 rings sometimes display systematic bond length alternation between *ca.* 1.85-Å single bonds and *ca.* 2.00-Å single bonds as shown in **10**, but this bond length alternation, when observed, is insufficiently large to distort the Type I molybdenum coordination geometry to Type I/II or I/III geometry.

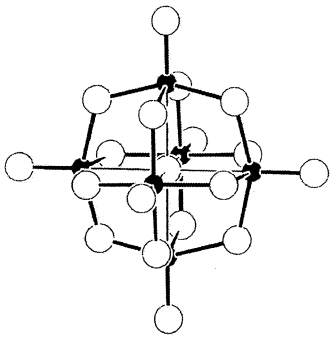

151

α-$Mo_{12}O_{36}$ Cages. The anions α-$PMo_{12}O_{40}^{3-}$ [262–267], α-$SiMo_{12}O_{40}^{4-}$ [268, 269], and α-$GeMo_{12}O_{40}^{4-}$ [270], all have the α-Keggin structure where an α-$Mo_{12}O_{36}$ cage (see **b** in Scheme II) is connected to an encapsulated tetrahedral oxoanion by weak molybdenum oxygen bonds. Molybdenum centers in the $PMo_{12}O_{40}^{3-}$ anion **152** all have Type I octahedral coordination geometry.

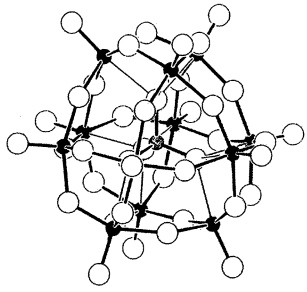

152

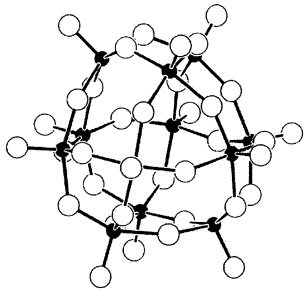

153

The α-$Mo_{12}O_{36}$ cage building unit **153** contains four approximately planar Mo_6O_6 rings that are analogues of the three Mo_4O_4 rings in the Mo_6O_{18} *closo* cage just described. As is the case with Mo_4O_4 rings in Mo_6O_{18} cages, bond length alternation is sometimes observed in these Mo_6O_6 rings such that ideally T_d cage symmetry is reduced to T symmetry.

In $[(n\text{-}C_6H_{13})_4N]_2(CH_3)(PMo_{12}O_{40})$ [267], all molybdenum centers have Type I coordination geometry, but binding of the methyl group to a bridging oxygen lengthens its Mo–O bonds significantly, initiating a pattern of bond length alternation in the Mo_6O_6 ring containing the methoxy group. The bond length alternation induced by methylation is superposed on the pattern of bond length alternation noted above for the parent anion. The remaining Mo_6O_{16} rings are unaffected by methylation, indicating that the methylation-induced bond length alternation is transmitted predominantly in a *trans* as opposed to a *cis* fashion.

β-$Mo_{12}O_{36}$ Cages. The β-$SiMo_{12}O_{40}^{4-}$ anion [271] has the structure shown in **154** where a β-$Mo_{12}O_{36}$ cage **155** (see **c** in Scheme II) is connected to a central SiO_4^{4-} group by weak Mo–O bonds. Although molybdenum centers in the β-$SiMo_{12}O_{40}^{4-}$ appear to have Type I coordination geometry, discussion of structural details is precluded by the poor precision of the structure determination.

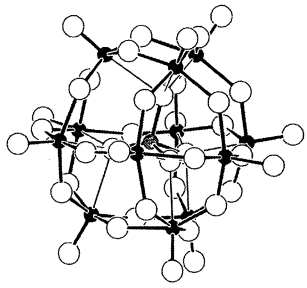

154

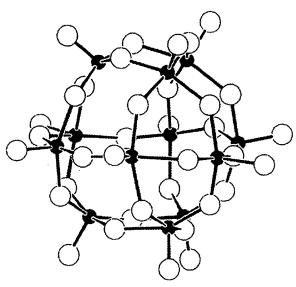

155

α-$Mo_{18}O_{54}$ Cages. The $S_2Mo_{18}O_{62}^{4-}$ or $[(SO_4^{2-})_2(Mo_{18}O_{54})]$ anion [272] has the structure shown in **156** where two SO_4^{2-} anions are encapsulated by an α-$Mo_{18}O_{54}$ cage building unit **157** (see **d** in Scheme II). *Trans* bond length alternation in all three Mo_8O_8 rings distorts the ideally D_{3h} $Mo_{18}O_{54}$ cage **157** to virtual D_3 symmetry. Here, bond length alternation is more exaggerated than bond length alternation noted above for $Mo_6O_{19}^{2-}$ and α-Keggin anions, and coordination geometry at several molybdenum centers is distorted to Type I/II geometry.

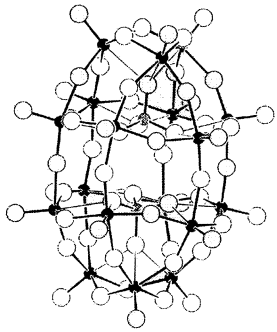

156

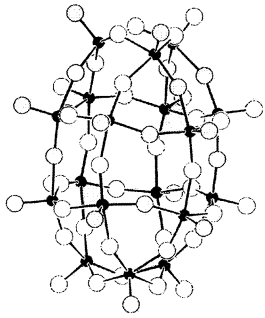

157

3.5.2. *Nido Cage Building Units*

$Mo_5O_{17}^{4-}$ Cages. Removal of an MoO^{4+} unit from an octahedral Mo_6O_{18} *closo* cage yields the square pyramidal $Mo_5O_{17}^{4-}$ *nido* cage observed as a structural building unit in several polyoxomolybdates, including $C_5H_5TiMo_5O_{18}^{3-}$ [273, 274], $ONMo_6O_{18}^{3-}$ [185], $C_6H_5N_2Mo_6O_{18}^{3-}$ [275], $C_6F_5N_2Mo_6O_{18}^{3-}$ [276], and $(C_6H_5)CH_3NNMo_6O_{18}^{2-}$ [277]. In the $C_5H_5TiMo_5O_{18}^{3-}$ anion **158**, all six molybdenum atoms have Type I octahedral coordination geometry, but in its MoO_2Cl^+ adduct, $C_5H_5TiMo_6O_{20}Cl^{2-}$ **159** [278], the $C_5H_5TiMo_5O_{18}^{3-}$ structure **158** is severely distorted.

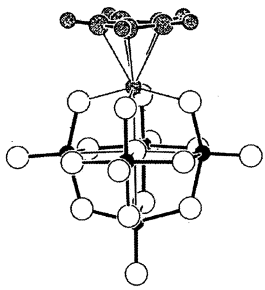

158

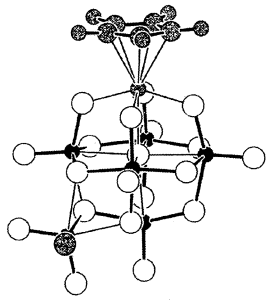

159

The consequences of MoO_2Cl^+ binding are not localized, but extend throughout the structure by a pattern of predominantly *trans* bond length alternation of the type described above for the methylated α-$PMo_{12}O_{40}^{3-}$ ion: two oxomolybdenum(VI) centers in **158** have Type I coordination geometry, two have Type I/II geometry, and one has Type II geometry.

Mo_9O_{27} Cages. *Trans* bond length alternation noted above for Mo_8O_8 rings in $S_2Mo_{18}O_{62}^{4-}$ anion **156** is far more pronounced in the $P_2Mo_{18}O_{62}^{6-}$ [279, 280] and $As_2Mo_{18}O_{62}^{6-}$ ions [281]. The two PO_4^{3-} ions in $P_2Mo_{18}O_{62}^{6-}$ are linked to molybdenum centers by weak Mo–O bonds as shown in **160**.

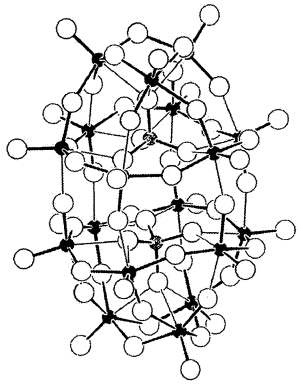

160

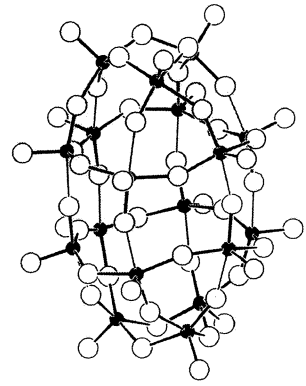

161

When both phosphate groups are removed from **160**, the resulting $Mo_{18}O_{54}$ group **161**, unlike the corresponding $Mo_{18}O_{54}$ group **157** in $S_2Mo_{18}O_{62}^{4-}$, is not a structural building unit. The $Mo_{18}O_{54}$ **161** group contains two Mo_9O_{27} groups linked together by weak molybdenum-oxygen bonds, and the $P_2Mo_{18}O_{62}^{6-}$ anion therefore has the structural formula $[(PO_4^{3-})_2(Mo_9O_{27})_2]$. This formulation reflects the coordination geometry observed at molybdenum centers in **160**, where the six central, equatorial molybdenum atoms have Type II coordination geometry and the two sets of three peripheral, axial molybdenum atoms have Type I/II geometry.

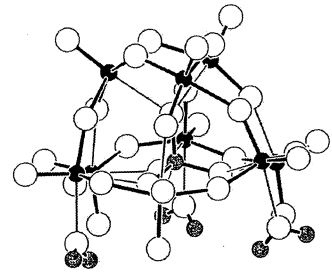

162

The $H_6PMo_9O_{34}^{3-}$ anion **162** [282, 283, 280, 284] has the structural formula $[(PO_4^{3-})(Mo_9O_{27})(H_2O)_3]$ and contains the same Mo_9O_{27} *nido*-cage building unit found in the $P_2Mo_{18}O_{62}^{6-}$ anion.

Note that the $H_6PMo_9O_{34}^{3-}$ anion does not adopt a symmetric structure where the PO_4^{3-} is weakly bonded to the hypothetical $H_6Mo_9O_{30}$ group **163**, where molybdenum centers in an $Mo_9O_{30}^{6-}$ monoxomolybdenum *nido* cage building unit have Type I coordination geometry. Instead, the $H_6PMo_9O_{34}^{3-}$ anion adopts structure **162**, where the six pairs of hydroxy ligands in **163** are replaced by three oxo ligands and three aquo ligands, presumably for the same reasons that "yl" ions adopt the oxo-aquo structure **5** instead of the dihydroxy structure **4**. Expressed in terms of off-center displacement as opposed to "yl" ion formation, the $P_2Mo_{18}O_{62}^{6-}$ and $H_6PMo_9O_{34}^{3-}$ ions display *trans* bond length alternation as in **7**, presumably because the alternative valence structure **6** implies stressed bonds, and hence a higher-energy structure (see Section 2.1).

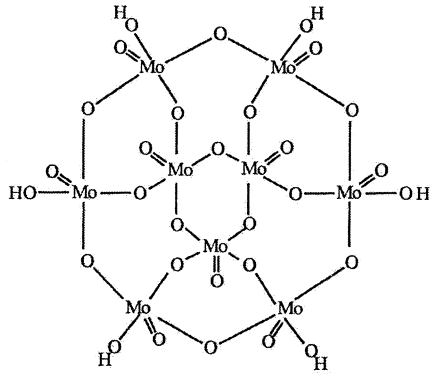

163

3.6. HYBRID DIOXOMOLYBDENUM/MONOXOMOLYBDENUM BUILDING UNITS

In Sections 3.1 to 3.5, most building units contained either dioxomolybdenum groups or monoxomolybdenum groups. Here, hybrid structural building units are described that contain both monoxomolybdenum and dioxomolybdenum groups.

3.6.1. *Hybrid Chain Building Units*

Valence structures for three simple hybrid chain building units, $Mo_2O_8^{4-}$, $Mo_3O_{11}^{4-}$, and $Mo_3O_{12}^{6-}$, are shown in **164**, **165** and **166**, respectively.

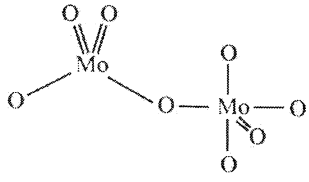

164

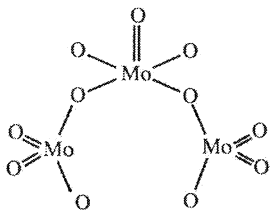

165

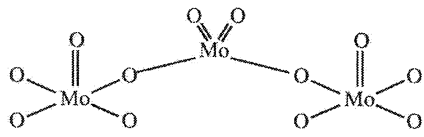

166

Betpakdalit, $H_{6-x}[K(H_2O)_6]_x[Ca(H_2O)_6]_4[Mo_{16}As_4Fe_6O_{74}]\cdot 4H_2O$ [285], contains the $As_2Mo_8O_{37}^{16-}$ group shown in **167**, where six molybdenum atoms have Type II coordination geometry and two molybdenum atoms have Type I/III coordination geometry.

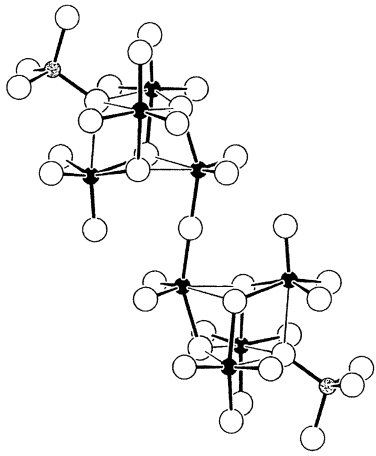

167

Reduction of this group to its structural building units yields the structural formula $[(Mo_2O_7^{2-})(Mo_3O_{11}^{4-})_2(AsO_4^{3-})]$. The $Mo_2O_7^{2-}$ dioxomolybdenum chain unit in **167** adopts the same conformation observed in the oxalate complex **40**. The $Mo_3O_{11}^{4-}$ groups each contain a central Type I/III molybdenum center and can be idealized in two ways. If this molybdenum center is treated as a distorted Type I center, the $Mo_3O_{11}^{4-}$ group is a distorted hybrid structural building unit **165**. If the Type I/III molybdenum center is treated as a distorted Type III center, the $Mo_3O_{11}^{4-}$ group contains three structural building units, two MoO_4^{2-} units plus a distorted MoO_3 trioxomolybdenum unit.

3.6.2. *Hybrid Ring Building Units*

In the $Mo_5O_{17}CH_3^{3-}$ or $[(Mo_5O_{16}^{2-})(OCH_3^-)]$ ion [115] **168**, four molybdenum centers have Type II coordination geometry and one has Type I/II geometry,

and when Type I/II coordination geometry is idealized to Type I geometry, the $Mo_5O_{16}^{2-}$ building unit has the valence structure **169**.

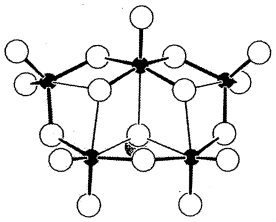

168

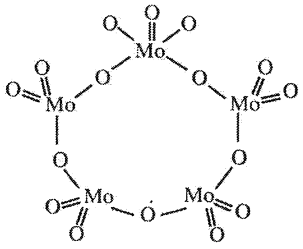

169

The $Mo_5O_{17}H^{3-}$ anion most likely has the $[(Mo_5O_{16}^{2-})(OH^-)]$ structure [115], not the $[(MoO_4^{2-})(Mo_4O_{12})(OH^-)]$ structure once assigned [286] by analogy with the $\{[(CH_3)_2AsO_2^{2-}](Mo_4O_{12})(OH^-)\}$ structure (see Section 3.2.1).

A hybrid ring structural building unit is also observed in the catecholate complex $[Mo_4O_{10}(OCH_3)_2(O_2C_6H_4)_2]^{2-}$ **170** [96, 97]. This building unit has the valence structure **171** and is a valence isomer of the $Mo_2O_7^{2-}$ dimer **33** found in the $Mo_4O_{10}(OCH_3)_6^{2-}$ anion **43** (see Section 3.2.1).

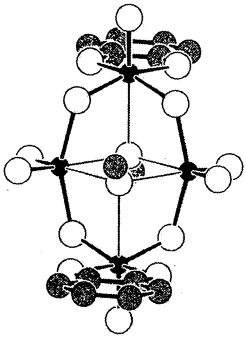

170

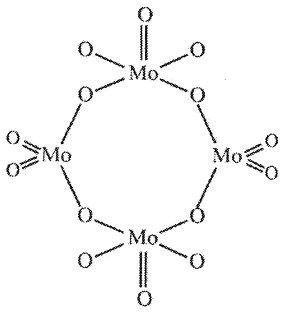

171

3.6.3. *Hybrid Polycyclic Building Units*

In the polycyclic dioxomolybdenum building units discussed in Section 3.3, trivalent oxygen atoms serve as ring junctions. The hybrid building units introduced in this Section illustrate how molybdenum atoms can also serve as ring junctions.

The $SiMo_9O_{33}^{8-}$ anion **172** [287] has the structural formula $[(SiO_4^{4-})(MoO_4^{2-})(Mo_8O_{25}^{2-})]$. Seven molybdenum atoms in **172** have Type II coordination geometry and two have Type I/II geometry, and when coordination geometry at the Type I/II centers is idealized to Type I geometry, the valence structure **173** is obtained.

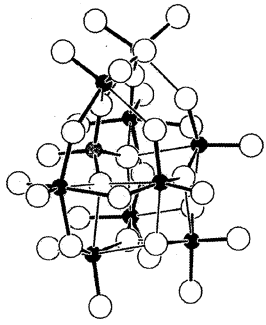

172

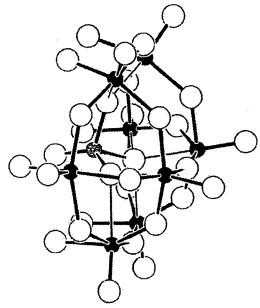

174

The $Mo_8O_{25}^{2-}$ building unit in **173** is a hybrid tricyclic unit, where all three rings are joined at two Type I/II molybdenum centers idealized as Type I centers in **173**. Idealization of Type I/II coordination geometry to Type II geometry would yield the alternative structural formula $[(SiO_4^{4-})(MoO_4^{2-})(Mo_2O_7^{2-})(Mo_6O_{18})]$. The $SiMo_9O_{33}^{8-}$ structure **172** may be derived from the β-$SiMo_{12}O_{40}^{4-}$ structure **154** in two steps. In the first step, the hypothetical β-$SiMo_8O_{31}^{10-}$ anion **174** is obtained by removing an $Mo_4O_9^{6+}$ group from **154** to form the hypothetical β-$SiMo_8O_{31}^{10-}$ anion **174**. In the second step, an MoO_2^{2+} group is added to **174** to form the $SiMo_9O_{33}^{8-}$ anion **172**.

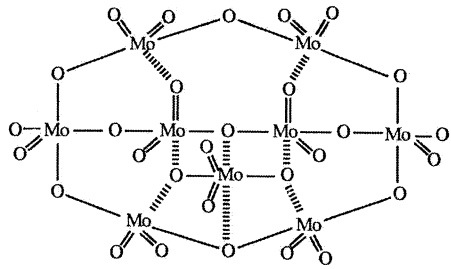

173

In $Mo_{36}O_{128}H_{32}^{8-}$ anion **175**, observed in $K_8[Mo_{36}O_{112}(H_2O)_{16}]\cdot nH_2O$ [288, 289] and $Na_8[Mo_{36}O_{112}(H_2O)_{16}]\cdot 58H_2O$ [290], has the structural formula $[(MoO_4^{2-})_2(Mo_{34}O_{104}^{4-})(H_2O)_{16}]$, where the hybrid polycyclic $Mo_{34}O_{104}^{4-}$ building unit **176** has eight ring junctions at four trivalent oxygen atoms and four seven-coordinate molybdenum atoms, junctions that are more readily identified in its valence structure **177**, where weak Mo–O bonds have been deleted for purposes of clarity.

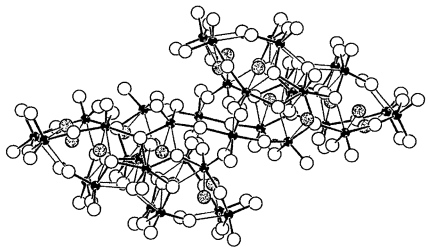

175

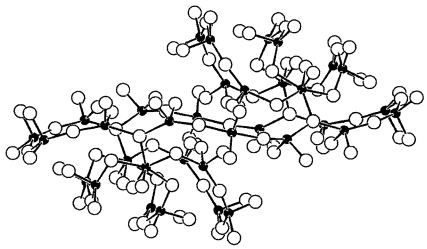

176

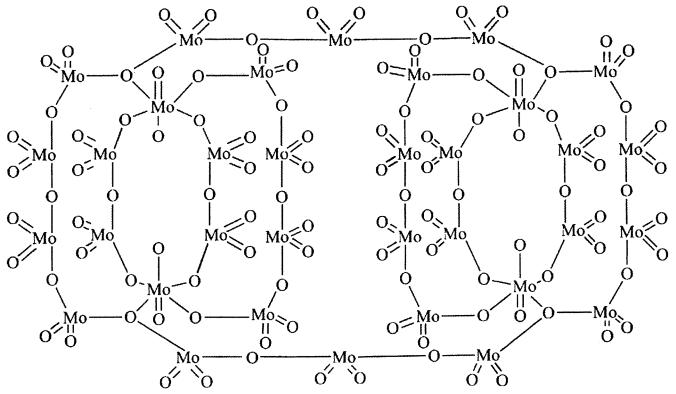

177

Cleavage of the four bonds connecting the oxygen and molybdenum junction atoms yields an $Mo_{14}O_{42}$ dioxomolybdenum ring plus two $Mo_{10}O_{31}^{2-}$ fragments. In the $Mo_{36}O_{128}H_{32}^{8-}$ anion **175**, each $Mo_{10}O_{31}^{2-}$ fragment is connected to three water molecules and a single orthomolybdate unit as shown in **178**.

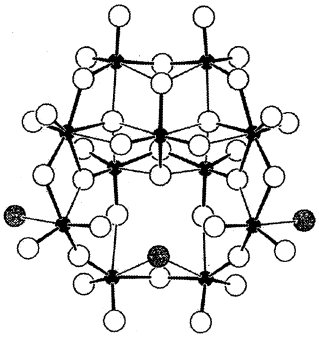

178

3.7. THE TRIOXOMOLYBDENUM BUILDING UNIT

The oxalate complex $NaNH_4[MoO_3C_2O_4]\cdot 2H_2O$ contains $(MoO_3)_\infty$ trioxomolybdenum chain polymers and $C_2O_4^{2-}$ oxalate ligands, where each bidentate oxalate ligand is bonded to one molybdenum center and one of the doubly-bonded oxygen atoms in each trioxomolybdenum unit is linked to a neighboring MoO_3 unit by a weak Mo–O bond [291, 292]. Here, Type III coordination geometry is quite symmetric: 2.21- and 2.17-Å bonds to oxalate ligands are *trans* to 1.72- and 1.74-Å bonds to the terminal oxygen atoms, and bonds to each doubly-bridging oxygen atom connecting MoO_3 units are 1.77 and 2.23 Å long.

The $Cu_6Mo_5O_{18}$ structure [293, 146] contains monomeric trioxomolybdenum building units, and its $[(MoO_4^{2-})_{3\infty}(MoO_3)_{2\infty}]$ oxomolybdenum (VI) structure **179** is obtained by adding MoO_3 groups to the $(MoO_4^{2-})_\infty$ structure observed in $HgMoO_4$ (see **31** in Section 3.1.1).

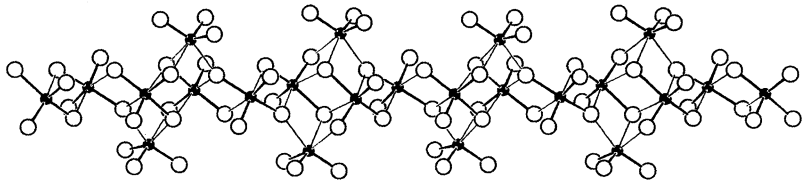

179

180

For purposes of comparison, the $HgMoO_4$ orthomolybdate polymer is drawn in **180** from the same viewpoint adopted in **179**. Type III, Type II and Type I/II octahedral coordination geometry is observed at molybdenum centers in $Cu_6Mo_5O_{18}$, and idealization of Type I/II centers to Type II geometry yields dioxomolybdenum orthomolybdate and trioxomolybdenum building units.

The $(NH_4)_4Cu_2Mo_8O_{28}(H_2O)_{10}$ structure [294] contains discrete $Mo_8O_{28}^{8-}$ or $[(Mo_2O_7^{2-})_2(MoO_4^{2-})_2(MoO_3)_2]$ anions, where molybdenum centers have Type II and Type III coordination geometry as shown in **181**. This anion is designated γ-$Mo_8O_{28}^{8-}$ to distinguish it from the

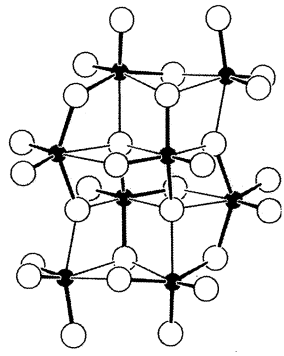

181

α, β, γ and ε isomers treated in Section 3.1.

Trioxomolybdenum building units are also found in the trinuclear squarate complex $[Mo_3O_8(OCH_3)(C_4O_4)_2]^{3-}$ [115] **182** and the binuclear 1-oxyethylidenediphosphonate complex $\{Mo_2O_6[CH_3C(O)(PO_3)_2]\}^{5-}$ **183** [295]. In addition to a trioxomolybdenum unit, the first complex contains an $Mo_2O_7^{2-}$ chain building unit and the second contains an orthomolybdate building unit.

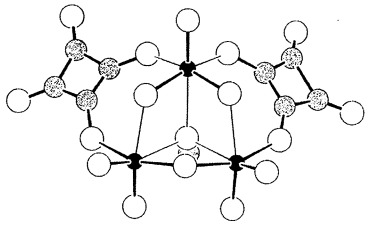

182

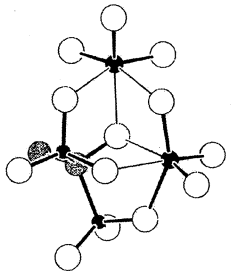

183

Three closely related trinuclear complexes containing trioxomolybdenum building units are shown in **184-186.** Molybdenum centers in the $\{Mo_3O_7[CH_3C(CH_2O)_2]_2\}^{2-}$ structure **184** [296] have Type II, Type II/III, and Type III coordination geometry and when Type II/III geometry is idealized to Type II geometry as in **184**, this complex has the structural formula $[(MoO_4^{2-})_2(MoO_3)]$. Its methylated derivative $\{Mo_3O_6(OCH_3)[CH_3C(CH_2O)_3]_2\}^-$ **185** [296, 297] also contains MoO_4^{2-} and MoO_3 building units but the CH_3O–Mo bond length is 1.87 Å and this molybdenum center therefore has Type II/III as opposed to Type III coordination geometry. Two alternative descriptions of the structure are valid, one involving two MoO_4^{2-} building units and one MoO_3 building unit as in **184** and another involving $Mo_2O_7^{2-}$ and MoO_4^{2-} building units. Precisely the same situation prevails in the $\{[C_5(CH_3)_5]Rh\}_2Mo_3O_9(OCH_3)_4$ structure **186** [95].

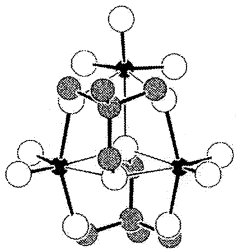

184

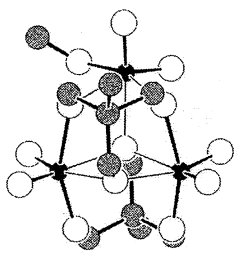

185

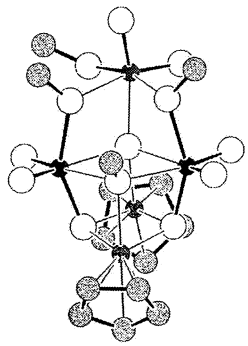

186

Portions of two larger structures treated in previous Sections are closely related to structures **184-186.** Removal of one $MoO_2(OCH_2CH_3)^+$ group from the tetranuclear $Mo_4O_8(CH_3CH_2O)_2[CH_3C(CH_2O)_3]_2$ complex **44** (see Section 3.1.2) yields the ethyl analogue of the$\{Mo_3O_6(OCH_3)[CH_3C(CH_2O)_3]\}^-$ anion **185.** Also, the central molybdenum atom of the $Mo_3O_{11}^{4-}$ hybrid chain building unit **165** in betpakdalit (see **167** in Section 3.6.1) has Type I/III coordination geometry that can be idealized to Type III geometry. From this point of view, the $Mo_3O_{11}^{4-}$ unit in **167** contains the same $[(MoO_4^{2-})_2(MoO_3)]$ configuration found in **184–186.**

For the sake of completeness, the $\{Mo_2O_4[O_2NC(CH_2O)_3]_2\}^{2-}$ anion **187** [296, 297] and the $I_2Mo_2O_{16}^{6-}$ anion **188** [298] are shown from about the same viewpoint adopted in **167.**

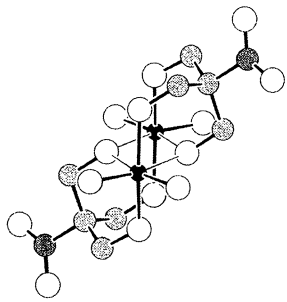

187

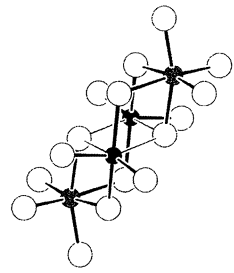

188

Both structures contain two monomeric orthomolybdate structural building units connected by a pair of bridging oxygen atoms as in **184–186.** The triolate ethoxide complex $\{MoO[(CH_3(CH_2O)_3](CH_3CH_2O)\}_2$ mentioned in Section 3.4.1 may be viewed as a derivative of **187** obtained by ethylating two centrosymmetrically-related terminal oxygen atoms. Although **187** and this ethoxy derivative both have the same M_2O_{10} metal-oxygen framework geometry defined by two MO_6 octahedra sharing an edge, they are valence isomers represented by the structural formulas $[(MoO_4^{2-})_2(O^{2-})_2]$ and $[(MoO_5^{2-})_2]$, respectively.

4. Structural Building Units in High-Valent Early Transition Metal Oxides

In Section 3, a large number of oxomolybdenum(VI) compounds were reduced to a relatively small number of molecular and polymeric structural building units. In the first parts of this Section, the identification of structural building units in other classes of high-valent early transition metal oxide compounds is briefly considered. Next, the possibility of treating dynamic behavior in terms of structural building units is explored. This discussion is followed by some general comments concerning the scope and limitations of the approach promoted in this Chapter.

4.1. MOLYBDENUM BLUES, BRONZES, AND OTHER DERIVATIVES

Unlike polynuclear oxomolybdenum(V) compounds, whose structures generally have little in common with the structures adopted by oxomolybdenum(VI) compounds [299], mixed-valence oxomolybdenum(V/VI) compounds frequently adopt structures based on the same building units encountered in oxomolybdenum(VI) chemistry. In addition, derivatives obtained by replacing metal and/or oxygen atoms in oxomolybdenum(VI) with heteroatoms often have the same structure as their parent compounds.

4.1.1. *Molybdenum Blues*

Mixed-valence Mo(V/VI) polyoxometalates are known as molybdenum blues [300, 301]. In some cases, molybdenum blues have structures very similar to those adopted by oxomolybdenum(VI) compounds, structures such as the α- and β-Keggin structures described above in Section 3.5.1 [302, 303]. In other cases, the structure of a molybdenum blue may be formally derived from a known oxomolybdenum(VI) structure by a condensation process involving formal loss of O^{2-}, as in the case of the $Mo_{14}O_{46}^{10-}$ anion [304], whose structure may be generated from two $Mo_7O_{24}^{6-}$ anions **121** by elimination of two O^{2-} anions to generate a hypothetical $Mo_{14}O_{46}^{8-}$ anion having the $Mo_{14}O_{46}^{10-}$ structure. In most cases, however, the structural relationship between molybdenum blues and Mo(VI) polyoxometalates is more tenuous. Consider, for example, the $[(MoO_3)_{176}(H_2O)_{63}(CH_3OH)_{17}H_n]^{(32-n)-}$ anion [305]. Its structure is based on an $Mo_{2n}O_{7n}$ double ring, $n = 32$, a cyclic version of the $Mo_{2\infty}O_{7\infty}$ monoxomolybdenum double chain **147**, where terminal oxygen atoms are directed away from the center of the ring. Orthomolybdate groups are bonded to the molybdenum atoms in this ring as shown in **108**: each MoO_4 group is bonded to four molybdenum atoms in the $Mo_{64}O_{224}$ ring such that six-coordination is achieved at all 64 molybdenum atoms, requiring 64/4 = 16 MoO_4 groups. The remaining molybdenum atoms form Mo_6O_{15} groups connected to the periphery of the $Mo_{64}O_{224}$ double ring as shown in **189**. Each

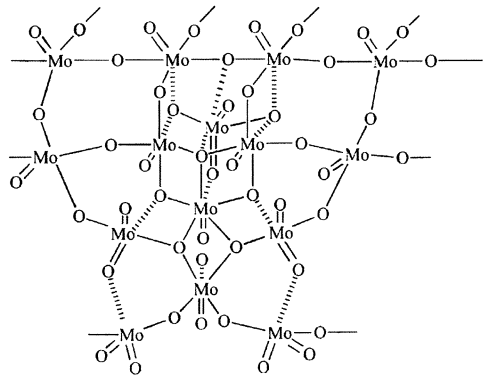

189

MoO_4 group is connected to one and only one Mo_6O_{15} group by a weak Mo–O bond, also shown in **189**, creating a total of 16 seven-coordinate molybdenum centers.

The complete structure is obtained by coordinating H_2O or CH_3OH ligands to the remaining five molybdenum centers in each Mo_6O_{15} group. There are a total of sixteen Mo_6O_{15} groups, one per MoO_4 group, accounting for all $16\times5 = 80$ H_2O/CH_3OH groups in the anion. Each pentagonal bipyramidal molybdenum center is linked to five neighboring octahedral molybdenum centers by sharing polyhedral edges, a configuration also observed in the $Mo_{36}O_{128}H_{32}^{8-}$ anion **175**. However, metal-oxygen bonding within this Mo_7O_{27} group is quite different in the mixed valence compound (see **190**) and the Mo(VI) compound (see **191**).

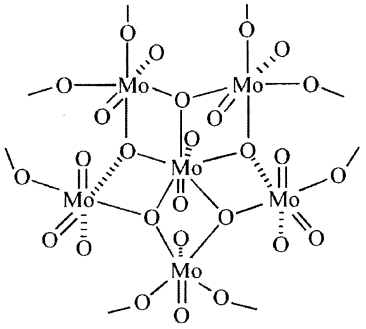

190

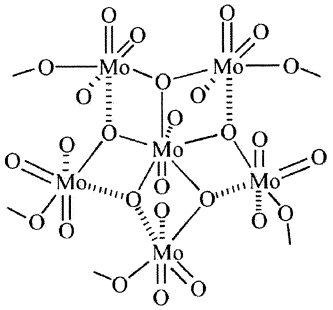

191

4.1.2. *Mixed-Valence Molybdenum Oxides and Molybdenum Bronzes*

In general, simple mixed-valence molybdenum(V/VI) oxides [306] and complex mixed-valence molybdenum(V/VI) oxides [307], known as molybdenum bronzes, may be reduced to their structural building units following the same procedures used for analyzing oxomolybdenum(VI) compounds. Some mixed-valence oxides like Mo_5O_{14} [308] and $Mo_{17}O_{47}$ [309] have structures based on monoxomolybdenum infinite sheet polymers. These particular compounds contain pentagonal Mo_7O_{27} groups of the type just described for the molybdenum blue $[(MoO_3)_{176}(H_2O)_{63}(CH_3OH)_{17}H_n]^{(32-n)-}$ (see **190**) and the Mo(VI) polyoxometallate $Mo_{36}O_{128}H_{32}^{8-}$ (see **191**). Other compounds such as the molybdenum bronze $K_3Mo_{10}O_{30}$ have a different type of structure containing both monoxomolybdenum and dioxomolybdenum groups [310]. The $K_3Mo_{10}O_{30}$ structure reduces to $Mo_\infty O_{3\infty}^{3-}$ quadruple chain building units **192**, and these infinite chain units are stacked into infinite sheets where weak Mo–O bonds are formed between five-coordinate molybdenum atoms and bridging oxygen atoms in neighboring $Mo_\infty O_{3\infty}^{3-}$ chains.

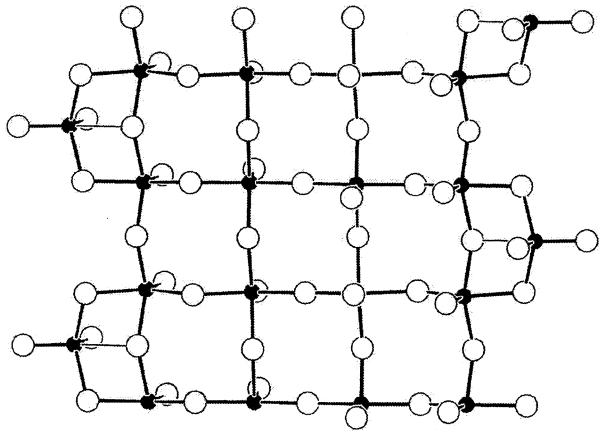

192

The quadruple chains stacked in this fashion form staircase-like infinite sheets curiously similar to the oxomolybdenum(VI) sheets **104** in $Cs_2Mo_7O_{22}$ described in Section 3.1.5.

Kihlborg has analyzed systematic patterns of *trans* bond length alternation in mixed-valence molybdenum(V/VI) oxides and pointed out how the "normal" long-short-long-short sequence is sometimes interrupted by a long-short-short-long sequence at the midpoint of the chain [311–314]. Consider, for example, the pattern of bond length alternation **193** observed in γ-Mo_4O_{11} [315]. Bond length alternation of the type discussed in Section 2.1 and illustrated in **7** is violated at the midpoint of the chain, and Mo=O groups at opposite ends of the chain are pointed in opposite directions, not in the same direction as shown in **7**.

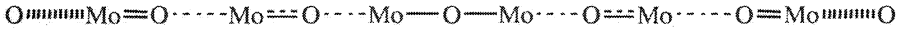

193

4.1.3. *Oxomolybdenum(VI) Derivatives*

The integrity of structural building units is often maintained when Mo(VI) centers in oxomolybdenum(VI) compounds are replaced by other d^0 early transition metal centers, and the α- and β-$V_2Mo_6O_{26}^{6-}$ ions mentioned in Section 3 are representative. Although replacement of oxygen atoms with heteroatoms has not been explored as extensively, many cases are known where structural building units are preserved, such as $NaMoO_3F$ [316], derived from α-$MoO_3 \cdot H_2O$ by replacing water ligands with fluoride ligands (see **111**), and $[Mo_5O_{18}(MoNC_6H_4CH_3)]^{2-}$ [317], derived from $Mo_6O_{19}^{2-}$ by replacing a doubly-bonded terminal oxo

ligand with a *p*-tolylimido group (see **151**). Sometimes, as in the case of $Mo_8O_{20}(NNPh)_6^{4-}$ **23**, where six terminal oxo ligands in α-$Mo_8O_{26}^{4-}$ **122** are replaced by phenyldiazenido ligands, structural building units remain intact, but their conformations are altered. Finally, it should be noted that ligand substitution can have significant repercussions even in mononuclear complexes. The mononuclear *cis*-dioxomolybdenum(VI) complex $MoO_2[SC(CH_3)_2CH_2N(CH_3)_2]$ is formally derived from $MoO_2(OCH_2CH_2OH)_2$, but molybdenum coordination geometry is clearly nonoctahedral and has been described as skew trapezoidal [318].

4.2. EARLY TRANSITION METAL OXIDES IN GENERAL

If the bond length criteria employed above for the identification of structural building units in oxomolybdenum(VI) compounds are applied to oxotungsten(VI) compounds, families of structural building units emerge that are in many respects similar to those observed for oxomolybdenum(VI) compounds. Oxovanadium(V) compounds may be approached in a similar fashion, and structural building units can in many cases be identified that are fragments of the V_2O_5 structure in the same sense that oxomolybdenum(VI) building units are fragments of the α- and β-MoO_3 structures as described in Section 3 [319]. Structural building units are generally not as readily identified in Nb(V), Ta(V), Ti(IV), Zr(IV), and Hf(IV) oxide materials. However, when attention is focused on perovskite-like materials, Kihlborg's approach to molybdenum oxides is applicable.

Structural building units may be unambiguously identified in early transition metal oxide compounds only in those cases where metal coordination is sufficiently irregular such that a clear distinction can be made between long bonds and short bonds. Moreover, the identification of structural building units is useful only if the distinction between strong and weak bonds is defined in such a fashion that a set characteristic structural building units emerge. Since irregular coordination geometry in early transition metal oxide compounds apparently has its physical origin in metal-oxygen d-p π bonding interactions as described in Section 2.1, it should come as no surprise that structural building units tend to be well-defined when high-valent, electron-deficient metal centers with appropriately low-lying, empty d orbitals are involved.

4.3. DYNAMIC BEHAVIOR OF OXOMOLYBDENUM(VI) BUILDING UNITS

Relatively little attention has been focused on the detailed mechanisms governing the interconversion of structural building units in oxomolybdenum(VI) compounds. An interesting pathway was proposed several years ago for conversion of the α-$Mo_8O_{26}^{4-}$ or $[(MoO_4^{2-})_2(Mo_6O_{18})]$ anion **119** into the isomeric β-$Mo_8O_{26}^{4-}$ or $[(Mo_4O_{12})_2(O^{2-})_2]$ anion **118**, a transformation known to pro-

ceed in solution [320]. Some of the reaction intermediates believed to be involved have since been isolated and characterized [238, 321], lending some plausibility to these speculations.

A structural rearrangement of the $C_6H_5AsMo_7O_{25}^{4-}$ or $[(C_6H_5AsO_3^{2-})(MoO_4^{2-})(Mo_6O_{18})]$ anion where structural building units remain intact has been characterized using variable-temperature ^{17}O NMR line-shape analysis, ^{17}O spin saturation transfer techniques, and ^{17}O label crossover experiments [322]. This anion is a derivative of the α-$Mo_8O_{26}^{4-}$ anion **122**, where $C_6H_5AsO_3^{2-}$ and MoO_4^{2-} groups are bonded to opposite sides of the Mo_6O_{18} ring. Structural rearrangement is intramolecular and involves inversion of the Mo_6O_{18} ring accompanied by reorientation of the MoO_4^{2-} building unit relative to the Mo_6O_{18} ring. Both of these processes are degenerate, that is, neither involves net structural change. The $C_6H_5AsMo_7O_{25}^{4-}$ anion is therefore a fluxional (stereochemically nonrigid) molecule [323], displaying the same type of behavior characteristic of small molecules such as ammonia. Fluxional processes such as Mo_6O_{18} ring inversion and MoO_4^{2-} reorientation in $C_6H_5AsMo_7O_{25}^{4-}$ or NH_3 inversion are often referred to as pseudorotations, since interconversion of reactant and product configurations gives the appearance of a simple rotation operation if the atoms are not labeled. For example, rotation of **194** by 180° about a vertical axis followed by a smaller rotation about a horizontal axis yields **195**.

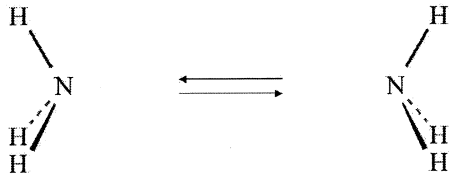

194 **195**

The significance of the fluxionality identified in $C_6H_5AsMo_7O_{25}^{4-}$ rests in the fact that MoO_4^{2-} reorientation and Mo_6O_{18} ring inversion are achieved without breaking any strong Mo–O bonds, that is, without breaking any M-O single or double bonds as defined in Section 2.2. This process involves breaking only weak Mo–O bonds, those interconnecting the MoO_4^{2-} and Mo_6O_{18} building units, and, in the case of Mo_6O_{18} ring inversion, a conformational change. A rapid structural rearrangement that preserves the integrity of structural building units offers physical support for the assumption that long bonds are weak bonds and short bonds are strong bonds, since breaking relatively weak bonds implies relatively low activation energies.

Generalizing the results obtained for the $C_6H_5AsMo_7O_{25}^{4-}$ isomerization, it is natural to ask whether intramolecular isomerizations in polymeric solids, usually referred to as structural phase transitions, might also have low activa-

tion energies if the integrity of structural building units is preserved. With this possibility in mind, interconversion of the low temperature and high temperature $Li_2Mo_4O_{13}$ polymorphs introduced in Section 3.1.4 warrants reexamination. Recall that interconversion of the H–$Li_2Mo_4O_{13}$ and L–$Li_2Mo_4O_{13}$ polymorphs may be achieved by a sheer motion within tetramolybdate double chains. Referring back to **84** and **86**, H–$Li_2Mo_4O_{13}$ double chains in **84** are generated from L–$Li_2Mo_4O_{13}$ double chains in **86** when the upper single chain is shifted to the right relative to the lower single chains in the double chain. This shear transformation involves shifting only the weak metal-oxygen bonds interconnecting $Mo_4O_{13}^{2-}$ building units as shown in valence structures **196** and **197**, where one $Mo_4O_{13}^{2-}$ unit is included from the relevant upper and lower single chains in **84** and **86**, respectively.

196

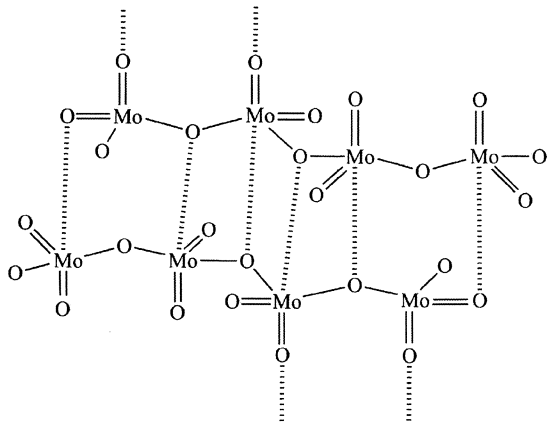

197

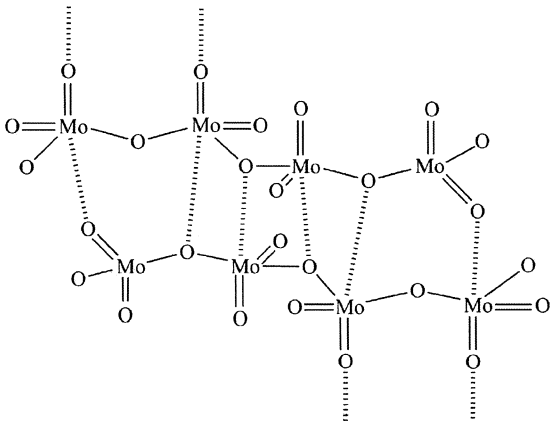

As far as the relationship between the two $Mo_4O_{13}^{2-}$ units are concerned, the **196/197** interconversion is a pseudorotation in precisely the same fashion that the **194/195** interconversion is a pseudorotation: in both cases one configuration is related to the other by a 180° rotation about a vertical axis followed by a smaller rotation about a horizontal axis such that the two configurations are related by a translation operation. Note, however, that interconversion of **196** and **197**, unlike the interconversion of **194** and **195**, does not require labeling of nuclei to distinguish between pseudorotation and rotation, since the weak bonds to adjacent single chains in the L– and H– $Li_2Mo_4O_{13}$ structures, indicated by dashed lines extending above and below the $Mo_4O_{13}^{2-}$ dimers in **196** and **197**, provide the required labeling. This is often the case when a molecular transformation is characterized solely by the relationship between initial and final configurations: processes that cannot be differentiated when the configurations rotate freely in space may nonetheless be distinguishable in the solid state if the configurations no longer have rotational freedom [324].

The purpose of the exercise just completed is not to suggest that structural phase transitions are energetically favorable only when the integrity of structural building units are retained. Instead, its purpose is to illustrate how the identification of structural building units may lead to an enormous conceptual simplification of complex structural transformations.

4.4. LIMITATIONS AND SCOPE OF THE MOLECULAR APPROACH

The exercise of first identifying molecular building units in high-valent early transition metal oxide compounds and then drawing their valence structures solely on the basis of bond length criteria is a purely formal procedure: its starting point is bond lengths and its endpoint is a diagrammatic representation of these very same bond lengths. For example, the valence structures included in this Chapter offer no insight into the relative charges on nonequivalent metal and oxygen centers [325], and from this point of view, they are no more informative than valence structures of simple organic molecules such as ethyl acetate **198**, which yield no information about the relative charges on nonequivalent carbon and oxygen atoms.

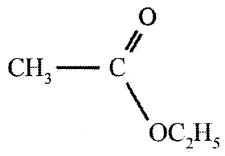

198

Nor can the formalisms described in this Chapter make predictions concerning the structures of complex oxides. Since structural information is a prerequisite, valence structures are no more capable of structural predictions than orbital

hybridization formalisms that also require structural information as input. Furthermore, the present formalism, although motivated by physical considerations such as π-bonding and off-center displacement, in no way embodies these physical considerations: valence structures **199** and **200**, drawn by Werner [326] well before the advent of σ and π bonding theory, convey the same structural information as valence structures **4** and **5**, respectively. The remaining valence structures drawn in this Chapter could also be redrawn using Werner's nomenclature without losing any of their significance.

199

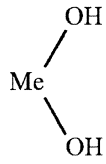

200

The significance of structural building units and their representation as valence structures becomes apparent only when the question of structure-property relationships is addressed. The closing paragraphs of this Chapter are therefore devoted to a brief discussion of how these valence structures serve as a bridge between structure and properties in high-valent early transition metal oxide compounds.

A key chemical property of many early transition metal oxides is there ability to catalyze the selective O_2 oxidation of small organic and inorganic molecules [1]. The selective oxidation of alcohols to aldehydes is a representative process, and when α-MoO_3 acts as the catalyst, oxidation proceeds after initial formation of a surface alkoxide complex [327]. Given that the molybdenum centers in $\alpha-MoO_3$ have Type II octahedral coordination geometry, this alkoxide group is most likely bonded to a Type II oxomolybdenum(VI) center as shown in **201**. This environment is observed in $[(P_3O_9)MoO_2(OCH_2CH_3)]^{2-}$, **25** in Section 3.1.1, and since thermolysis of this complex yields acetaldehyde [328], the oxidation reaction may be represented as conversion of **201** into **202**.

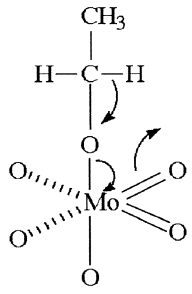

201

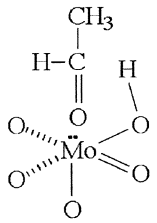

202

Arrows drawn in **201** indicate the net rearrangement of valence electron pairs implied by reduction of the hexavalent Mo(VI) center to a tetravalent Mo(IV) center and oxidation of the alkoxide ligand to acetaldehyde. Since valence structures **201** is Lewis structure [329], the "arrow convention" may be used to represent its transformation into **202** [330]. Free radical reactions may be treated in a similar fashion by using single-headed arrows to follow the movement of single electrons. For example, photolysis of $[(P_3O_9)MoO_2(OCH_2CH_3)]^{2-}$ yields ethylene as the organic product [328], a β elimination reaction known as a Norrish Type II cleavage in carbonyl chemistry [331]. The mechanism shown in Scheme III may be justified by drawing an analogy between molybdenyl and carbonyl chemistry: $n \rightarrow \pi^*$ electronic excitation generates a molybdenum(V) center plus an oxygen anion radical capable of γ-hydrogen atom abstraction.

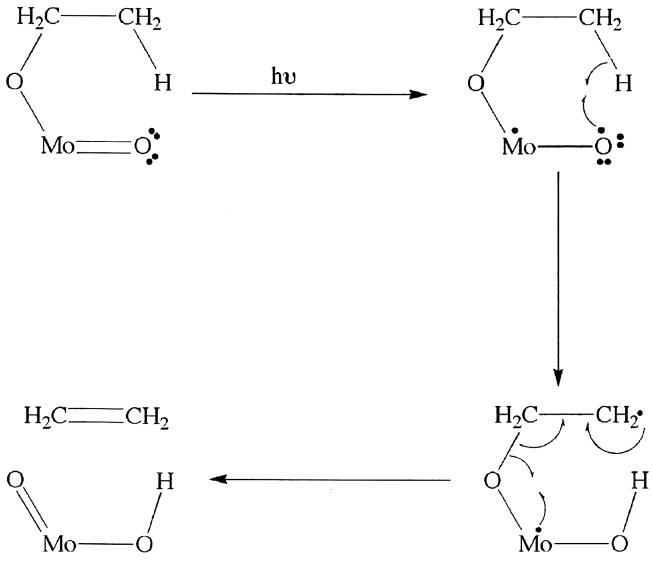

Scheme III

Metal-oxygen multiple bonding affects the physical as well as the chemical properties of high-valent transition metal oxide compounds. Electrons in π bonds, unlike electrons in σ bonds, are not localized in the strongly bonding region along the internuclear axis, and they are therefore relatively responsive to externally applied electric fields. The electrooptic effect, where permittivity and therefore the refractive index are altered by application of an electric field, therefore tends to be large in high-valent early transition metal oxides, particularly when chains of M=O units are aligned in parallel arrays [332]. This is the case in materials like lithium metaniobate, $LiNbO_3$, where trioxoniobium(V) building units **203** are arranged such that three polar M=O chains intersect at each niobium center. Since this structure is polar, the electrooptic effect is linear and therefore unusually large. Lithium metaniobate is also a very robust material, retaining its polar structure up

to about 1200° C, only about 100° below its melting temperature [333]. Its various nonlinear optical properties have therefore been studied in great detail and found widespread practical application [334].

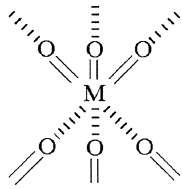

203

Many of the unusual electrical properties associated with high-valent early transition metal compounds have their origin in M=O chains whose polarity may be reversed at temperatures far below their melting temperatures. For example, barium metatitanate is a tetragonal, polar material at ambient temperature, but it loses its polarity at 130°C, its Curie temperature T_C [335]. In *t*-$BaTiO_3$, titanium(IV) centers all have Type I octahedral coordination geometry and are linked together as shown in **204** such that all of the titanyl groups are oriented in the same direction. Tetragonal barium metatitanate is spontaneously polarized at temperatures below 130° C, and since the direction of polarization may be reversed by application of an electric field, *t*-$BaTiO_3$ is classified as a ferroelectric material.

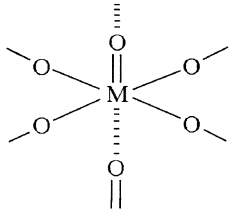

204

The degree of polarization is sensitive to small changes in metal-oxygen bond lengths, and polarization can be modulated by application of external mechanical forces: *t*-$BaTiO_3$ is a piezoelectric material.

Spontaneous polarization is a well-defined concept on the molecular level in *t*-$BaTiO_3$ and related materials. For example, the direction of polarization in **205** and **206** may be reversed by transferring two protons from one end of the chain to the opposite end, but these chains are not necessarily ferroelectric because their polarization might be induced by unsymmetric protonation.

205

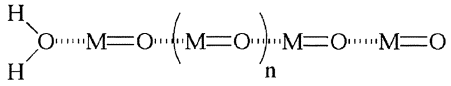

206

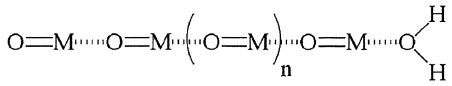

207

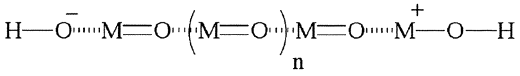

Polarization is spontaneous when it arises in an otherwise symmetric environment as in **207**, and spontaneous polarization in an otherwise symmetric environment is accompanied by polarization charges, also shown in **207**. Note that valence structures **205** and **206** represent Mo=O chains in the $[H_6PMo_5O_{34}]^{3-}$ anion discussed in Section 3.5.2 (*cf.* **162** and **163**).

In the absence of an externally applied electric field, single-domain crystals of ferroelectric materials like *t*-$BaTiO_3$ tend to be thermodynamically unstable due to polarization charge that accumulates on crystal surfaces. This charge accumulation is mitigated by formation of domain structures that allow for neutralization of polarization charges at 90^circ domain walls. In *t*-$BaTiO_3$, for example, characteristic domain boundaries are formed between domains related by 90° and 180° polarization rotation [336]. Both types of domain wall are illustrated in **208**, where dashed lines represent the centers of domain walls. Here, diagonal 180° domain boundaries intersect vertical 90° domain boundaries. The antiparallel dipole configuration at 180° domain walls serves to separate regions of positive and negative charge on the same side of a 90° domain wall, and the head-to-tail configuration at 90° domain walls insures that negative charge on one side of the domain wall is counterbalanced by positive charge on the opposite side of the wall. Note that 180° polarization rotation implies no macroscopic mechanical strain at 180° domain walls, but 90° polarization rotation implies macroscopic mechanical strain since the distance spanned by two metal-oxygen single bonds at a Type I octahedral titanium(IV) center is different from the distance spanned by a double bond and a weak bond. As a result, electrostatic forces that tend to reduce the width of 90° domain walls are opposed by mechanical forces favoring domain walls sufficiently thick to accommodate the mechanical strain implied by the structural mismatch at 90° domain boundaries [337].

Domains and domain wall configurations in high-valent early transition metal ferroelectrics differ in two respects from the idealized valence structures shown in

207 and **208**. First, metal coordination geometry does not change discontinuously at domain boundaries, particularly when polarization charge is created. In reality, the degree of bond length alternation changes continuously in order to minimize mechanical strain and/or delocalize charge. Second, ferroelectric domain boundaries are dynamic entities, not static structures. Domain wall dynamics plays a key role during polarization reversal, since polarization reversal is not a concerted process but a stepwise process involving domain wall migration as well as the creation and elimination of domain walls [336].

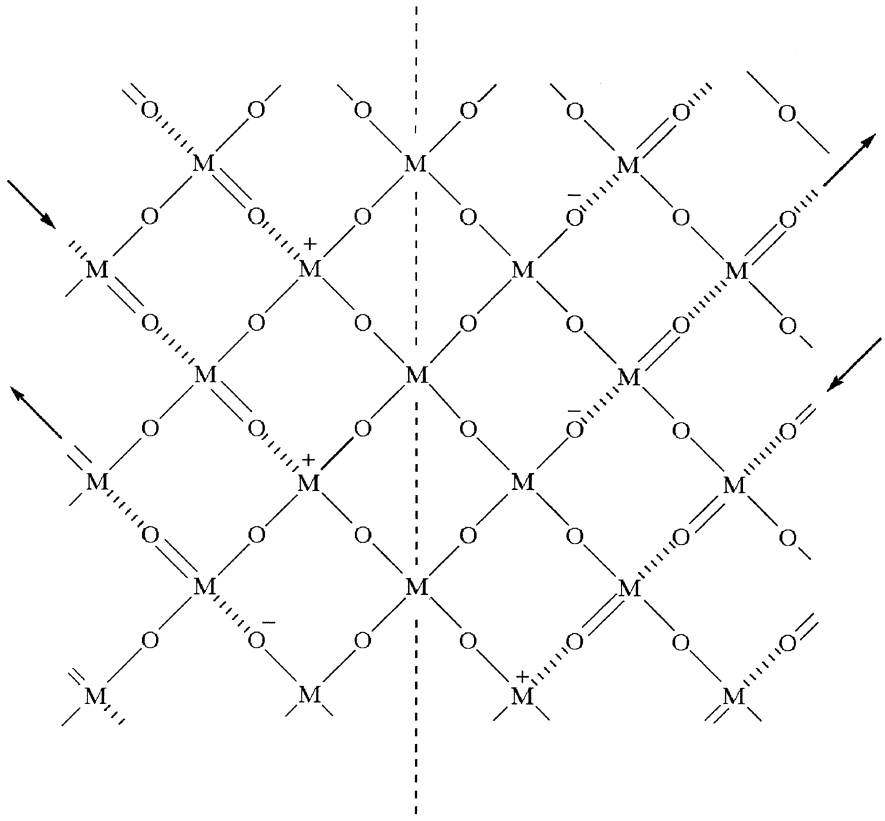

208

Domain wall dynamics also play a key role in determining the dielectric properties of ferroelectric materials like *t*-$BaTiO_3$ at temperatures just above the Curie temperature T_C, where exceptionally high permittivities are observed. The ferroelectric and high-κ properties of high-valent early transition metal oxides have a common origin, namely, bond length alternation along metal-oxygen chains. The domain wall dynamics involved are conveniently described using soliton terminology [338], following the approach successfully adopted for analysis of bond length alternation in homoatomic chains in materials like polyacetylene [339], het-

eroatomic chains in materials like polynitriles [340, 341], and hydrogen-bonded chains like $(HF)_x$ [342]. Entropic considerations and the presence of vacancies and defects dictate that bond length alternation of the type shown in **207** cannot extend indefinitely in real materials [343]. Structural domains are formed, domains of the type shown in **209**, where domain boundaries have been artificially compressed to single atoms.

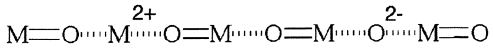

209

These boundaries can expand and contract as shown in **210** and **211** for dipositive domain walls ("dipositive solitons") and dinegative domain walls ("dinegative solitons"), respectively, and in this fashion delocalize charge and reduce electrostatic repulsion between opposite ends of the domain wall. Dinegative and dipositive domain walls migrate by expanding in one direction and contracting in the opposite direction, and when they collide, a dipolar domain wall ("bipolaron") is formed as shown in **212**. Here, opposite ends of the domain wall have opposite charges, and contraction of a dipolar domain wall ultimately leads to its elimination as shown in **213**. Since **212** and **213** are reversible processes, creation of a dipolar domain wall according to **213** followed by division according to **212** provides a mechanism for generating dipositive and dinegative domain walls. Note that dinegative and dipositive domain walls separate domains having opposite polarity ("twin domains") and dipolar domain walls separate domains having the same polarity ("antiphase domains").

210

211

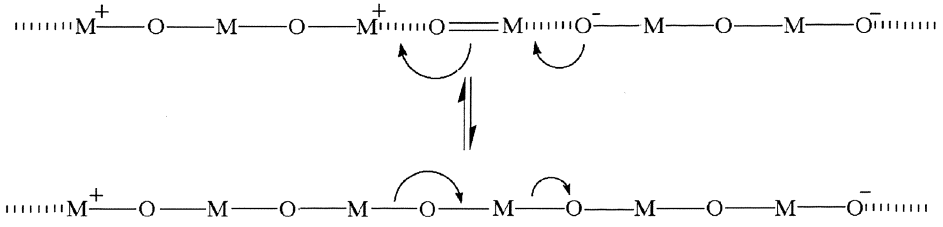

212

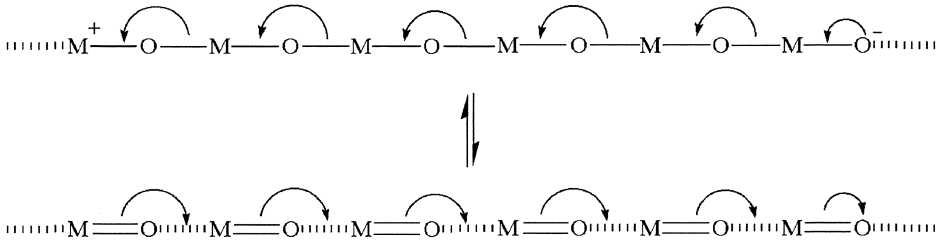

213

Although entropically favorable, the formation of dynamic domain walls is energetically unfavorable. At low temperatures, domain boundaries and hence polar domains are largely "frozen" into electrostatically stabilized domain wall configurations of the type shown in **208** for *t*-$BaTiO_3$, where a dipositive soluton is highlighted. With increasing temperature, entropic factors become increasingly important: domain walls grow in size and/or number and their mobility increases [344]. Polar domains eventually become sufficiently small and sufficiently isolated by domain walls that bulk spontaneous polarization disappears. In cases like *t*-$BaTiO_3$ where mechanical forces influence the stability of domain wall configurations, the disappearance of spontaneous polarization is associated with a structural phase transition [345]. However, formation of a nonpolar bulk phase does not imply disappearance of locally polar domains. These domains persist in the nonpolar phase as relatively short, polar metal-oxygen chains [346, 347], and since domain walls in these chains are very mobile, they are very responsive to externally applied electric fields. This facile response is the basis for the high permittivity observed at temperatures just above T_C in *t*-$BaTiO_3$ and related materials. At temperatures near T_C, these materials are fluxional [348], and their structural/dynamic behavior is characterized by a collective reaction coordinate or "soft mode" [349].

When d^0 early transition metal oxides are partially reduced to form blues and bronzes of the type discussed in Sections 4.1.1 and 4.1.2, the extra valence electrons occupy metal-oxygen d-p π^* antibonding orbitals localized largely at

the metal centers. Bond length alternation is inhibited in two directions at the reduced metal centers, stabilizing Type I octahedral coordination relative to Type II and Type III geometry. In soliton terminology, polarons are formed, and in polyoxometalates, these polarons may condense to form bipolarons, as described by Kazansky in this book. Larger clusters may form in polymeric systems, and in systems like $K_3Mo_{10}O_{30}$ where the number of electrons occupying π^* antibonding orbitals is less than the number of π^* antibonding orbitals available at Type I metal centers (see **192**), complex phase behavior is observed. Specifically, an incommensurate phase is observed at low temperatures, and the d-electron charge density wave associated with this phase is mobile. At very low temperatures, bond length alternation is still a viable option at d^0 Type I molybdenum(VI) centers in $K_3Mo_{10}O_{30}$ [350], and "memory effects" have been observed that are in some respects analogous to the dielectric behavior just described for *t*-$BaTiO_3$ [6].

When high-valent early transition metal oxide compounds are reduced to their structural building units and represented using valence structures, apparently different materials are revealed to have much in common. The same coordination geometries are observed in molecular and polymeric systems; molecular and polymeric materials both reduce to the same structural building units. "Spontaneous" patterns of bond length alternation observed in rings and cages also appear in chains and sheets, and patterns of bond length alternation may be "induced" by chemical substitution or by electric fields. Temperature-dependent fluxionality is observed both in molecular and polymeric systems. Dinegative metal-oxygen chains of the type found in dioxomolybdenum(VI) building units appear as dinegative domain boundaries in ferroelectrics; "abnormal" patterns of bond length alternation found in mixed-valence molybdenum(V/VI) oxides appear as dipositive domain boundaries. The pattern of behavior is unmistakable: structural building units and their valence structures provide a simple means for relating structure and properties in a large class of complex materials.

Acknowledgments

This material is based upon work supported by the U.S. Department of Energy, Division of Materials Sciences under Award No. DEFG02-91ER45439, through the Frederick Seitz Materials Research Laboratory at the University of Illinois at Urbana-Champaign. Ball and stick structures were drawn using Dr. Egbert Keller's SCHAKAL program.

WGK is grateful to Professor F.A. Cotton, whose patience and support have been greatly appreciated. This Chapter is offered as a birthday present long overdue.

References

1. Gates, B.C., Katzer, J.R., and Schuit, G.C.A. (1979) *Chemistry of Catalytic Processes*, McGraw-Hill, New York, p. 311.
2. Prokhorov, A.M. and Kuz'minov, Y.S. (1990) *Physics and Chemistry of Crystalline Lithium Niobate (Engl. Ed.)*, Adam Hilger, Bristol.
3. Burfoot, J.C. and Taylor, G.W. (1979) *Polar Dielectrics and their Applications*, University of California Press, Berkeley.
4. Moulson, A.J. and Herbert, J.M. (1990) *Electroceramics*, Chapman and Hall, London.
5. Lines, M.E. and Glass, A.M. (1977) *Principles and Applications of Ferroelectrics and Related Materials*, Clarendon Press, Oxford.
6. Greenblatt, M. (1988) Molybdenum Oxide Bronzes with Quasi-Low-Dimensional Properties, *Chem. Rev.* **88**, 31–53.
7. Kepert, D.L. (1972) *The Early Transition Metals*, Academic Press, London.
8. Wells, A.F. (1984) *Structural Inorganic Chemistry, 5th ed.* Clarendon Press, Oxford, pp. 575–625.
9. Müller, A., Peters, F., Pope, M.T. and Gatteschi, D. (1998) Polyoxometalates: Very Large Clusters–Nanoscale Magnets, *Chem. Rev.* **98**, 239–271.
10. Dickens, P.G. and Wiseman, P.J. (1975) Oxide Bronzes and Related Phases, in L.E. Roberts (ed.), *MTP International Review of Science, Series 2, Inorg. Chem., Vol. 10*, pp. 211–254.
11. Cheetham, A.K. (1981) Structural Studies on Nonstoichiometric Oxides Using X-Ray and Neutron Diffraction, in O.T. Sorensen (ed.), *Nonstoichiometric Oxides*, Academic Press, New York, pp. 399–433.
12. Porai-Koshits, M.A. and Atovmyan, L.O. (1974) *Crystalchemistry and Sterreochemistry of Coordination Compounds of Molybdenum (in Russian)*, Izd. Nauka, Moscow.
13. Porai-Koshits, M.A. and Atovmyan, L.O. (1975) Peculiarities of the Structures of Oxygen Compounds of Group V and VII Transition Metals and the Formation of Iso- and Heteropoly Anions, *Sov. J. Coord. Chem. (Engl. Transl.)* **1**(9), 1065–1074.
14. Goodenough, J.B. (1982) The Solid State Chemistry of Molybdenum, in H.F. Barry and P.C.H. Mitchell (eds.), *Proceedings of the Climax Fourth International Conference on the Chemistry and Uses of Molybdenum*, Climax Molybdenum Company, Ann Arbor, p. 1–23.
15. Mayer, J.M. (1988) Metal-Oxygen Multiple Bond Lengths: A Statistical Study, *Inorg. Chem.* **27**(22), 3899–3903.
16. Nugent, W.A. and Mayer, J.M. (1988) *Metal-Ligand multiple bonds: the chemistry of transition metal complexes containing oxo, nitrido, imido, alkylidene, or alkylidyne ligands*, Wiley, New York.
17. Ouahab, L. (1997) Organic/Inorganic Supramolecular Assemblies and Synergy between Physical Properties, *Chem. Mater.* **9**, 1909–1926.
18. Coronado, E. and Gomez-Garcia, C.J. (1998) Polyoxometalate-Based Molecular Materials, *Chem. Rev.* **98**, 273–296.
19. Werner, A. (1911) *New Ideas on Inorganic Chemistry* (Engl. Transl.), Longmans, Green, and Co., London, p. 98.
20. Kihlborg, L. (1963) Least squares refi nement of the crystal structure of molybdenum trioxide, *Ark. Kemi* **21**(34): 357–364.
21. Clark, G.M. (1972) *The Structures of Non-Molecular Solids*, Wiley, New York.
22. Hyde, B.G. and Anderson, S. (1989) *Inorganic Crystal Structures*, Wiley-Interscience, New York, p. 14.
23. Taube, H. (1978) Observations on Atom-Transfer Reactions, in D.B. Rorabacher and J.F. Endicott (eds.), *Mechanistic Aspects of Inorganic Reactions (ACS Symposia Series, No. 198)*, American Chemical Society, Washington, D.C., pp. 151–171.

24. Ballhausen, C.J. and Gray, H.B. (1961) The Electronic Structure of the Vanadyl Ion, *Inorg. Chem.* **1**(1), 111–122.
25. Megaw, H.D. (1957) *Ferroelectricity In Crystals*, Methuen, London, pp. 126–129.
26. Megaw, H.D. (1968) A Simple Theory of the Off-Centre Displacement of Cations in Octahedral Environments, *Acta. Cryst.* **B24**, 149–153.
27. Wheeler, R.A., Whangbo, M.-H., Hughbanks, T., Hoffmann, R., Burdett, J.K. and Albright, T.A. (1986) Symmetric vs. Asymmetric Linear M-X-M Linkages in Molecules, Polymers, and Extended Networks, *J. Am. Chem. Soc.* **108**, 2222–2236.
28. Orgel, L.E. (1958) Ferroelectricity and the Structure of Transition-Metal Oxides, *Faraday Disc. Chem. Soc.* **26**, 138–144.
29. Donohue, J. (1965) Bond Angles in the Binuclear Molybdenum(VI) Complex Anion $[MoO_2(C_2O_4)(H_2O)]_2O^{2-}$, *Inorg. Chem.* **4**(6), 921–922.
30. Wells, A.F. (1984) *Structural Inorganic Chemistry, 5th ed.* Clarendon Press, Oxford, pp. 510–512, 585–587.
31. Pope, M.T. (1972) Heteropoly and Isopoly Anions as Oxo Complexes and Their Reducibility to Mixed-Valence 'Blues", *Inorg. Chem.* **11**(8), 1973–1974.
32. Pope, M.T. (1983) *Heteropoly and Isopoly Oxometalates*, Springer-Verlag, Berlin, pp. 18–19.
33. Steward, E.G. and Rooksby, H.P. (1951) Pseudo-Cubic Alkaline-Earth Tungstates and Molybdates of the R_3MX_6 Type, *Acta Cryst.* **4**, 503–507.
34. Pierpont, C.G. and Downs, H.H. (1975) Bridging and Terminal *o*-Benzoquinone Coordination. The Crystal and Molecular Structure of Hexakis(tetrachloro-1,2-benzoquinone)dimolybdenum, *J. Am. Chem. Soc.* **97**(8), 2123–2127.
35. Chiu, N.-S. and Bauer, S.H. (1984) Note on the Structure of Ba_2CaMoO_6, *Acta. Cryst.* **C40**, 1646–1647.
36. deLearie, L.A. and Pierpont, C.G. (1988) Catecholate Complexes of High-Oxidation-State Metal Ions. Synthesis and Characterization of Dimeric Hexakis(tetrachlorocatecholato)ditungsten(VI), *Inorg. Chem.* **27**, 3842–3845.
37. Schröder, F.A. and Hartman, P. (1972) Some Aspects of the Structure of WO_3 and a Contribution to the Understanding of the so-called 'Shear Structures", *Z. Naturforsch.* **27b**, 902–908.
38. Allmann, R. (1975) Beziehungen zwischen Bindungslägen und Bindungsstärken in Oxidstrukturen, *Montash. Chem.* **106**, 779–793.
39. Schröder, F.A. (1975) Contributions to the Chemistry of Mo and W. XIV. The Mo-O Bond Length/Bond Order Relationship. A Systematical Treatment, *Acta Cryst.* **B31**, 2294–2309.
40. Brown, I.D. and Wu, K.K. (1976) Empirical Parameters for Calculating Cation-Oxygen Bond Valences, *Acta. Cryst.* **B32**, 1957–1959.
41. Cotton, F.A. and Wing, R.M. (1965) Properties of Metal-to-Oxygen Multiple Bonds, Especially Molybdenum-to-Oxygen Bonds, *Inorg. Chem.* **4**(6), 867–873.
42. Griffi th, W.P. and Wickins, T.D. (1968) *cis*-Dioxo- and Trioxo-complexes, *J.Chem.Soc (A)*, 400–402.
43. Cotton, F.A. (1974) Structure and Bonding in Molecular Oxo-Molybdenum Compounds, *J. Less-Common Met.* **36**, 13–22.
44. Cotton, F.A. and Wilkinson, G. (1988) *Advanced Inorganic Chemistry, 5th ed.* Wiley, New York, p. 68.
45. Strandberg, R. (1973) Multicomponent Polyanions IV. The Molecular and Crystal Structure of $Na_6Mo_5P_2O_{23}(H_2O)_{13}$, a Compound Containing Sodium-coordinated Pentamolybdodiphosphate Anions, *Acta Chem. Scand.* **27**, 1004–1018.
46. Hedman, B. (1977) Multicomponent Polyanions. 16. The Molecular and Crystal Structure of $Na_6Mo_5P_2O_{23}(H_2O)_{14}$, a Compound Containing Sodium-coordinated Pentamolybdodiphosphate Anions. *Acta Cryst.* **B33**, 3083–3090.

47. Lee, M.R. and Jaulmes, S. (1987) Nouvelle serie d'oxydes derives de la structure de $\alpha-U_3U_8$: $M^{II}UMo_4O_{16}$. *J. Solid State Chem.* **67**, 364–368.
48. Antipin, M.Y., Didenko, L.P., Kachapina, L.M., Shilov, A.E., Shilova, A.K. and Struchkov, Y.T. (1989) Polynuclear Molybdenum(VI)-Molybdenum(V) Complex: A Precursor of the Catalyst for Dinitrogen Reduction, *J. Chem. Soc., Chem. Commun.*, 1467–1468.
49. Pope, M.T. (1991) Molybdenum Oxygen Chemistry: Oxides, Oxo Complexes, and Polyoxoanions, in S.J. Lippard (ed.), *Progress in Inorganic Chemistry, Vol. 39*, John Wiley & Sons, New York, p. 181–257.
50. Chen, Q. and Zubieta, J. (1992) Coordination chemistry of soluble metal oxides of molybdenum and vanadium, *Coord. Chem. Rev.* **114**, 107–167.
51. Chippindale, A.M. and Cheetham, A.K. (1994) The Oxide Chemistry of Molybdenum, in E.R. Braithwaite and J. Haber (eds.), *Studies in Inorganic Chemistry 19. Molybdenum: An Outline of its Chemistry and Uses*, Elsevier, Amsterdam, pp. 146–184.
52. Bräkken, H. (1931) Die Kristallstrukturen der Trioxyde von Chrom, Molybdän und Wolfram, *Z. Kristallogr.* **78**, 484–488.
53. Wooster, N. (1931) The Crystal Structure of Molybdenum Trioxide, MoO_3, *Z. Kristallogr.* **80**, 504–512.
54. Andersson, G. and Magnéli A. (1950) On the Crystal Structure of Molybdenum Trioxide, *Acta Chem. Scand.* **4**, 793–797.
55. Nagano, O. (1979) Structure of the Potassium Molybdate Complex of 1,4,7,10,13,16-Hexacyclooctadecane (18-Crown-6) *Acta. Cryst.* **B35**, 465–467.
56. Klemperer, W.G., Mainz, V.V., Wang, R.-C. and Shum, W. (1985) Organosilicates as Silica Surface Models: The Molybdenum Trioxide Complexes $[R_3SiOMoO_3]^-$, Where R = Phenyl and *tert*-Butyl, *Inorg. Chem.* **24**, 1968–1970.
57. Hsieh, T.-C. and Zubieta, J. (1985) Synthesis and Characterization of Oxomolybdate Clusters Containing Co-ordinatively Bound Diazenido Units. The Crystal and Molecular Structure of the Octanuclear Oxomolybdate $(NHEt_3)_2(NBu_4)_2[Mo_8O_{20}(NNPh)_6]$, *J. Chem. Soc., Chem. Commun.*, 1749–1750.
58. Hsieh, T.-C., Schaikh, S.N. and Zubieta, J. (1987) Derivatized Polyoxomolybdates. Synthesis and Characterization of Oxomolybdate Clusters Containing Coordinatively Bound Diazenido Units. Crystal and Molecular Structure of the Octanuclear Oxomolybdate $(NHEt_3)_2(n\text{-}Bu_4)_2[Mo_8O_{20}(NNPh_6]$ and Comparison to the Structures of the Parent Oxomolybdate $\alpha\text{-}(n\text{-}Bu_4)_4[Mo_8O_{26}]$ and the Tetranuclear (Diazenido)oxomolybdates $(n\text{-}Bu_4)_2[Mo_4O_{10}(OMe)_2(NNPh)_2]$ and $(n\text{-}Bu_4)_2[Mo_4O_8(OMe)_2(NNC_6H_4NO_2)_4]$, *Inorg. Chem.* **26**, 4079.
59. Schröder, F.A., Scherle, J. and Hazell, R.G. (1975) The Structure of *cis*-Dioxobis-(2-hydroxyethyl-1-oxo)molybdenum(VI). *Acta. Cryst.* **B31**, 531–536.
60. Kojic-Prodic, B., Ruzic-Toros, Z.,Grdenic, D. and Golic, L. (1974) The Crystal Structure of Dioxobis-(1,3-diphenylpropanedionato)molybdenum(VI), $(C_{15}H_{11}O_2)_2MoO_2$ *Acta. Cryst.* **B30**, 300–305.
61. Day, V.W., Klemperer, W.G., Schwartz, C. and Wang, R.-C. (1988) Molecular Models of Early Transition Metal Oxides: Polyoxoanions as Organic Functional Groups, in G.J.-M. Basset , B.C. Candy , J.-P. Choplin, A. Leconte, M. Quignard, F, and C. Santini (eds.), *NATO ASI Series, Series C., Vol. 231*, Kluwer Academic Publishers, Dordrecht, pp. 173–186.
62. van den Elzen, A.F. and Rieck G.D. (1973) The Crystal Structure of $Bi_2(MoO_4)_3$, *Acta Cryst.* **B29**, 2433–2437.
63. Teller, R.G., Brazdil, J.F., Grasselli, R.K., Thomas, R., Corliss, L. and Hastings, J. (1984) The Structure of Ce-Doped $Bi_2(MoO_4)_3$ as Determined by Neutron Profi le Refi nement, *J. Solid State Chem.* **52**, 313–319.
64. Daran, J.-C., Prout, K., Adam,G.J.S., Green, M.L.H., and Sala-Pala, J. (1977) Organo-

Transition Metal Oxides and Sulphides: A Tetranuclear η-cyclopentadienylmolybdenum Oxide and Related Compounds, *J. Organomet. Chem.* **131**, C40-C42.

65. Prout, K. and Daran, J.-C. (1978) The Crystal and Molecular Structures of Bis(η-methylcyclopentadienyl)-molybdenum(IV)di-μ−sulphido-disulphidomolybdenum(VI) and Di-μ-oxo-di-μ_3-oxo-bis[bis(η-methylcyclopentadienyl)molybdenum(IV)dioxomolybdenum(VI)]. *Acta. Cryst.* **B34**, 3586–3591.
66. Chew, C.K. and Penfold, B.R. (1975) Structural Studies of molybdenum(VI) coordination chemistry: Crystal and Molecular structure of Mo_2O_4(2,2-dimethylpropane-1,3-diolate)$_2\cdot(H_2O)_2$ containing a μ-dioxo bridge, *J. Cryst. Mol. Struct.* **5**, 413–421.
67. Hayashi, Y., Toriumi, K. and Isobe, K. (1988) Novel Triple Cubane-Type Organometallic Oxide Clusters: $[MCp^*MoO_4]_4\cdot nH_2O$ (M = Rh and Ir; $Cp^* = C_5Me_5$; n = 2 for Rh and 0 for Ir), *J. Am. Chem. Soc.* **110**, 3666–3668.
68. Jeitschko, W. and Sleight, A.W. (1973) The Crystal Structure of $HgMoO_4$ and Related Compounds, *Acta Cryst.* **B29**, 869–875.
69. Klevtsov, P.V., Solodovnikov, S.F., Perepelitsa, A.P. and Klevtsova, R.F. (1984) Crystal Structure and Thermal Stability of $AgIn(MoO_4)_2$, *Sov. Phys.-Crystallogr. (Engl. Transl.)* **29**, 415–419.
70. van den Elzen, A.F. and Rieck, G.D. (1973) Redetermination of the Structure of Bi_2MoO_6, Koechlinite, *Acta Cryst.* **B29**, 2436–2438.
71. Teller, R.G., Brazdil, J.F. and Grasselli, R.K. (1984) The Structure of γ-Bismuth Molybdate, Bi_2MoO_6, by Powder Neutron Diffraction, *Acta Cryst.* **C40**, 2001–2005.
72. Laarif, A., Theobald, F.R., Vivier, H. and Hewat, A.W. (1984) Crystal Structure of Sb_2MoO_6, *Z. Kristallogr.* **167**, 117–124.
73. Day, V.W., Fredrich, M.F., Klemperer, W.G. and Shum, W. (1977) Synthesis and Characterization of the Dimolybdate Ion, $Mo_2O_7^{2-}$, *J. Am. Chem. Soc.* **99**(18), 6146–6148.
74. Fredrich, M.F. (1981) Ph.D. Dissertation. Lincoln, Nebraska, The University of Nebraska-Lincoln.
75. Stadnicka, K., Haber, J. and Kozlowski, R. (1977) The Crystal Structure of Magnesium Dimolybdate, *Acta Cryst.* **B33**, 3859–3862.
76. Gatehouse, B.M. (1977) The Crystal and Molecular Structures of $Ce_6Mo_{10}O_{39}$ and $K_2Mo_2O_7\cdot H_2O$ and the Refi nement of the 'Lindqvist" Octamolybdate $(NH_4)_4Mo_8O_{26}4H_2O$, *J. Less-Common Met.* **54**, 283–288.
77. Gatehouse, B.M. and Same, R. (1978) The Crystal Structure of a Complex Cerium(III) Molybdate; $Ce_6(MoO_4)_8(Mo_2O_7)$, *J. Solid State Chem.* **25**, 115–120.
78. Becher, H.J. and Fenske, D. (1978) Crystal and Anion Structure of the Double Salt Potassium Bromide-Potassium Dimolybdate, *J. Chem. Res. (S)*, 167.
79. Braunstein, P., de Meric de Belleton, C., Lanfranchi, M. and Tiripicchio, A. (1984) First Heterobimetallic Complexes with Bridging and Chelating $Ph_2PCH_2Ph_2$ (dppm): Crystal Structure of $[(\eta-C_5H_4Me)Mo(CO)_2(\mu$-dppm)Pt(dppm)$]_2[Mo_2O_7]$. Air Oxidation of the Anions $[(\eta-C_5H_4R)Mo(CO)_3]^-$ Into $[Mo_2O_7]^{2-}$, *Organometallics* **3**, 1772–1774.
80. Pierpont, C.G. and Buchanan, R.M. (1982) Molybdenum Complexes Containing Catecholate Ligands. Structural Studies on Complexes of the Pentaoxobis(quinone)dimolybdate(n-) (n = 0, 1, 2) Redox Series, *Inorg. Chem.* **21**, 652–657.
81. Atovmyan, L.O., Tkachev, V.V. and Shishova, T.G. (1972) Crystal Structure of a Binuclear Dioxo Compound of Mo(VI), *Dokl. Phys. Chem.* **205**, 622–623.
82. Pierpont, C.G. and Buchanan, R.M. (1975) Radical-Anion Coordination of 9,10-Phenanthrequinone in $Mo_2O_5(PQ)_2$, *J. Am. Chem. Soc.* **97**(22), 6450–6455.
83. Tkachev, V.V. and Atovmyan, L.O. (1976) Crystal And Molecular Structures of Binuclear (VI) Oxo Complexes: $(NH_4)_2[Mo_2O_5(C_6H_4O_2)_2]\cdot 2H_2O$ and

$Ba[Mo_2O_5(C_6H_4O_2)_2]\cdot 5H_2O\cdot C_6H_4(OH)_2$, *Sov. J. Coord Chem. (Engl. Transl.)* **2**, 89–92.

84. Liu, S., Shaikh, S.N. and Zubieta, J. (1988) Synthesis and Structural Characterisation of an Unusual Tetranuclear Oxomolybdenum(VI) Complex of Dihydroxybenzoquinone, $[Mo_4O_{10}(O_4C_6H_2)_2]^{2-}$, and a Comparison with the Mononuclear Chloranilate Complex $[MoO_2(HO_4C_6Cl_2)(O_4C_6Cl_2)]^{1-}$, *J. Chem. Soc., Chem. Commun.*, 1017–1019.
85. El-Hendawy, A.M., Griffi th, W.P., O'Mahoney, C.A. and Williams, D.J. (1989) Complexes of Naphthalene-2,3-diol (H_2ND) With Group VI and Group VII Metals, and the X-Ray Crystal Structure of *cis*-$(NH_4)_2[Mo_2O_5(ND)_2]\cdot 2H_2O$, *Polyhedron* **8**(4), 519–525.
86. Liu, S., Shaikh, S. and Zubieta, J. (1989) Synthesis and Chemical Characterization of Complexes Containing Semiquinone Groups Bridged by Pentaoxodimolybdate Groups. Structural and Electrochemical Studies of $[(n\text{-}C_4H_9)_4N]_2[Mo_4O_{10}(C_6H_2O_4)_2]$ and $[(n\text{-}C_4H_9)_4N]_3[Mo_6O_{15}(C_6O_6)_2]$ and of an Analogous Tetraoxydibenzofuran Complex, $[(n\text{-}C_4H_9)_4N]_2[Mo_4O_{10}(C_{12}H_4O_5)_2]$, Prepared from Metal-Mediated Radical Coupling of 1,2,4-Trihydroxybenzene Precursors, *Inorg. Chem.* **28**(4), 723–732.
87. Godfrey, J.E. and Waters, J.M. (1975) Ammonium μ-Oxo-μ-Mannitolate-Tetraoxodimolybdate(VI) Monohydrate $[C_6H_{11}O_{11}Mo_2]NH_4\cdot H_2O$, *Cryst. Struct. Comm.* **4**, 5–8.
88. Hedman, B. (1977) Multicomponent Polyanions. 15. The Molecular and Crystal Structure of $Na[Mo_2O_5\{O_3(OH)C_6H_8(OH)_2\}]\cdot 2H_2O$, *Acta Cryst.* **B33**, 3077–3083.
89. Ma, L., Liu, S. and Zubieta, J. (1989) Polyoxomolybdate-Alkoxide Interactions. The Crystal and Molecular Structures of the Erythritolate Complexes $[(n\text{-}C_4H_9)_4N]_2[Mo_2O_5(eryth)]$ and$[(n\text{-}C_4H_9)_4N][Mo_2O_5(Heryth)]$, *Polyhedron* **8**(12), 1571–1573.
90. Taylor, G.E. and Waters, J.M. (1981) The Structure of a Compound of Unexpected Conformation Involved in the Xylose-Lyxose Epimerization, *Tetrahedron Lett.* **22**(13), 1277–1278.
91. Liu, S. and Zubieta, J. (1989) Polyoxomolybdate-Hydrocarbon Interactions. Synthesis and Structure of $[(n\text{-}C_4H_9)_4N][Mo_2O_5(C_8O_{13}O_5)]\cdot 0.5(C_2H_5)_2O$, From the Reaction of 3-hydroxy-2-butanone with $[(n\text{-}C_4H_9)_4N]_2[Mo_2O_7]$, *Polyhedron* **8**(9), 1213–1215.
92. Cotton, F.A., Morehouse, S.M. and Wood, J.S. (1964) The Identifi cation and Characterization by X-Ray Diffraction of a New Binuclear Molybdenum(VI) Oxalate Complex, *Inorg. Chem.* **3**(11), 1603–1608.
93. Cotton, F.A., Morehouse, S.M. and Wood, J.S. (1965) Bond Angles in the Binuclear Molybdenum(VI) Complex Anion $[MoO_2(C_2O_4)(H_2O)]_2O^{-2}$, *Inorg. Chem.* **4**(6), 921–922.
94. Takeuchi, Y., Kobayashi, A. and Sasaki, Y. (1982) Structure of the Tetrahydrogentetramolybdotetraarsenate(V)(4-) Polyanion, *Acta Cryst.* **B38**, 242–244.
95. Do, Y., You, X.-Z., Zhang, C., Ozawa, Y. and Isobe, K. (1991) Trishomocubane-type methoxide cluster as a novel mediator in the extension of cube size in organometallic oxide clusters synthesis and structures of $[(RhCp^*)_2Mo_3O_9(OMe)_4]\cdot MeOH$ and a linear quadruple cubane-type cluster $[(RhCp^*)_4Mo_6O_{22}]\cdot 4CH_2Cl_2$ ($Cp^* = \eta^5\text{-}C_5Me_5$), *J. Am. Chem. Soc.* **113**(15), 5892–5893.
96. Liu, S., Shaikh, S.N. and Zubieta, J. (1987) Coordination Complexes of Polyoxomolybdate Anions. Characterization of a Tetranuclear Core from Reactions in Methanol: Syntheses and Structures of Two Polyoxomolybdate Alcoholates, $(MePPh_3)_2[Mo_4O_{10}(OCH_3)_6]$ and $[(n\text{-}C_4H_9)_4N]_2[Mo_4O_{10}(OCH_3)_2(OC_6H_4O)_2]$, and Their Relationship to a General Class of Tetranuclear Cluster Types $[Mo_4O_x(OMe)_2(L)_y(LL)_z]^{2-}$, *Inorg. Chem.* **26**, 4303–4305.
97. Kang, H., Liu, S. Shaikh, S.N., Nicholson, T. and Zubieta, J. (1989) Synthesis and Structural Investigation of Polyoxomolybdate Coordination Compounds Displaying a Tetranuclear Core. Crystal and Molecular Structures of $[n\text{-}Bu_4N]_2[Mo_4O_{10}(OMe)_4X_2]$ (X = -OMe, -Cl) and Their Relationship to the Catecholate Derivative $[n\text{-}Bu_4N]_2[Mo_4O_{10}(OMe)_2(OC_6H_4O)_2]$ and to the

Diazenido Complexes of the *o*-Aminophenolate and the Naphthalene-2,3-diolate Derivatives $[n\text{-}Bu_4N]_2[Mo_4O_6(OMe)_2(HNC_6H_4O)_2(NNC_6H_5)_4]$ and $[n\text{-}Bu_4N]_2[Mo_4O_6(OMe)_2(C_{10}H_6O_2)_2(NNC_6H_5)_4]$. Comparison to the Structure of a Binuclear Complex with the $[Mo_2(OMe)_2(NNC_6H_5)_4]^{2+}$ Core, $[Mo_2(OMe)_2(H_2NC_6H_4O)_2(NNC_6H_5)_4]$, *Inorg. Chem.* **28**, 920–933.

98. Wilson, A.J., Robinson, W.T. and Wilkins, C.J. (1983) 1,3-Diethoxy-1,2;1,4;2,3,4:2,3;3,4;1,2,4-bis-μ_4-{2-hydroxymethyl-2-methyl-1,3-propanediolato(3-)}-μ-*O*,μ-*O'*,μ-*O''*}-tetrakis[*cis*-dioxomolybdenum(VI)], $C_{14}H_{28}Mo_4O_{16}$, *Acta Cryst.* **C39**, 54–56.
99. Björnberg, A. (1980) Multicomponent Polyanions. 28. The Structure of $K_7Mo_8V_5O_{40}{\sim}8H_2O$, a Compound Containing a Structurally New Potassium-Coordinated Octamolybdopentavanadate Anion, *Acta Cryst.* **B36**, 1530–1536.
100. Dexter, D.D. and Silverton, J.V. (1968) A New Structural Type for Heteropoly Anions. T he Crystal Structure of $(NH_4)_2H_6(CeMo_{12}O_{42})\cdot 12H_2O$, *J. Am. Chem. Soc.* **90**, 3589–3590.
101. Evans Jr., H.T. (1971) in J.D. Dunitz and J.A. Ibers (eds.), *Perspectives in Structural Chemistry, Vol. 4*, Wiley, New York, p. 1–59.
102. Tat'yanina, I.V., Chernaya, T.S., Gorchenkova, E.A., Simonov, V.I. and Spitsyn, V.I. (1979) Crystal Structure of the U(IV) Heteropolymolybdate $CuH_6[UMo_{12}O_{42}]\cdot 12H_2O$, *Dokl. Chem. (Engl. Transl.)* **247**, 387–389.
103. Molchanov, V.N., Tatjanina, I.V., Torchenkova, E.A. and Kazansky, L.P. (1981) A Novel Type of Heteropolynuclear Complex Anion: X-Ray Crystal Structure of the Polymeric Complex Anion $[Th(H_2O)_3UMo_{12}O_{42}]_n^{4n-}$, *J. Chem. Soc., Chem. Commun.*, 93–94.
104. Tat'yanina, I.V., Fomicheva, E.B., Molchanov, V. N., Zavodnik, V.E., Bel'skii, V.K. and Torchenkova, E.A. (1982) The Crystal Structure of $(NH_4)_2[Er_2UMo_{12}O_{42}]\cdot 22H_2O$, *Sov. Phys. Crytallogr. (Engl. Transl.)* **27**(2), 142–145.
105. Tat'yanina, I.V., Molchanov, V.N., Popov, V.M., Torchenkova, E.A. and Spitsyn, V.I. (1982) Crystal Structures of Cerium Molybdenum and Uranium Molybdenum Heteropoly Acids, *Bull. Acad. Sci. USSR, Div. Chem. Sci. (Engl. Transl.)* **31**, 707–710.
106. Kotvanova, M.K., Molchanov, V.N., Torchenkova, E.A. and Spitsyn, V.I. (1984) The Crystal Structure of $(NH_4)_4[(UO_2)_2(OH_2)_3UMo_{12}O_{42}]\cdot 18H_2O$, *Russ. J. Inorg. Chem. (Engl. Transl.)* **29**(7), 1027–1030.
107. Knöpnadel, I., Hartl, H., Hunnius, W.-D. and Fuchs, J. (1974) Anionic Structure of the So-called Ammonium Dimolybdate $(NH_4)_2Mo_2O_7$, *Angew. Chem., Int. Ed. Engl.* **13**, 823.
108. Armour, A.W., Drew, M.G.B. and Mitchell, P.C. H. (1975) Crystal and Molecular Structure and Properties of Ammonium Dimolybdate, *J. Chem. Soc., Dalton Trans.*, 1493–1496.
109. Magarill, S.A. and Klevtsova, R.F. (1972) Crystal Structure of Potassium Bimolybdate $K_2Mo_2O_7$. *Sov. Phys. Crystallogr. (Engl. Transl.)* **16**(4), 645–648.
110. Fallon, G.D. and Gatehouse, B.M. (1982) The Crystal Structure of a Complex Cerium (III) Molybdate Containing Dimolybdate Chain, $Ce_2(MoO_4)_2(Mo_2O_7)$, *J. Solid State Chem.* **44**, 156–161.
111. Efremov, V.A., Davydova, N.N. and Trunov, V.K. (1988) The Crystal Structure of $Pr_2Mo_4O_{15}$, *Russ. J. Inorg. Chem.* **33**(12), 1729–1732.
112. Gatehouse, B.M. and Jozsa, A.J. (1987) The Crystal Structure of Potassium Dimolybdate Hydrate, *J. Solid State Chem.* **71**, 34–39.
113. Gatehouse, B.M. and Leverett, P. (1976) Crystal Structures of Silver Dimolybdate, $Ag_2Mo_2O_7$, and Silver Ditungstate, $Ag_2W_2O_7$, *J. Chem. Soc., Dalton Trans.*, 1316–1320.
114. Shaikh, S.N. and Zubieta, J. (1986) Organonitrogen Derivatized Polyoxomolybdate Anion Clusters. Synthesis and Characterization of a Tetranuclear Oxomolybdate Containing a Single *cis*-Bisphenyldiazenido-molybdenum Unit: $[Mo_4O_{10}(OCH_3)_2(NNC_6H_5)_2]^{2-}$, *Inorg. Chim. Acta* **121**, L43-L44.

115. Chen, Q., Ma, L., Liu, S. and Zubieta, J. (1989) Structural Characterization of the Pentamolybdate Anion, $[(MoO_4)_2\{Mo_3O_8(OMe)\}]^{3-}$, and Isolation of the $[Mo_3O_8(OMe)]^+$ Trinuclear Core in the Squarate Complex $[\{Mo_3O_8(OMe)\}(C_4O_4)_2]^{3-}$, *J. Am. Chem. Soc.* **111**, 5944–5946.
116. Ichida, H. private communication.
117. Nenner, A.-M. (1985) Multicomponent Polyanions. 38. Structure of $K_5NaMo_6V_2O_{26}\cdot 4H_2O$, a Compound Containing a New Configuration of the Hexamoldybdodivanadate Anion, *Acta Cryst.* **C41**, 1703–1707.
118. McCarron III, E.M. and Harlow, R.L. (1983) Synthesis and Structure of $Na_4[Mo_8O_{24}(OCH_3)_4]\cdot 8MeOH$: A Novel Isopolymolybdate That Decomposes with the Loss of Formeldahyde, *J. Am. Chem. Soc.* **105**, 6179–6181.
119. Isobe, M., Marumo, F., Yamase, T. and Ikawa, T. (1978) The Crystal Structure of Hexakis(isopropylammonium) Dihydrogenoctamolybdate(6-) Dihydrate, $(C_3H_{10}N)_6[H_2Mo_8O_{28}].2H_2O$, *Acta Cryst.* **B34**, 2728–2731.
120. Adams, R.D., Klemperer, W.G. and Liu, R.-S. (1979) Synthesis and X-Ray Structure of a Formylated Octamolybdate Cluster $[(HCO)_2(Mo_8O_{28})]^{6-}$, *J. Chem. Soc., Chem. Commun.*, 256–257.
121. Kamenar, B., Korpar-Colig, B., Penavic, M. and Cindric, M. (1990) Synthesis and Characterization of Octamolybdates containing Co-ordinatively Bound Salicylideneiminato and Methioninato (MetO) Ligands. Crystal Structures of $[NH_3Pr]_2[Mo_8O_{22}(OH)_4(OC_6H_4CH{=}NPr\text{-}2)_2]\cdot 6MeOH$ and $[Hmorph]_4[Mo_8O_{24}(OH)_2(MetO)_2]\cdot 4H_2O$ (morph = morpholine), *J. Chem. Soc., Dalton Trans.*, 1125–1130.
122. Moini, A., Peascoe, R., Rudolf, P.R. and Clearfield, A. (1986) Hydrothermal Synthesis of Copper Molybdates, *Inorg. Chem.* **25**, 3782–3785.
123. Gatehouse, B.M. and Leverett, P. (1968) The Crystal Structure of Dipotassium Trimolybdate, $K_2Mo_3O_{10}$; A Compound with Five co-ordinate Molybdenum(VI), *J. Chem. Soc. (A)*, 1398–1405.
124. Forster, A., Kreusler, U. and Fuchs, J. (1985) Die kristallinen Phasen der Alkalitrimolybdate, *Z. Naturforsch.* **40b**, 1139–1148.
125. Seleborg, M. (1966) The Crystal Structure of Dipotassium Trimolybdate, *Acta. Chem. Scand.* **20**, 2195–2201.
126. Porai-Koshits, M.A., Aslanov, L.A., Ivanova, G.V. and Polynova, T.N. (1968) X-Ray Structural Study of Ammonium Dimolybdomalate. *J. Struct. Chem. (Engl. Transl.)* **9**, 401–405.
127. Berg, J.-E., Brandänge, S., Lindblom, L. and Werner, P.-E. (1977) Crystal and Molecular Structure of Tetra-ammonium *aa'*-μ-Oxobis-{[*gied'*-μ_3-(S)-malato-$O^1,O^2,O^4,O^{4'}$]. di-μ-oxobis[dioxomolybdate(VI)]} Monohydrate. ^{13}C NMR Studies, *Acta Chem. Scand.* **A31**, 325–328.
128. Berg, J.-E. and Werner P.-E. (1977) The crystal structure of tetraammounim *aa'*-μ-oxobis-{[*gied'*-μ_3-(S)-malato-O(1),O(2),O(4),O(4')]- di-μ-oxobis[dioxomolybdate(VI)]} monohydrate, *Z. Kristallogr.* **145**, 310–320.
129. Alcock, N.W., Dudek, M., Grybos, R., Hodorowicz, E., Kanas, A. and Samotus, A. (1990) Complexation between Molybdenum(VI) and Citrate: Structural Characterisation of a Tetrameric Complex, $K_4[(MoO_2)_4O_3(cit)_2]\cdot 6H_2O$, *J. Chem. Soc., Dalton Trans.*, 707–710.
130. Day, V.W., Thompson, M.R., Day, C.S.,Klemperer, W.G. and Liu, R.-S. (1980) Substitutive Intramolecular Carbonyl Insertion in a Carbomolybdate Cluster: Formation of a Polycentric, Conformationally Flexible Anion Binding Cavity, *J. Am. Chem. Soc.* **102**, 5971–5973.
131. Liu, S., Shaikh, S.N. and Zubieta, J. (1988) Polyoxomolybdate-*o*-Benzoquinone Interactions. Synthesis and Structure of a Diacetal Derivative, $[Mo_4O_{15}(OH)(C_{14}H_8)]^{3-}$ from 9,10-Phenanthrequinone Carbonyl Insertion. Comparison to the Reaction Prod-

ucts with Tetrachloro-1,2-benzoquinone, the Ligand-Bridged Binuclear Complexes $[(MoO_2Cl_2)_2L]^{2-}$, L = $(C_6Cl_2O_4)^{2-}$ and $(C_2O_4)^{2-}$, Formed via Carbonyl Insertion and Chloride Transfer, *Inorg. Chem.* **27**(18), 3064–3066.

132. Fuchs, J., Hartl, H., Hunnius, W.-D. and Mahjour, S. (1975) Anion Structure of Ammonium Decamolybdate $(NH_4)_8Mo_{10}O_{34}$. *Angew. Chem. Int. Ed. Engl.* **14**, 644.
133. Garin, J.L. and Costamagna, J.A. (1988) The Structure of Ammonium Decamolybdate $(NH_4)_8Mo_{10}O_{34}$, *Acta Cryst.* **C44**, 779–782.
134. Benchrifa, R. and De Pape R. (1990) Isotypism of the triclinic $Tl_8Mo_{10}O_{34}$ and $(NH_4)_8Mo_{10}O_{34}$ molybdates, *Acta Cryst.* **C46**, 728.
135. Touboul, M., Idoura, C. and Tolédano, P. (1984) Structure du Décamolybdate(VI) d'Octathallium(I), $Tl_8Mo_{10}O_{34}$, *Acta Cryst.* **C40**, 1652–1655.
136. Bharadwaj, P.K., Ohashi, Y. and Sasada, Y. (1986) Structure of Octakis(methylammonium) Decamolybdate(8-) Dihydrate, *Acta Cryst.* **C42**, 545–547.
137. Koop, M. and Müller-Buschbaum (1985) Zur Kenntnis eines neuen Kupfermolybdates: $Cu_4Mo_5O_{17}$, *Z. Anorg. Allg. Chem.* **530**, 7–15.
138. McCarron III, E.M. and Calabrese, J.C. (1986) Synthesis and Structure of $Cu_4{}^{1+}Mo_5{}^{6+}O_{17}$, *J. Solid State Chem.* **65**, 215–224.
139. Richter, H. and Fuchs, J. (1984) Die wahrscheinliche Struktur des gelben Natriumpolymolybdats, *Z. Naturforsch.* **39b**, 623–627.
140. Gatehouse, B.M. and Leverett, P. (1970) The Chain Structure of Potassium Tetramolybdate, $K_2Mo_4O_{13}$, *Chem. Commun.*, 740–741.
141. Gatehouse, B.M. and Leverett, P. (1971) Crystal Structure of Potassium Tetramolybdate, $K_2Mo_4O_{13}$, and its Relationship to the Structures of Other Univalent Metal Polymolybdates, *J. Chem. Soc. (A)*, 2107–2112.
142. Benchrifa, R., Leblance, M. and De Pape, R. (1989) Synthesis and crystal structure of two polymorphs of $(NH_4)_2Mo_4O_{13}$, orthorhombic (*o*) and triclinic (*t*), *Eur. J. Solid State Inorg. Chem.* **26**, 593–601.
143. Gatehouse, B.M. and Miskin, B.K. (1975) Structural Studies in the LI_2MoO_4-MoO_3 System: Part 2. The High Temperature Form of Lithium Tetramolybdate, *H*-$Li_2Mo_4O_{13}$, *J. Solid State Chem.* **15**, 274–282.
144. Gatehouse, B.M. and Miskin, B.K. (1974) Structural Studies in the LI_2MoO_4-MoO_3 System: Part 1 The Low Temperature Form of Lithium Tetramolybdate, L–$Li_2Mo_4O_{13}$, *J. Solid State Chem.* **9**, 247–254.
145. Tolédano, P. and Touboul, M. (1978) Structure Cristalline du Tétramolybdate de Thallium(I), $Tl_2Mo_4O_{13}$, *Acta Cryst.* **B34**, 3547–3551.
146. McCarron III, E.M. and Calabrese, J.C. (1986) Hydrothermal Synthesis and Structure of $Cu^{1+}{}_6Mo^{6+}{}_5O_{18}$, *J. Solid State Chem.* **62**, 64–74.
147. Krebs, B. and Paulat-Böschen I. (1976) Kristallstruktur des sogennannten Kaliumdekamolybdats $KMo_5O_{15}OH.2H_2O$, *Acta Cryst.* **B32**, 1697–1704.
148. McCarron III, E.M., Thomas, D.M. and Calabrese, J.C. (1987) Hexagonal Molybdates: Crystal Structure of $(Na{\cdot}2H_2O)Mo_{5.33}[H_{4.5}]_{0.67}O_{18}$, *Inorg. Chem.* **26**, 370–373.
149. Garin, J.L. and Blanc, J.M. (1985) Synthesis and Crystal Chemistry of $NH_2(MoO_3)_3$, *J. Solid State Chem.* **58**, 98–102.
150. Caiger, N.A., Crouch-Baker, S., Dickens, P.G. and James, G.S. (1987) Preparation and Structure of Hexagonal Molybdenum Trioxide, *J. Solid State Chem.* **67**, 369–373.
151. Evans Jr., H.T. and Showell, J.S. (1969) Molecular Structure of the Decamolybdodicobaltate(III) Ion, *J. Am. Chem. Soc.* **91**, 6881–6882.
152. Krol, I.A., Starikova, Z.A., Sergienko, V.S. and Tolkacheva, E.O. (1990) A new type of linear polyanion $[Mo_6O_{17}(HL_2)]^{6-}$ in the structure of $(NH_4)_6$ $[Mo_6O_{17}(HL_2)]{\cdot}10H_2O$ (where HL is an anion of 1-hydroxy-ethylidenediphosphonic acid), *Zh. Neorg. Khim.* **35**, 2817–2827.

153. Böschen, I., Buss, B., Krebs, B. and Glemser, O. (1970) Polymeric Octamolybdate Ions in the Crystal Structure of $(NH_4)_6Mo_8O_{27}\cdot 4H_2O$, *Angew. Chem. Int. Ed. Engl.* **9**(8), 638–639.
154. Böschen, V.I., Buss, B. and Krebs, B. (1974) Die Kristallstruktur des polymeren Oktamolybdats $(NH_4)_6Mo_8O_{27}\cdot 4H_2O$, *Acta Cryst.* **B30**, 48–56.
155. Gatehouse, B.M. and Miskin, B.K. (1975) The Crystal Structures of Caesium Pentamolybdate, $Cs_2Mo_5O_{16}$, and Caesium Heptapolymolybdate, $Cs_2Mo_7O_{22}$, *Acta Cryst.* **B31**, 1293–1299.
156. Tolédano, P., Touboul, M. and Herpin, P. (1976) Structure Cristalline de l'Heptapolymolybdate de Thallium(I), $Tl_2Mo_7O_{22}$, *Acta Cryst.* **B32**, 1859–1863.
157. McCarron III, R.M. and Harlow, R.L. I (1983) Synthesis and Chain Structure of $Mo_3O_9\cdot 4DMSO$ (DMSO = dimethyl sulphoxide): a Novel Chain Structure, *J. Chem. Soc., Chem. Commun.*, 90–91.
158. McKee, V. and Wilkins, C.J. (1984) Structure of a Second Crystalline Form of a Molybdenum Trioxide-Dimethyl Sulphoxide Polymer, $Mo_3O_9\cdot 4(CH_3)_2SO$, *Acta Cryst.* **C40**, 1676–1681.
159. Lindqvist, I. (1950) Crystal Structure Studies on Anhydrous Sodium Molybdates and Tungstates, *Acta Chem. Scand.* **4**, 1066.
160. Seleborg, M. (1967) A Refi nement of the Crystal Structure of Disodium Dimolybdate, *Acta Chem. Scand.* **21**, 499–504.
161. Range, K.-J. and Fässler A. (1990) Diammonium Trimolybdate(VI), $(NH_4)_2Mo_3O_{10}$, *Acta Cryst.* **C46**, 488–489.
162. Kreusler, H.-U., Förster, A. and Fuchs, J. (1980) Die Struktur des Rubidiumtrimolybdathydrats $Rb_2Mo_3O_{10}\cdot H_2O$, *Z. Naturforsch.* **35b**, 242–244.
163. Gatehouse, B.M., Jenkins, C.E. and Miskin, B.K. (1983) The Crystal Structure of a Sodium Molybdenum Oxide, $Na_6Mo_{10}O_{33}$, Containing Cross-Linked Chains of Octahedra and Square Pyramids, *J. Solid State Chem.* **46**, 269–274.
164. Böschen, I. and Krebs, B. (1974) Kristallstruktur der 'weissen Molybdänsäure' $\alpha-MoO_3\cdot H_2O$, *Acta Cryst.* **B30**, 1795–1800.
165. Oswald, H.R., Günter, J.R. and Dubler, E. (1975) Toptactic Decomposition and Crystal Structure of White Molybdenum Trioxide-Monohydrate: Prediction of Structure by Topotaxy, *J. Solid State Chem.* **13**, 330–338.
166. Fuchs, J., Kreusler, H.-U. and Förster, A. (1979) Die Kristallstruktur des Rubidiumtrimolybdatosulfats $Rb_2SMo_3O_{13}$, *Z. Naturforsch.* **34b**, 1683–1685.
167. Krebs, B. (1970) The Crystal Structure of MoO_3,$2H_2O$: a Metal Aquoxide with Both Coordinated and Hydrate Water, *Chem Commun.*, 50–51.
168. Åsbrink, S. and Brandt, B.G. (1971) A Study of the Crystal Structure of $MoO_3\cdot 2H_2O$ including Localization and Refi nement of the Hydrogen Atom Positions, *Chem. Scr.* **1**, 169–181.
169. Krebs, B. (1972) Die Kristallstruktur von $MoO_3\cdot 2H_2O$, *Acta Cryst.* **B28**, 2222–2231.
170. McCarron III, E.M. and Calabrese, J.C. (1991) The Growth And Single-Crystal Structure of a High-Pressure Phase of Molybdenum Trioxide - MoO_3-II, *J. Solid State Chem.* **91**(1), 121–125.
171. Berkowitz, J., Inghram, M.G. and Chupka, W.A. (1957) Polymeric Gaseous Species in the Sublimation of Molybdenum Trioxide, *J. Chem. Phys.* **26**(4), 842–846.
172. Blackburn, P.E., Hoch, M. and Johnston, H.L. (1958) The Vaporization of Molybdenum and Tungsten Oxides, *J. Phys. Chem.* **62**(7), 769–773.
173. Kazenas, E.K., Chizhika, D. and Tsvetkov, Y.V. (1969) Thermodynamics of the Sublimation of Tungsten and Molybdenum Trioxide, *Akad. Nauk SSSR. Inst. Met. Iss. Prots. Mets. Tsv. Red. Met.*, 19–27.
174. Kazenas, E.K. and Tsvetkov, Y.V. (1969) Mass-Spectrometric Determination of the Com-

position and Pressure of Molybdenum Trioxide Vapour, *Russ. J. Inorg. Chem.* **14**(1), 5–7.

175. Charlu, T.V. and Kleppa, O.J. (1971) A calorimetric determination of the enthalpy of vaporization of MoO_3, *J. Chem. Thermodynamics* **3**, 697–700.
176. Egorova, N.M. and Rambidi, N.G. (1972) The Material Point Method in the Interpretation of Electron Diffraction Data, in S.J. Cyvin (ed.), *Molecular Structures and Vibrations*, Elsevier, Amsterdam, p. 212–227.
177. Kazenas, E.K., Chizhika, D. and Tsvetkov, Y.V. (1972) *Termodin. Kinet. Protssessov Vosstranov. Met., Mater. Konf., 1969*, 14–19.
178. Perov, P.A., Novikov, V.N. and Mal'tsev, A.A. (1972) Investigation of IR Absorption Spectra of Vapors Over MoO_3 by the Isolation Method in an Argon Matrix at the Temperature of Liquid Helium, *Vestn. Mosk. Univ.: Khim.* **27**(1), 89–90.
179. Stomberg, R. private communication.
180. Stomberg, R., Trysberg, L. and Larking, I. (1970) Studies on Peroxomolybdates VIII. The Structure of the Diperoxotetramolybdate(VI) Ion, $[Mo_4O_{12}(O_2)_2]^{4-}$, and of the Diperoxoheptamolybdate(VI) Ion, $[Mo_7O_{22}(O_2)_2]^{6-}$, *Acta Chem. Scand.* **24**(7), 2679.
181. Day, V.W., Fredrich, M.F., Klemperer, W.G. and Liu, R.-S. (1979) Polyoxomolybdate-Hydrocarbon Interactions. Synthesis and Structure of the $CH_2Mo_4O_{15}H^{3-}$ Anion and Related Methylenedioxymolybdates, *J. Am. Chem. Soc.* **101**, 491–492.
182. Barkigia, K.M., Rajkovic-Blazer, L.M., Pope, M.T. and Quicksall, C.O. (1975) A New Type of Heteropoly Anion. Tetramolybdo Complexes of Dialkyl- and Diarylarsenates, *J. Am. Chem. Soc.* **97**, 4146.
183. Matsumoto, K.Y. (1979) Heteropolyanions of Methylarsonate and Dimethylarsinate: The Crystal Structures of Guanidinium Hexamolybdomethylarsonate Hexahydrate, $(CN_3H_6)_2[CH_3AsMo_6O_{21}(H_2O)_6]\cdot 6H_2O$ and Guanidinium Tetramolybdodimethylarsinate Monohydrate, $(CN_3H_6)_2[(CH_3)_2AsMo_4O_{14}(OH)]\cdot H_2O$. *Bull. Chem. Soc. Japan* **52**(11), 3284–3291.
184. Barkigia, K.M., Rajkovic-Blazer, L.M., Pope, M.T., Prince, E. and Quicksall, C.O. (1980) Molybdoarsinate Heteropoly Complexes. Structure of the Hydrogen Tetramolybdodimethylarsinate(2-) Anion by X-Ray and Neutron Diffraction, *Inorg. Chem.* **19**, 2531–2537.
185. Gouzerh, P., Jeannin, Y., Proust, A. and Robert, F. (1989) Two Novel Polyoxomolybdates Containing the $(MoNO)^{3+}$ Unit: $[Mo_5Na(NO)O_{13}(OCH_3)_4]^{2-}$ and $[Mo_6(NO)O_{18}]^{3-}$, *Angew. Chem. Int. Ed. Engl.* **28**(10), 1363–1364.
186. Gatehouse, B.M. and Leverett, P. (1969) The Crystal Structure of Silver Decamolybdate, $Ag_6Mo_{10}O_{33}$, *Chem. Commun.*, 1093–1094.
187. Gatehouse, B.M. and Leverett, P. (1970) The Crystal Structure of Silver Decamolybdate, $Ag_6Mo_{10}O_{33}$, *J. Solid State Chem.* **1**, 484–496.
188. Lindqvist, I. (1950) The structure of the tetramolybdate ion, *Ark. Kemi* **2**(20), 349–355.
189. Weakley, T.J.R. (1982) The Crystal Structure of Ammonium β-Octamolybdate Pentahydrate, *Polyhedron* **1**(1), 17–19.
190. Atovmyan, L.O. and Krasochka, O.N. (1972) X-Ray Diffraction Investigation of the Crystals of the Octamolybdate $(NH_4)_4Mo_8O_{26}\cdot 4H_2O$, *J. Struct. Chem. (Engl. Transl.)* **13**, 319–320.
191. Vivier, H., Bernard,J. and Djomaa, H. (1977) Structure cristalline de $(NH_4)_4Mo_8O_{26}$, $4H_2O$, *Rev. Chim. Minér.* **24**(6), 584–604.
192. Esteban-Calderon, C., Martinez-Ripoll, M., Garcia-Blanco, S. and Roman, P. (1984) Synthesis and Crystal Structure of Pyridinium β-Octamolybdate, *An. Quim., Ser. B* **80**, 470–473.
193. Giter, L., Roman, P., Jaud, J. and Galy, J. (1981) Structure cristalline de l'octamolybdate de 3-ethyl pyridinium à polyanions discrets $[Mo_8O_{26}]^{4-}$, *Z. Kristallogr.* **154**, 59–68.

194. Romàn, P., Martinez-Ripoll, M. and Jaud, J. (1982) Crystal Structure of 4-ethyl pyridinium octamolybdate, *Z. Kristallogr.* **158**, 141–147.
195. Román, P. and Gonzalez-Aguado, M.E. (1983) Crystal structure of 3-methylpyridinium β-octamolybdate, *Z. Kristallogr.* **165**, 271–276.
196. Román, P., Gutiérrez-Zorrilla, J.M., Martinez-Ripoll, M. and Garcia-Blanco, S. (1986) Structure of 2-Methylpyridinium β-Octamolybdate(VI), *Acta Cryst.* **C42**, 956–958.
197. Wilson, A.J., McKee, V., Penfold, B.R. and Wilkins, C. J. (1984) Structure of Tetrakis(dimethylammonium) β-Octamolybdate Bis(*N,N*-dimethylformamide), $[NH_2(CH_3)_2]_4[Mo_8O_{26}].2C_3H_7NO$, with Comments on Relationships among Octamolybdate Anions, *Acta Cryst.* **C40**, 2027–2030.
198. Fuchs, J. and Knöpnadel I. (1982) Die Kristallstruktur des Dinatriumditetramethylammonium-octamolybdatdihydrats, $Na_2[N(CH_3)_4]_2Mo_8O_{26}\cdot 2H_2O$ und die Beziehung zwischen Mo–O-Abstand und Bindungsordnung in Polymolybdaten, *Z. Kristallogr.* **158**, 165–179.
199. Kroenke, W.J., Fackler Jr., J.P. and Mazany, A.M. (1983) Structure and Bonding of Melaminium β-Octamolybdate, *Inorg. Chem.* **22**, 2412–2416.
200. Bharadwaj, P.K., Ohashi, Y., Sasada, Y., Sasaki, Y. and Yamase, T. (1984) Structure of Oxonium Tris(triethylammonium) Octamolybdate(4-) Dihydrate, $(C_6H_{16}N)_3(H_3O)[Mo_8O_{26}].2H_2O$. *Acta Cryst.* **C40**, 48–50.
201. McCarron III, E.M. and Harlow, R.L. (1984) Di-μ-aqua-tetrakis[μ-(methanol)-(methanol)sodium] Octamolybdate, $[Na_4(CH_4O)_8(H_2O)_2][Mo_8O_{26}]$, *Acta Cryst.* **C40**, 1140–1141.
202. Arzoumanian, H., Baldy, A., Lai, R., Odreman, A., Metzger, J. and Pierrot, M. (1985) An Unusual Route to the Isopolymolybdates; Octamolybdate β-$[Mo_8O_{26}]^{4-}$ and Hexamolybdate $[Mo_6O_{19}]^{2-}$. Reaction of Dioxomolybdenum Complexes with Triphenylphosphonium Ylides. Crystal Structures of the Salts $[PPh_3CH_2COOEt]^+{}_2[NH_2Et]^+{}_2[Mo_8O_{26}]^{4-}$, $[PPh_3CH_2COOEt]^+{}_2[Mo_6O_{19}]^{2-}$, and $[[PPh_3CH_2Ph]^+{}_2[Mo_6O_{19}]^{2-}$, *J. Organomet. Chem.* **295**, 343–352.
203. Roman, P., Gutiérrez-Zorrilla, J.M., Esteban-Calderon, C., Martinez-Ripoll, M. and García-Blanco, S. (1985) Synthesis, Characterization and Crystal Structure of the Anilinium β-Octamolybdate Dihydrate, *Polyhedron* **4**(6), 1043–1046.
204. Román, P., Gutiérrez-Zorrilla, J.M., Martínez-Ripoll, and García-Blanco (1986) Preparation, Characterization and Crystal Structure of *N,N*-dimethylanilinium β-Octamolybdate Dihydrate, *Polyhedron* **5**(11), 1799–1803.
205. Fischer, J., Ricard, L. and Toledano, P. (1974) A Novel Phosphomolybdate Structure: Crystal Structure of $[NH_4]_5[(MoO_3)_5(PO_4)(HPO_4)]\cdot 3H_2O$, *J.Chem. Soc., Dalton Trans.*, 941–946.
206. Hedman, B. and Strandberg, R. (1979) Multicomponent Polyanions. 19. The Molecular and Crystal Structure of $Na_5HMo_5P_2O_{23}(H_2O)_{11}$, a Superstructure with Sodium-coordinated Monohydrogenentamolybdodiphosphate Anions, *Acta Cryst.* **B35**, 278–284.
207. Hedman, B. (1973) Multicomponent Polyanions VI. The Molecular and Crystal Structure of $Na_4H_2Mo_5P_2O_{23}(H_2O)_{10}$, a Compound Containing Sodium-coordinated Dihydrogenpentamolybdodiphosphate Anions, *Acta. Chem. Scand.* **27**, 3335–3354.
208. Stalick, J.K. and Quicksall, C.O. (1976) Two Heteropoly Anions Containing Organic Groups. Crystal and Molecular Structures of Ammonium Pentamolybdis(methylphosphonate) Pentahydrate, $(NH_4)_4[CH_3P)_2Mo_5O_{21}]\cdot 5H_2O$ and Tetramethylammonium Pentamolybdis(ethylammoniumphosphonate) Pentahydrate, $Na[N(CH_3)_4][NH_3C_2H_4P)_2Mo_5O_{21}]\cdot 5H_2O$, *Inorg. Chem.* **15**(7), 1577–1584.
209. Lyxell, D.-G. and Strandberg, R. (1988) The Structure of Tetraguanidinium Pentamolybdodiphenylphosphonate, *Acta Cryst.* **C44**, 1535–1538.

210. Ozeki, T., Ichida, H., Miyamae, H. and Sasaki, Y. (1988) Crystal Structure of $K_4[H_2P_2Mo_5O_{21}]\cdot 2H_2O$, *Bull. Chem. Soc. Japan* **61**, 4455–4457.
211. Liu, B.-Y., Ku, Y.-T., Wang, M. and Zheng, P.-J. (1988) Synthesis and Characterization of a New Type of Heteropolyanion: Pentamolybdobis(*n*-propylarsonate), Having Two Types of Crystals under the Same pH Conditions in the Same Solution, *Inorg. Chem.* **27**, 3868–3871.
212. Wang, M., Zheng, P., Liu, B. and Gu, Y. (1988) Structure of Guanidinium Pentamolybdis(*n*-Propylarsenate) Dihydrate. *Acta Cryst.* **C44**, 1503–1505.
213. Matsumoto, K.Y., Kato, M. and Sasaki, Y. (1976) The Crystal Structure of Ammonium Pentamolybdodisulfate(IV)(4-) trihydrate $(NH_4)_4[S^{IV}{}_2Mo_5O_{21}]\cdot 3H_2O$, *Bull. Chem. Soc. Japan* **49**(1), 106–110.
214. Lee, U. (1984) Ph.D. Dissertation. Tokyo, The University of Tokyo.
215. Lee, U. and Sasaki, Y. (1984) Isomerism of the Hexamolybdo-Platinate(IV) Polyanion. Crystal Structures of $K_{3.5}[\alpha\text{-}H_{4.5}PtMo_6O_{24}]\cdot 3H_2O$ and $(NH_4)_4[\beta\text{-}H_4PtMo_6O_{24}]\cdot 1.5H_2O$, *Chem. Lett.*, 1297–1300.
216. Evans Jr., H.T. (1968) Refi ned Molecular Structure of the Heptamolybdate and Hexamolybdotellurate Ions, *J. Am. Chem. Soc.* **90**, 3275–3276.
217. Evans Jr., H.T. (1974) The Molecular Structure of the Hexamolybdotellurate Ion in the Crystal Complex with Telluric Acid, $(NH_4)_6[TeMo_6O_{24}]\cdot Te(OH)_6\cdot 7H_2O$, *Acta Cryst.* **B30**, 2095–2100.
218. Perloff, A. (1970) The Crystal Structure of Sodium Hexamolybdochromate(III) Octahydrate $Na_3(CrMo_6O_{24}H_6)\cdot 8H_2O$, *Inorg. Chem.* **9**(10), 2228–2239.
219. Ito, F., Ozeki, T., Ichida, H., Miyamae, H. and Sasaki, Y. (1989) Structure of Tetraammonium Hexahydrogenhexamolybdocuprate(II) Tetrahydrate, *Acta Cryst.* **C45**, 946–947.
220. Kondo, H., Kobayashi, A. and Sasaki, Y. (1980) The Structure of the Hexamolybdoperiodate Anion in Its Potassium Salt, *Acta Cryst.* **B36**, 661–664.
221. Ogawa, A., Yamato, H, Lee., U., Ichida, H., Kobayashi, A. and Sasaki, Y. (1988) Structure of Pentapotassium Dihydrogenhexamolybdoantimonate Heptahydrate, *Acta Cryst.* **C44**, 1879–1881.
222. Lindqvist, I. (1950) The structure of the paramolybdate ion, *Acta Cryst.* **3**, 159–160.
223. Lindqvist, I. (1950) A crystal structure investigation of the paramolybdate ion, *Ark. Kemi* **2**(18), 325–341.
224. Shimao, E. (1967) The Structure of $Mo_7O_{24}{}^{6-}$ Ion in the Crystal of Ammonium Heptamolybdate Tetrahydrate, *Bull. Chem. Soc. Japan* **40**, 1609–1613.
225. Gatehouse, B.M. and Leverett, P. (1968) The Crystal Structure of Potassium Heptamolybdate Tetrahydrate, $K_6Mo_7O_{24},4H_2O$. *Chem. Commun.*, 901–902.
226. Sjöbom, K. and Hedman, B. (1973) Multicomponent Polyanions VII. The Molecular and Crystal Structure of $Na_6Mo_7O_{24}(H_2O)_{14}$, a Compound Containing Sodium-coordinated Heptamolybdate Anions, *Acta Chem. Scand.* **27**, 3673–3691.
227. Evans Jr., H.T., Gatehouse, B.M. and Leverett, P. (1975) Crystal Structure of the Heptamolybdate(VI) (Paramolybdate) Ion, $[Mo_7O_{24}]^{6-}$, in the Ammonium and Potassium Tetrahydrate Salts, *J. Chem. Soc., Dalton Trans.*, 505–514.
228. Don, A. and T.J.R. Weakley (1981) Guanidinium Heptamolybdate Monohydrate, *Acta Cryst.* **B37**, 451–453.
229. Ohashi, Y., Yanagi, K., Sasada, Y. and Yamase, T. (1982) Crystal Structure and Photochemistry of Isopolymolybdates. I. The Crystal Structures of Hexakis(propylammonium)heptamolybdate(VI) Trihydrate and Hexakis(isopropylammonium)heptamolybdate(VI) Trihydrate, *Bull. Chem. Soc. Japan* **55**(4), 1254–1260.
230. Fedoseev, A.M., Grigor'ev, M.S., Yanovskii, A.I., Struchkov, Y.T. and Spitsyn, V.I. (1987)

Synthesis and Crystal and Molecular Structure of a New Praseodymium(III) Compound $(NH_4)_{28}Pr_8Mo_{58}O_{200}\cdot 40H_2O$, *Dokl. Phys. Chem. (Engl. Transl.)* **297**, 477–479.

231. Fuchs, J. and Hartl, H. (1976) Anion Structure of Tetrabutylammonium Octamolybdate $[N(C_4H_9)_4]_4Mo_8O_{26}$, *Angew. Chem. Int. Ed. Engl.* **15**(6), 375–376.
232. Day, V.W., Fredrich, M.F., Klemperer, W.G. and Shum, W. (1977) Structural and Dynamic Stereochemistry of α-$Mo_8O_{26}^{4-}$, *J. Am. Chem. Soc.* **99**, 952–953.
233. Kwak, W., Rajkovic, L.M., Stalick, J.K., Pope, M.T. and Quicksall, C.O. (1976) Synthesis and Structure of Hexamolybdobis(organoarsenates), *Inorg. Chem.* **15**(11), 2778–2783.
234. Wang, M., Zheng, P., Liu, B. and Gu, Y. (1987) Crystal and Molecule Structure of Guanidinium Hexamolybdo-bis(*n*-propylarsonate), $(CN_3H_6)_4(n\text{-}C_3H_7As)_2Mo_6O_{24}$, *Acta Phys.-Chim. Sin.* **3**, 485–489.
235. Björnberg, A. (1979) Multicomponent Polyanions. 26. The Crystal Structure of $Na_6Mo_6V_2O_{26}(H_2O)_{16}$, a Compound Containing Sodium-Coordinated Hexamolybdodivanadate Anions, *Acta Cryst.* **B35**, 1995–1999.
236. Kwak, W., Rajkovic, L.M., Pope, M.T., Quicksall, C.O., Matsumoto, K.Y. and Sasaki, Y. (1977) A New Molybdoarsonate. Structure of $(PhAs)_2Mo_6O_{25}H_2^{4-}$and Solution Interconversion of Heteropoly Anions That Differ by a Constitutional Water Molecule, *J. Am. Chem. Soc.* **99**(19), 6463–6464.
237. Matsumoto, K.Y. (1978) The Crystal Structure of Guanidinium Hexamolybdobis(phenylarsonate) Tetrahydrate, $(CN_3H_6)_4[(C_6H_5As)_2Mo_6O_{25}H_2]\cdot 4H_2O$, *Bull. Chem. Soc. Japan* **51**(2), 492–498.
238. Niven, M.L., Cruywagen, J.J. and Heyns, J.B.B. (1991) The First Observation of γ–Octamolybdate: Synthesis, Crystal, and Molecular Structure of $[Me_3N(CH_2)_6NMe_3]_2[Mo_8O_{26}]\cdot 2H_2O$, *J. Chem. Soc., Dalton Trans.*, 2007.
239. Ozawa, Y. and Sasaki, Y. (1987) Synthesis and Crystal Structure of $[(CH_3)_4N]_4Na_2[As_2Mo_{12}O_{42}]\cdot 6H_2O$, *Chem. Lett.*, 1733–1736.
240. Nenner, A.-M. and Pettersson, L. private communication.
241. Chen, Q., Liu, S. and Zubieta, J. (1990) Coordination Chemistry of Polyoxomolybdates: The Structure of a Dodecanuclear Molybdate Cage Incorporating Hydrogen Squarate Ligands, $[(C_4H_9)_4N]_4[Mo_{12}O_{36}(C_4O_4H)_4]\cdot 10Et_2O$, *Angew. Chem. Int. Ed. Engl.* **29**(1), 70–72.
242. Ichida, H. and Yagasaki, A. (1991) Synthesis and Structure of a Novel Polymolybdate which contains Five-coordinated Molybdenum(VI), *J., Chem. Soc., Chem.Commun.*, 27–28.
243. Waugh, J.L.T., Shoemaker, D.P. and Pauling, L. (1954) On the Structure of the Heteropoly Anion in Ammonium 9-Molybdomanganate, $(NH_4)_6MnMo_9O_{32}\cdot 8H_2O$, *Acta Cryst.* **7**, 438–441.
244. Allmann, R. and D'Amour, H.(1975) Strukturverfeinerung von Ammonium-9-molybdomanganat, $(NH_4)_6[MnMo_9O_{32}]\cdot nH_2O$, ($n$=6–8), *Z. Kristallogr.* **141**, 342–353.
245. Weakley, T.J.R. (1977) The Crystal Structure of Potassium Nonamolybdomanganate(IV) Hexahydrate, $K_6[MnMo_9O_{32}]\cdot 6H_2O$, *J. Less-Common Met.* **54**, 289–296.
246. Weakley, T.J.R. (1987) Ammonium Nonamolybdenionickelate(IV) Hexahydrate, *Acta Cryst.* **C43**, 2221–2222.
247. Nishikawa, T. and Sasaki, Y. (1975) The Crystal Structure of Ammonium Dodecamolybdotetraarsenate(V) Tetrahydrate, $(NH_4)_4\ H_4As_4Mo_{12}O_{50}\cdot 4H_2O$, *Chem. Lett.*, 1185–1186.
248. Barkigia, K.M., Rajkovic-Blazer, L.M., Pope, M.T. and Quicksall, C.O. (1981) Dodecamolybdotetrakis(organoarsenates) and the Structure of a Neutral Zwitterionic Heteropoly Complex, *Inorg. Chem.* **20**(10), 3318–3323.
249. Kessler, V.G., Mironov, A.V., Yurova, N.Y., Yanovsky, A.I. and Struchkov, Y.T. (1993) The Synthesis and X-Ray Crystal Structure of Molybdenum Oxomethoxide $[MoO(OMe)_4]_2$, *Polyhedron* **12**(12), 1573–1576.

250. Buchanan, R.M. and Pierpont, C.G. (1979) Synthesis, Structure, and Properties of the Oxygen Defi cient Bis(3,5-di-*tert*-butylcatecholato)oxomolybdenum(VI) Dimer, $[MoO(O_2C_6H_2(t\text{-}Bu)_2)_2]_2$, *Inorg. Chem.* **18**(6), 1616–1620.
251. McKee, V. and Wilkins, C.J. (1987) Some Binculear Molybdenum(VI) Complexes obtained from Condensation Reactions: Their Crystal and Molecular Structures, *J. Chem. Soc., Dalton Trans.*, 523–528.
252. Hoffmann, R. and Hoppe, R. (1989) Zwei neue Ordnungs-Varianten des NaCl-Typs: Li_4MoO_5 und Li_4WO_5, *Z. anorg. allg. Chem.* **573**, 157–169.
253. Martin-Frère, J., Jeannin, Y., Robert, F. and Vaisserman, J. (1991) Synthesis and Structures of Two Unprecedented Heteropolyoxometalates $[As_3M_3O_{15}]^{3-}$ (M=Mo, W) and $[As_6CoMo_6O_{30}]^{4-}$. First Examples of Linear Triarsenate(III) and Cyclic Triarsenate(III), *Inorg. Chem.* **30**, 3635–3639.
254. Matheson, A.J. and Penfold, B.R. (1979) μ-Oxo-bis{[2,3-dimethyl-2,3-butanediolato(1-)][2,3-dimethyl-2,3-butanediolato(2-)]oxomolybdenum(VI)}, *Acta Cryst.* **B35**, 2707–2709.
255. Cremers, T.L., Eller, P.G., Penneman, R.A. and Herrick, C.C. (1983) Orthorhombic Uranium(IV) Molybdenum(VI) Oxide UMo_2O_8, *Acta Cryst.* **C39**, 1163–1165.
256. Parise, J.B., McCarron III, E.M. and Sleight, A.W. (1987) A New Modifi cation of ReO_3-type MoO_3 and the Deuterated Intercalation Compound from which it is Derived: $D_{0.99}MoO_3$, *Mat. Res. Bull.* **22**, 803–811.
257. Parise, J.B., McCarron III, E.M., Sleight, A.W. and Prince, E. (1988) Refi nement of the Structure of Beta'-MoO_3, *Mater. Sci. Forum* **27–28**, 85–88.
258. Allcock, H.R., Bissell, E.C. and Shawl, E.T. (1973) Crystal and Molecular Structure of a New Hexamolybdate-Cyclophosphazene Complex, *Inorg. Chem.* **12**(12), 2963–2968.
259. Garner, C.D., Howlader, N.C., Mabbs, F.E., McPhail, A.T., Miller, R.W. and Onan, P.M. (1978) Studies in Eight-Co-ordination. Part 5 Crystal and Molecular Structure and Electron Spin Resonance Spectra of Tetrakis(diethyldithiocarbamato)molybdenum(V) Hexamolybdate and Chloride, *J. Chem. Soc., Dalton Trans.*, 1582.
260. Nagano, O. and Sasaki, Y. (1979) Structure of the Hydrated Potassium Hexamolybdate Complex of Hexaoxacyclooctadecane (18-Crown-6), *Acta Cryst.* **B35**, 2387–2389.
261. Dahlstrom, P. and Zubieta, J. (1982) Crystal and Molecular Structure of The tetrabutylammonium salt of the Nonadecaoxo-Hexamolybdate(VI) Dianion, $[(n\text{-}C_4H_9)_4N]_2[Mo_6O_{19}]$, *Cryst. Struct. Comm.* **11**, 463–469.
262. Strandberg, R. (1975) Multicomponent Polyanions. 13. The Crystal Structure of a Hydrated Dodecamolybdophosphoric Acid, $H_3Mo_{12}PO_{40}(H_2O)_{29-31}$, *Acta Chem. Scand.* **A29**, 359–364.
263. Allmann, R. (1976) About the Space Group of $H_3Mo_{12}PO_{40}(H_2O)_{29-31}$; a Discussion, *Acta. Chem. Scand.* **A30**, 152–156.
264. Boeyens, J.C.A., McDougal, G.J. and Smit, J.V.R. (1976) Crystallographic Study of the Ammonium/Potassium 12-Molybdophosphate Ion-Exchange System, *J. Solid State Chem.* **18**, 191–199.
265. Clark, C.J. and Hall, D. (1976) Dodecamolybdophosphioric Acid *circa*30-Hydrate, *Acta Cryst.* **B32**, 1545–1547.
266. D'Amour, H. and Allmann, R. (1976) Ein Kegginkomplex mit erniedrigter Pseudosymmetric in der Struktur des $H_3[PMo_{12}O_{40}]\cdot(13\text{–}14)H_2O$, *Z. Kristallogr.* **143**, 1–13.
267. Knoth, W.H. and Harlow, R.L. (1981) Derivatives of Heteropolyanions. 3. O-Alkylation of $Mo_{12}O_{40}^{3-}$ and $W_{12}O_{40}^{3-}$, *J. Am. Chem. Soc.* **103**, 4265–4266.
268. Feist, M., Molchanov, V.N., Kazanskii, L.P., Torchenkova, E.A. and Spitsyn, V.I. (1980) Crystal Structure of $H_4SiMo_{12}O_{40}\cdot 13H_2O$, *Russ. J. Inorg. Chem.* **25**(3), 401–406.
269. Ichida, H., Kobayashi, A. and Sasaki, Y. (1980) The Structure of Tetraguanidinium

α-Dodecamolybdosilicate Monohydrate, $(CH_6N_3)_4[SiMo_{12}O_{40}]\cdot H_2O$, *Acta Cryst.* **B36**, 1382–1387.

270. Strandberg, R. (1977) Multicomponent Polyanions. 17. The Crystal Structure of $Na_4Mo_{12}GeO_{40}(H_2O)_8$, a Compound Containing Sodium-Coordinated Dodecamolybdogermanate Anions, *Acta Cryst.* **B33**, 3090–3096.
271. Ichida, H. (1981) Ph.D. Dissertation. Tokyo, The University of Tokyo.
272. Hori, T., Tamada, O. and Himeno, S. (1989) The Structure of 18-Molybdodisulphate(VI)(4-) Ion in $(NEt_4)_4S_2Mo_{18}O_{62}\cdot CH_3CN$, *J. Chem. Soc., Dalton Trans.*, 1491–1497.
273. Day, V.W., Fredrich, M.F.,Thompson, M.R., Klemperer, W.G.,Liu, R.-S. and Shum, W. (1981) Reactivity of the $[(\eta^5\text{-}C_5H_5)Ti(Mo_5O_{18})]^{3-}$ Anion: Synthesis and Structure of MoO_2Cl^+ and $Mn(CO)_3{}^+$Adducts, *J. Am. Chem. Soc.* **103**, 3597–3599.
274. Che, T.M., Day, V.W., Francesconi, L.C., Fredrich, M. F. and Klemperer, W.G. (1985) Synthesis and Structure of the $[(\eta^5\text{-}C_5H_5)Ti(Mo_5O_{18})]^{3-}$ and $[(\eta^5\text{-}C_5H_5)Ti(W_5O_{18})]^{3-}$ Anions, *Inorg. Chem.* **24**, 4055–4062.
275. Hsieh, T.-C. and Zubieta, J.A. (1986) Synthesis and Characterization of Oxomolybdate Clusters Containing Coordinatively Bound Organo-Diazenido Units: The Crystal and Molecular Structure of the Hexanuclear Diazenido-Oxomolybdate, $(NBu_4)_3[Mo_6O_{18}(N_2C_6H_5)]$, *Polyhedron* **5**(10), 1655–1657.
276. Bank, S., Liu, S., Shaikh, S.N., Sun, X., Zubieta, J. and Ellis, P.D. (1988) ^{95}Mo NMR Studies of (Aryldiazenido)- and (Organohydrazido)molybdates. Crystal and Molecular Structure of $[n\text{-}Bu_4N]_3[Mo_6O_{18}(NNC_6F_5)]$, *Inorg. Chem.* **27**, 3535–3543.
277. Kang, H. and Zubieta, J. (1988) Co-ordination Complexes of Polyoxomolybdates with a Hexanuclear Core: Synthesis and Structural Characterization of $[NBu^n{}_4]_2[Mo_6O_{18}(NNMePh)]$, *J. Chem. Soc., Dalton Trans.*, 1192–1193.
278. Thompson, M.R. (1981) Ph.D. Dissertation. Lincoln, Nebraska, University of Nebraska-Lincoln.
279. Strandberg, R. (1975) Multicomponent Polyanions. 12. The Crystal Structure of $Na_6Mo_{18}P_2O_{62}(H_2O)_{24}$, a Compound Containing Sodium-coordinated 18-Molybdodiphosphate Anions, *Acta Chem. Scand.* **A29**, 350–358.
280. d'Amour, H. (1976) Vergleich der Heteropolyanionen $[PMo_9O_{31}(H_2O)_3]^{3-}$, $[P_2Mo_{18}O_{62}]^{6-}$ und $[P_2W_{18}O_{62}]^{6-}$, *Acta Cryst.* **B32**, 729–740.
281. Ichida, H. and Sasaki, Y. (1983) The Structure of Hexaguanidinium Octadecamolybdodiarsenate Enneahydrate, $(CH_6N_3)_6[As_2Mo_{18}O_{62}]\cdot 9H_2O$, *Acta Cryst.* **C39**, 529–533.
282. d'Amour, H. and Allmann, R. (1974) Nanomolybdophosphat, $[PMo_9O_{31}(OH_2)_3]^{6-}$, ein neuer Phosphormolybdatkomplex, *Naturwissenschaften* **61**, 31.
283. Strandberg, R. (1974) Multicomponent Polyanions. VIII. On the Crystal Structure of $Na_3H_6Mo_9PO_{34}(H_2O)_x$, a Compound Containing Protonized Enneamolybdomonophosphate Anions, *Acta Chem. Scand.* **A28**, 217–225.
284. Hedman, B. (1978) Multicomponent Polyanions. 18. A Neutron Diffraction Study of $Na_3Mo_9PO_{31}(OH_2)_3\cdot 12\text{–}13H_2O$, a Compound Containing 9-Molybdomonophosphate Anions with Molybdenum-coordinated Water Molecules, *Acta Chem. Scand.* **A32**, 439–446.
285. Schmetzer, K., Nuber, B. and Tremmel, G. (1984) Betpakdalit aus Tsumeb, Namibia: Mineralogie, Kristallchemie und Struktur, *Neues Jahrb. Mineral, Montsh*, 393.
286. Filowitz, M., Klemperer, W.G. and Shum, W. (1978) Synthesis and Characterization of the Pentamolybdate Ion, $Mo_5O_{17}H^{3-}$, *J. Am. Chem. Soc.* **100**, 2580–2581.
287. Fukushima, H.F., Kobayashi, A. and Sasaki, Y. (1981) Structure of a Novel Type of Heteropolyanion: Dicupro(II)-18-molybdodisilicate(12-), $[Cu_2Si_2Mo_{18}O_{66}]^{12-}$, *Acta Cryst.* **B37**, 1613–1615.
288. Paulat-Böschen, I. (1979) X-Ray Crystallographic Determination of the Structure of the

Isopolyanion $[Mo_{36}O_{112}(H_2O)_{16}]^{8-}$ in the Compound $K_8[Mo_{36}O_{112}(H_2O)_{16}]\cdot 36H_2O$, *J. Chem. Soc., Chem. Commun.*, 780–782.

289. Krebs, B. and Paulat-Böschen I. (1982) The Structure of the Potassium Isopolymolybdate $K_8[Mo_{36}O_{112}(H_2O)_{16}]\cdot nH_2O$ (n=36···40), *Acta Cryst.* **B38**, 1710–1718.
290. Krebs, B., Stiller, S., Tytko, K.H. and Mehmke, J. (1991) Structure and bonding in the high molecular weight isopolymolybdate ion, $[Mo_{36}O_{112}(H_2O)_{16}]^{8-}$. The crystal structure of $Na_8[Mo_{36}O_{112}(H_2O)_{16}]\cdot 58H_2O$, *Eur. J. Solid State Inorg. Chem.* **28**, 883–903.
291. Day, V.W., Klemperer, W.G. and Richard, D.L. Manuscript in Preparation.
292. Atovmyan, L.O. and Bokii, G.B. (1963) The Crystal Structure of $NaNH_4[MoO_3C_2O_4]\cdot 2H_2O$, *J. Struct. Chem.* **4**, 524–530.
293. Koop, M. and Müller-Buschbaum H. (1985) Synthese und Kristallstruktur von $Cu_6Mo_5O_{18}$, *Z. Anorg. Allg. Chem.* **531**, 140–146.
294. Ito, F., Ozeki, T., Ichida, H., Miyamae, H. and Sasaki, Y. (1988) Structure of Tetraammonium Octamolybdobis(diaquacuprate(II)) Hexahydrate, *Chem. Lett.*, 467–468.
295. Krol, I.A., Starikova, Z.A., Sergienko, V.S. and Tolkacheva, E.O. (1991) Deprotonation of an α-hydroxy Group in 1-Hydroxyethylidenediphosphonic Acid and an Unusual Type of Dimeric Anion in the Structure of $Na_5[Mo_2O_6(L^*)]\cdot 14H_2O$, *Mendeleev Commun.*, 7–8.
296. Ma, L., Liu, S. and Zubieta, J. (1989) Synthesis and Characterization of a Trinuclear Polyoxomolybdate Containing a Reactive $[MoO_3]$ Unit, $[(n\text{-}C_4H_9)_4N]_2[Mo_3O_7\{CH_3C(CH_2O)_3\}_2]$, and Its Conversion to the Methoxy Derivative $[(n\text{-}C_4H_9)_4N][Mo_3O_6(OCH_3)\{CH_3C(CH_2O)_3\}_2]$, *Inorg. Chem.* **28**, 175.
297. Liu, S., Ma, L., McGowty, D. and Zubieta, J. (1990) Molybdenum (VI) Complexes of Branched Ligands with [N,O,O,O] and [O,O,O] Donor Sets. The Crystal and Molecular Structures of $[MoO_2\{HOC_2H_4N(C_2H_4O)_2\}]$, $[(n\text{-}C_4H_9)_4N]_2[Mo_2O_4\{O_2NC(CH_2O)_3\}_2]\cdot 2O_2NC(CH_2OH)_3$, $[(n\text{-}C_4H_9)_4N]_2[Mo_2O_5\{HO_2CCH_2N(CH_2O)_3\}_2]\cdot H_2O$ and $[(n\text{-}C_4H_9)_4N][Mo_3O_6(OCH_3)\{CH_3C(CH_2O)_3\}_2]$, *Polyhedron* **9**(13), 1541–1553.
298. Mattes, R., Matz, Ch. and Sicking, E. (1977) Die Kristallstruktur von $K_6[Mo_2J_2O_{16}]\cdot 10H_2O$, *Z. Anorg. Allg. Chem.* **435**, 207–213.
299. Chae, H.K., Klemperer, W.G. and Marquart, T.A. (1993) High-nuclearity oxomolybdenum(V) complexes, *Coord. Chem. Rev.* **128**, 209–224.
300. Müller, A., Kögerler, P. and Bögge, H. (2000) Pythagorean Harmony in the World of Metal Oxygen Clusters of the $\{Mo_{11}\}$ Type: Giant Wheels and Spheres both Based on a Pentagonal Type Unit, in M. Fujita (ed.), *Molecular Self-Assembly: Organic Versus Inorganic Approaches*, Springer-Verlag, Berlin, pp. 203–236.
301. Müller, A. and Serain, C. (2000) Soluble Molybdenum Blues–"des Pudels Kern", *Acc. Chem. Res.* **33**, 2–10.
302. Barrows, J.N., Jameson, G.B. and Pope, M.T. (1985) Structure of a Heteropoly Blue. The Four-Electron Reduced β-12-Molybdophosphate Anion, *J. Am. Chem. Soc.* **107**, 1771–1773.
303. Müller, A., Krickmeyer, E., Penk, M., Wittneben, V. and Döring, J. (1990) $[H_6As_{10}Mo_{24}O_{90}]^{8-}$, a Heteropolyanion Comprising Two Linked Spherical Fragments, and Reduced Keggin Anions as Its Degradation Products, *Angew. Chem. Int. Ed. Engl.* **29**, 88–90.
304. Yamase, T. (1991) Photochemical Studies of Alkylammonium Molybdates. Part 9. Structure of Diamagnetic Blue Species involved in the Photoredox Reaction of $[Mo_7O_{24}]^{6-}$, *J. Chem. Soc., Dalton Trans.*, 3055–3063.
305. Müller, A., Koop, M., Bögge, H., Schmidtmann, M. and Beugholt, C. (1998) Exchanged ligands on the surface of a giant cluster: $[(MoO_3)_{176}(H_2O)_{63}(CH_3OH)_{17}H_n]^{(32-n)-}$, *Chem. Commun.*, 1501–1502.
306. Kepert, D.L. (1972) *The Early Transition Metals*. Academic Press, London, pp. 256–264.
307. Vincent, H. and Marezio, M. (1989) On Structural Aspects of Molybdenum Bronzes and

Molybdenum Oxides in Relation to Their Low-Dimensional Transport Properties, in C. Schlenker (ed.), *Low-Dimensional Properties of Molybdenum Bronzes and Oxides*, Kluwer, Dordrecht, pp. 49–85.

308. Yamazoe, N. and Kihlborg, L. (1975) Mo_5O_{14}–Twinning and Three-Dimensional Structure, Determined from a Partly Tantalum-Substituted Crystal, *Acta Cryst.* **B31**, 1666–1672.
309. Kihlborg, L. (1963) Least Squares Refi nement of the Structure of $Mo_{17}O_{47}$, *Acta Chem. Scand.* **17**(5), 1485–1486.
310. Ghedira, M., Chenavas, J., Marezio, M. and Marcus, J. (1985) Crystal Structure, Dimensionality, and 4*d* Electron Distribution in $K_{0.30}MoO_3$ and $Rb_{0.30}MoO_3$, *J. Solid State Chem.* **57**, 300–313.
311. Kihlborg, L. (1963) Least squares refi nement of the structure of Mo_8O_{23}, *Arkiv Kemi* **21**(43), 461–469.
312. Kihlborg, L. (1963) The structural chemistry of the higher molybdenum oxides, *Arkiv Kemi* **21**(44), 471–495.
313. Kihlborg, L. (1963) The crystal structure of $Mo_{18}O_{52}$ and the existence of homologous series of structures based on MoO_3, *Arkiv Kemi* **21**(42), 443–460.
314. Kihlborg, L. (1963) Crystal structure studies on monoclinic and orthorhombic Mo_4O_{11}, *Arkiv Kemi* **21**(35), 365–377.
315. Ghedira, M., Vincent, H., Marezio, M., Marcus, J., and Furcaudot, G. (1985) Structure cristalline du conducteur métallique bidimensionnel $Mo_4O_{11-\gamma}$, *J. Solid State Chem.* **56**, 66–73.
316. Moutou, J.-M., Chaminade, J.-P., Puchard, M. and Hagenmuller, P. (1986) Structure Cristalline de l'oxyfluoromolybdate de sodium $NaMoO_3F$, *Revue de Chimie minérale* **23**(1), 27–34.
317. Du, Y., Rheingold, A.L. and Maatta, E.A. (1992) A Polyoxometalate Incorporating an Organoamido Ligand: Preparation and Structure of $[Mo_5O_{18}(MoNC_6H_4CH_3)]^{2-}$, *J. Am. Chem. Soc.* **114**, 345–346.
318. Berg, J.M., Spira, D.J., Hodgson, K.O., Bruce, A.E., Miller, K.F. , Corbin, J.L. and Stiefel, E.I. (1984) Six-Coordinate Dioxomolybdenum(VI) Complexes Containing a Nonoctahedral Structure with a Short Sulfur-Sulfur Contact, *Inorg. Chem.* **23**, 3412–3418.
319. Klemperer, W.G., Marquart, T.A. and Yaghi, O.M. (1992) New Directions in Polyvanadate Chemistry: From Cages and Clusters to Baskets, Belts, Bowls, and Barrels, *Angew. Chem. Int. Ed. Engl.* **31**, 49–51.
320. Klemperer, W.G. and Shum, W.J. (1976) Synthesis and Interconversion of the Isomeric α- and β- ($Mo_8O_{26}^{4-}$) Ions, *J. Am. Chem. Soc.* **98**, 8291–8293.
321. Xi, R., Wang, B., Isobe, K., Nishioka, T., Toriumi, K. and Ozawa, Y. (1994) isolation and X-Ray Crystal Structure of a New Octamolybdate: $[(RhCp^*)_2(\mu_2\text{-}SCH_3)_3]_4[Mo_8O_{26}]\cdot 2CH_3CN$ ($Cp^*=\eta^5\text{-}C_5Me_5$), *Inorg. Chem.* **33**, 833–836.
322. Klemperer, W.G., Schwartz, C. and Wright, D.A. (1985) Mechanistic Polyoxoanion Chemistry: Intramolecular Rearrangements of the α-$Mo_8O_{26}^{4-}$, $C_6H_5AsMo_7O_{25}^{4-}$, and $(C_6H_5As)_2Mo_6O_{24}^{4-}$ Anions, *J. Am. Chem. Soc.* **107**, 6941–6950.
323. Cotton, F.A., Wilkinson, G., Murillo, C.A. and Bochmann, M. (1999) *Advanced Inorganic Chemistry, 6th ed.*, Wiley, New York, pp. 13–14.
324. Klemperer, W.G. (1972) Enumeration of Permutational Isomerization Reactions, *J. Chem. Phys.* **56**(11), 5478–5489.
325. Tytko, K.H., Mehmke, J. and Fischer, S. (1999) Bonding and Charge Distribution in Isopolyoxometalate Ions and Relevant Oxides–A Bond Valence Approach, in D.M.P. Mingos (ed.), *Bonding and Charge Distribution in Polyoxometalates —A Bond Valence Approach*, Springer, Berlin, pp. 129–321.

326. Werner, A. (1911) *New Ideas on Inorganic Chemistry* (Engl. Transl.), Longmans, Green, and Co., London, p. 124.
327. Farneth, W.E., Staley, R.H., and Sleight, A.W. (1986) Stoichiometry and Structural Effects in Alcohol Chemisorption/Temperaure-Programmed Desorption on MoO_3, *J. Am. Chem. Soc.* **108**, 2327–2332.
328. Day, V.W., Klemperer, W.G., Lockledge, S.P., Main, D. J., Rosenberg, F.S., Wang, R.-C., and Yaghi, O.M. (1990) Selective Oxidation on Soluble Oxides: A Progress Report, in J.P. Fackler (ed.), *Metal-Metal Bonds in Chemistry and Catalysis*, Plenum Press, New York, pp. 161–174.
329. Zumdahl, S.S. and S.A. Zumdahl (2000) *Chemistry, 5th ed.*, Houghton Miffln, Boston, p. 376.
330. March, J. (1985) *Advanced Organic Chemistry, 3rd ed.*, John Wiley & Sons, New York, p. 182.
331. March, J. (1985) *Advanced Organic Chemistry, 3rd ed.*, John Wiley & Sons, New York, p. 214.
332. Lines, M.E. and Glass, A.M. (1977) *Principles and Applications of Ferroelectrics and Related Materials*, Clarendon Press, Oxford, pp. 477–497.
333. Boysen, H. and Altorfer, F. (1994) A Neutron Powder Investigation of the High-Temperature Structure and Phase Transition in $LiNbO_3$, *Acta Cryst.* **B50**, 405–414.
334. Lawrence, M. (1993) Lithium niobate integrated optics, *Reg. Prog. Phys.*, 363–429.
335. Moulson, A.J. and J.M. Herbert (1990) *Electroceramics*, Chapman and Hall, London, pp. 68–79.
336. Jona, F. and G. Shirane (1993) *Ferroelectric Crystals*, Dover Publications, New York, pp. 160–181.
337. Klein, C. and Hurlbut Jr., C.S. (1993) *Manual of Mineralogy, 21st ed.*, John Wiley & Sons, New York, p. 167.
338. Krumhansl, J.A. and Schrieffer, J.R. (1975) Dynamics and statistical mechanics of a one-dimensional model Hamiltonian for structural phase transitions, *Phys. Rev. B.* **11**(9), 3535–3545.
339. Heeger, A.J., Kivelson, S., Schrieffer, J.R., and Su, W.-P. (1988) Solitons in conducting polymers, *Rev. Mod. Phys.* **60**(3), 781–850.
340. Rice, M.J. and Mele, E.J. (1982) Elementary Excitations of a Linearly Conjugated Diatomic Polymer, *Phys. Rev. Lett.* **49**(19), 1455–1459.
341. Campbell, D.K. (1983) Polarons in a Diatomic Polymer, *Phys. Rev. Lett.* **50**(11), 865.
342. Zolotaryuk, A.V., Peyrard, M., and Spatschek, K.H. (2000) Collective proton transport with weak proton-proton coupling, *Phys. Rev. E* **62**(4), 5706–5710.
343. Park, C.H. and Chadi, D.J. (1998) Microscopic study of oxygen-vacancy defects in ferroelectric perovskites, *Phys. Rev. B* **57**(22), 961–964.
344. Barsch, G.R. and Krumhansl, J.A. (1984) Twin Boundaries in Ferroelastic Media without Interface Dislocations, *Phys. Rev. Lett.* **53**(11), 1069–1072.
345. Mazor, A. and Bishop, A.R. (1989) Model for a decorated twin boundary in ferroelastic martensites, *Phys. Rev. B* **40**(7), 5084–5093.
346. Comes, R., Lambert, M., and Guinier, A. (1968). The chain structure of $BaTiO_3$ and $KNbO_3$, *Solid State Comm.* **6**(10), 715–719.
347. Lambert, M. and Comes, R. (1969) The chain structure and phase transition of $BaTiO_3$ and $KNbO_3$, *Solid State Comm.* **7**(2), 305–308.
348. Klemperer, W.G. and Richard, D.L. (1999) A ^{17}O Solid State NMR Study of the Lead Zirconium Titanate System ($PbZr_xTi_{1-x}O_3$), in J.J. Fitzgerald (ed.): *Solid-State NMR Spectroscopy of Inorganic Materials*, American Chemical Society, Washington DC, p. 256–263.

349. Brennan, C.J. and Nelson, K.A. (1997) Direct time-resolved measurement of anharmonic lattice vibrations in ferroelectric crystals, *J. Chem. Phys.* **107**(22), 9691–9694.
350. Tian, M., Chen, L., and Zhang, Y. (2000) Temperature dependence of the structural parameters of the host lattice in blue bronze $K_{0.3}MoO_3$, *Phys. Rev. B* **62**(3), 1504–1506.